

Hydrogen Generation through Solar Powered Methanol Electrolysis

A Major Qualifying Project Report

Submitted to

the Faculty of the

WORCESTER POLYTECHNIC INSTITUTE

Chemical Engineering Department

in partial fulfillment of the requirements

for the Degree of Bachelor of Science

by

Thomas W. Cormier

Oliver P. Lizotte

Joseph N. Pizzuto

Date: April 30, 2016

Adviser: Ravindra Datta

Table of Contents

List of Figures	6
Abstract	10
Executive Summary	11
Acknowledgements	13
Chapter 1. Introduction	14
1.1 Rationale and Goals	14
1.1.1 Coupling Energy Storage and CO ₂ Mitigation	14
1.1.2 Power-to-Gas	15
1.1.3 Hydrogen Economy	17
1.1.4 Methanol Economy	17
1.1.5 eRedux of CO ₂ to Methanol.....	18
1.1.6 Hydrogen from Methanol	19
1.1.7 Hydrogen from Methanol Electrolysis.....	20
1.2 Summary of Work Accomplished	22
Chapter 2. Background and Vision.....	23
2.1. Energy Storage and Energy Vectors	23
2.2. Hydrogen Economy	26
2.3 Hydrogen Generation.....	29
2.3.1 Steam Reforming	30

2.3.2 Hydrogen from Electrolysis	34
2.4 Electrolyzer Anatomy	36
2.4.1 Membrane	37
2.4.2 Catalyst	39
2.4.3 Gas Diffusion Layer.....	39
2.4.4 Bipolar Plates	40
2.5 Cell Polarization.....	40
2.6 Degradation.....	43
2.6.1 Membrane degradation	43
2.6.2 Catalyst Degradation.....	44
2.6.3 Gas Diffusion Layer Degradation	44
2.7 Methanol Electrolysis Literature Review	45
2.7.1 Methanol Electrolyzer Performance	46
2.7.2 Methanol Electrolyzer Application Potential.....	48
2.7.3 Optimizing Operating Conditions and Electrolyzer Design	51
2.7.4 Effect of Temperature on Methanol Electrolysis Performance	51
2.7.5 Effect of Methanol Concentration	54
2.7.6 Performance of Different Anode Catalysts.....	55
2.7.7 Performance of Different Membranes	56
2.7.8 Advanced Methanol Electrolysis Systems.....	60

2.7.9 Conclusions on Methanol Electrolysis Literature.....	61
2.8 Solar Panels.....	62
2.8.1 Solar Power Issues.....	63
Chapter 3. Methodology.....	65
3.1 Single Cell Test Stand at Envirowerks.....	65
3.1.1 Design and Assembly of the Cell.....	69
3.1.2 Experimental Procedure.....	71
3.2 Four-Cell Performance and Durability Testing.....	73
3.2.1 Setup.....	74
3.2.2 Data Acquisition.....	76
3.2.2 Experimental Procedure.....	77
3.3 Fuel Cell Center Lab Single Cell Testing.....	78
3.3.1 FCC Single Cell Setup.....	79
3.3.2 FCC Single Cell Tests.....	82
3.4 Solar Powered Methanol Electrolysis System.....	83
3.4.1 Designing the setup.....	83
3.4.2 Test Procedure.....	87
Chapter 4. Results and Discussion.....	88
4.1 FCC Single Cell Tests.....	88
4.1.1 Effect of Feed Flow Rate.....	89

4.1.2: Effect of Feed Concentration	91
4.1.3 Effect of Temperature at a Given Concentration.....	100
4.2 Performance of the Standalone Solar Powered System.....	105
4.2.1 System Pressure	106
4.2.2 System Temperature	107
4.2.3 System Voltage and Current Density.....	108
4.3 Concluding Remarks.....	109
Chapter 5. Conclusions and Recommendations for Future Work	110
5.1 Single Cell Methanol Electrolyzer Performance	110
5.2 Standalone Solar Powered Methanol Electrolyzer System.....	111
5.3 Recommendations for Future Work.....	111
References.....	114
Appendices.....	122

List of Figures

Figure 1.1. Power and energy characteristics of various grid storage technologies (California Hydrogen Business Council, 2015).	14
Figure 1.2. Energy density of electrochemical energy storage versus conventional fuels (Centi and Perathoner, 2011; Ganesh, 2014).....	15
Figure 1.3. The grid storage concept power-to-gas (P2G) (Jentsch et al., 2014).	16
Figure 1.4. Carbon neutral cycle of methanol produced from CO ₂ as a common energy vector (Olah et al., 2008).	18
Figure 1.5. Schematic of a renewable methanol economy, wherein excess grid energy is used to electrochemically convert anthropogenic CO ₂ into methanol, which can be stored, and utilized when needed for producing electricity either directly in a DMFC, or first in an electrolyzer to produce H ₂ on demand which is then used in a fuel cell.	20
Figure 2.1. Current cost estimates for alternate electrical energy storage technologies (DOE, 2008).	24
Figure 2.2. Discharge times and power ratings for different electrochemical energy storage technologies (Dunn et al., 2011).	25
Figure 2.3. Volumetric versus gravimetric energy densities of selected chemical and batteries (Wikipedia, 2016).	26
Figure 2.4. Solar derived hydrogen fuel for producing electricity on demand with a fuel cell. ...	29
Figure 2.5. Alternate pathways to produce hydrogen from renewable, nuclear, and fossil resources (Florida Solar Energy Center).....	30
Figure 2.6. A typical steam reforming diagram (Gumilar, 2010).	31

Figure 2.7. Tank volumes for various storage options for 4 kg of hydrogen on board a car (Schlapbach and Züttel, 2001).	33
Figure 2.8. Comparison of various hydrogen storage options (Schlapbach and Züttel, 2001).....	33
Figure 2.9. A typical electrolyzer cell.....	35
Figure 2.10. Nafion [®] Membranes with Carbon Cloth GDL.	38
Figure 2.11. A schematic polarization plot and the various overpotentials within the PEM-water electrolyzer (Datta et al., 2015).....	41
Figure 2.12 Comparison of prediction with experiments for polarization plot of a PEM-WE based on Nafion [®] 117 at different temperatures.	43
Figure. 2.13. Schematic of methanol electrolyzer developed by NASA's Jet Propulsion Laboratory (Jefferies-Nakamura et al., 2002).....	46
Figure 2.14. Polarization plots at 90 °C for a 2 M methanol feed for 2.5 mg/cm ² Pt-Ru/C anode, and 1.5 mg/cm ² Pt/C (1), and Pt-WC/C (2) cathode (Hu et al., 2007).	47
Figure 2.15. A comparison of the polarization and current efficiency of methanol and water electrolysis (Uhm et al., 2012).....	49
Figure 2.16 Effect of operating temperature on current density (a) and on hydrogen production rate (b) by methanol electrolyzer with Nafion-117 and 4 M methanol, at 30 °C (lowest curve), 40 °C, 50 °C, 60 °C, 70 °C and 80 °C (highest curve) (Sasikumar et al. 2008).....	53
Figure 2.17: Volume of evolved hydrogen after 20 min of electrolysis as a function of the current intensity <i>I</i> for two methanol concentrations and two working temperatures (Guenot et al., 2015).	53
Figure 2.18. Polarization plots for methanol electrolysis at different temperatures for different methanol feed concentrations (Lamy et al., 2015a).....	55

Figure 2.19. The polymer structure of Nafion [®]	57
Figure 2.20. Schematic of methanol electrolyzer based on an anion-exchange membrane (AEM) (Tuomi et al., 2013).	59
Figure 2.21. Chemical structure of polyethersulfone (PES) and sulfonated polyethersulfone (SPES, right) (Muthumeenal et al. 2016).	60
Figure 2.22. A typical solar panel schematic.	63
Figure 3.1: Envirowerks Original Single Cell Test Stand.	66
Figure 3.2: Control System for Envirowerks Test Stand.	68
Figure 3.3: Cell Design & Assembly Used Throughout Entire Project.	70
Figure 3.4: Carbon bipolar plates used throughout the project.	71
Figure 3.5. A fully assembled single cell electrolyzer.	72
Figures 3.6 & 3.7: Modified Test Stand at Envirowerks.	74
Figure 3.8. The flow schematic of the four cell test stand.	75
Figure 3.9. Schematic of the four cell test stand relay circuit.	76
Figure 3.10: Single cell setup used for FCC testing.	79
Figure 3.11: Power supply used during FCC testing.	80
Figure 3.12: A version of a voltage divider circuit diagram, with V_{out} calculation.	81
Figure 3.13: Solidworks Design of a Solar Methanol Electrolyzer.	84
Figure 3.14: The monocrystalline solar panel mounted on the stand alone system.	84
Figure 3.15 & 3.16: The solar powered methanol electrolyzer system prototype.	87
Figure 4.1. A picture of the single cell electrolyzer used in FCC.	89
Figure 4.2: Effect of feed flow rate on the performance of the cell operating at 20 °C and a methanol concentration of 5 M.	90

Figure 4.3: Repeat experiment of feed flow rate of 5mL/min on the performance of the cell operating at 20 °C and a methanol concentration of 5 M.....	91
Figure 4.4: Effect of concentration at 20 °C and 10 ml/min flow rate.....	92
Figure 4.5: Effect of concentration at 30 °C and 10 ml/min flow rate.....	93
Figure 4.6: Effect of Concentration at 40 °C and 10 ml/min flow rate.....	94
Figure 4.7: Effect of Concentration at 50 °C and 10 ml/min flow rate.....	96
Figure 4.8: Effect of Concentration at 60 °C and 10 ml/min flow rate.....	97
Figure 4.9: Effect of Concentration at 70 °C and 10 ml/min flow rate.....	98
Figure 4.10: The effect of temperature on a 1M feed solution.	101
Figure 4.11: The effect of temperature on 3M solution.....	102
Figure 4.12: The effect of temperature on 5M solution.....	103
Figure 4.13: The effect of temperature on 10M solution.....	104
Figure 4.14: Column pressure as a function of time, before and after a leak.	106
Figure 4.15: Recorded cell and ambient temperature data from the standalone solar powered methanol electrolysis system.	108
Figure 4.16: Average voltage and current density of the solar powered system between 25 °C and 40 °C.....	109

Abstract

Because of the unpredictable nature of most renewable energy sources, effective energy storage is needed. The methanol economy suggests that methanol can be used as an efficient means of storing energy. Hydrogen from methanol can be used as a fuel for fuel cells, a clean way to produce energy. By coupling a solar panel to a methanol electrolyzer, hydrogen can be produced, harnessing the power of the sun. In this project, methanol electrolysis was performed under different operating conditions in order to understand the characteristics of electrolysis. Experimental data showed that increasing temperature and methanol concentration, improved methanol electrolysis performance. Additionally a solar powered methanol electrolyzer was made to assess the viability of solar methanol electrolysis.

Executive Summary

As global demand for power increases, conventional fossil fuels, such as coal and gas, will not be a viable option to provide energy because of climate change concerns. On the other hand, renewable sources such as wind and solar power are intermittent and do not always produce power when needed. Peak energy demands occur during the early evening hours after both wind and solar power supplies may no longer be available. This discrepancy between renewable energy generation and usage calls for grid level energy storage. Besides hydropower, current means of energy storage, e.g., batteries, are too costly and bulky to be of practical use for grid storage.

Fuel Cells are a very clean and efficient way of producing energy, but the transportation and storage of hydrogen needed for their operation is currently difficult as well as costly. The method of hydrogen production in industry is steam reforming of methane. An alternate hydrogen production method is using water electrolysis in fuel cells using excess grid energy for storage. Water electrolysis however requires a larger amount of energy and also produces oxygen besides the needed hydrogen. A practical alternative to water for electrolysis is to use methanol, which is easier to electrolyze than water, requiring a thermodynamic potential of only .02 V vs water's 1.2 volts. Besides, a molecule of methanol produces 3 molecules of H₂ rather than a single molecule from a molecule of water.

A scheme that couples all of the above and involves fuel cells in each of the following steps: 1) Excess renewable grid electricity is utilized to produce methanol via electrochemical reduction of anthropogenic CO₂ which can be readily stored/transported as the energy vector; 2) Methanol is electrolyzed to produce hydrogen on demand; 3) Hydrogen produced is utilized in a fuel cell to produce electricity when demand exceeds grid availability.

The focus of this work was step 2 in the above closed-cycle sustainable scheme, i.e., an investigation of methanol electrolysis in a PEM fuel cell because there is only limited research in the field reported in the literature so far. Thus, methanol electrolysis experiments were conducted in a PEM electrolyzer to study its performance characteristics. Further, a commercial solar cell was coupled to the PEM electrolysis cell to investigate the direct use of a solar cell for methanol electrolysis.

During the course of this project, thus, a methanol electrolyzer was designed, constructed, and also paired with a solar panel in order to generate hydrogen in a renewable fashion. The solar powered setup was tested during optimal sunlight conditions, and data was acquired during a three hour period to track the performance of the cell.

In order to further optimize the performance and efficiency of the methanol electrolyzer, experiments were conducted on a Nafion[®] 212 membrane electrode assembly (MEA) under a variety of conditions to maximize performance. These experiments consisted of testing the MEA at six different temperatures and four different methanol concentrations. In order to conduct these tests, an existing fuel cell test setup was modified in order to run the electrolysis tests. During these tests, the current density was varied upward from a minimal density to obtain polarization plots until reaching around 1.1 V, furthermore beyond 1.23 V is where water electrolysis occurs. These polarization plots are used to determine optimal operating conditions for methanol electrolysis with a Nafion[®] 212 MEA, which were found to be 3M at 60 C.

Acknowledgements

Firstly, we would like to thank Professor Datta for advising our group, as well as helping and guiding us throughout the duration of this project. We would also like to thank Patrick Emerick for allowing us to work in his facility, partially funding experiments and for providing us with years of knowledge to expedite our learning curve. Without the help of Patrick our group would not have been able to accomplish close to what was done in the same amount of time. Finally, we would like to thank the FCC for allowing us space to work and perform tests.

Chapter 1. Introduction

1.1 Rationale and Goals

1.1.1 Coupling Energy Storage and CO₂ Mitigation

There is now incontrovertible evidence that the unabated use of fossil fuels is causing dramatic climate change, and a shift to renewable energy is needed now. In fact, solar and wind power have started to make inroads into the energy sector so far exclusively reliant on fossil resources. However, the intermittency and lack of reliability of these renewable resources requires grid level electrical energy storage (EES) (Figure 1.1).

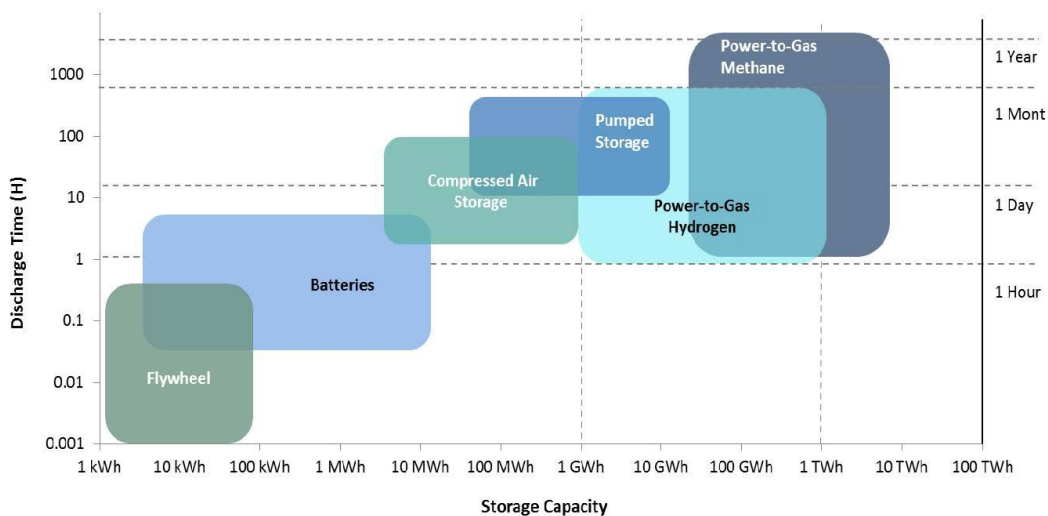


Figure 1.1. Power and energy characteristics of various grid storage technologies (California Hydrogen Business Council, 2015).

EES technologies (USDOE, 2013) can be divided into four types: 1) mechanical, 2) electrical, 3) chemical, and 4) electrochemical (Dunn et al., 2011). Pumped hydroelectric storage, in which water is pumped back into the reservoir from downstream in a dam when excess power is available, accounts for 99% of the worldwide storage capacity, with compressed air storage is a distant second. Only a tiny fraction of the total energy generation in the US uses electrical energy storage,

limited mostly to pumped hydroelectric storage. The electrochemical energy storage includes batteries, flow batteries (Dunn et al., 2011) and reversible fuel cells, e.g., for electrolysis of water into H_2 .

It turns out that to take advantage of energy and hydrogen density of conventional hydrocarbon fuels (Figure 1.2), it is attractive to store excess grid energy as some of these fuels (Centi and Perathoner, 2011). This is shown schematically in Figure 1.1 as Power-to-Gas or P2G, where the electrical energy is stored, e.g., as hydrogen from the electrolysis of water. Further, of course, if the anthropogenic CO_2 could be converted into useful fuels, it would mitigate the CO_2 emissions. Such an approach would combine grid storage and carbon recycling by using CO_2 as a feedstock in the P2G process for methane as shown in Figure 1.1.

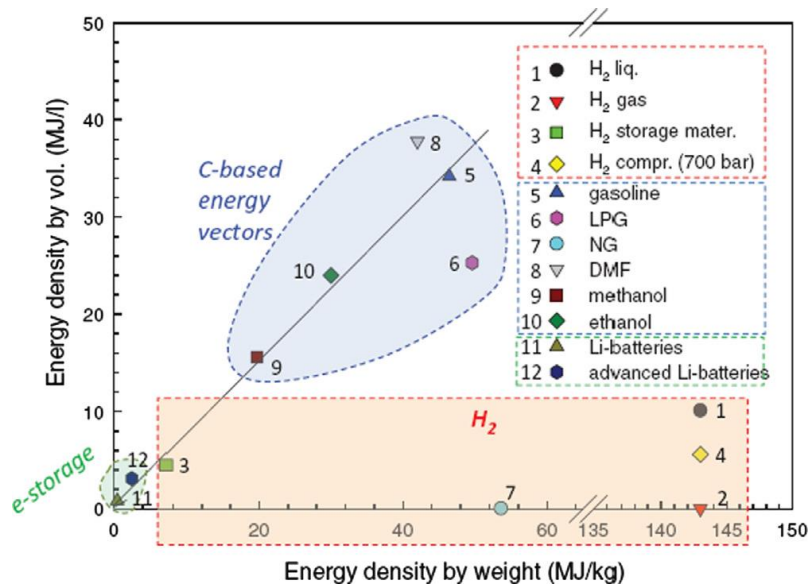


Figure 1.2. Energy density of electrochemical energy storage versus conventional fuels (Centi and Perathoner, 2011; Ganesh, 2014).

1.1.2 Power-to-Gas

A key advantage of the P2G scheme is that the produced methane could be directly sent to the existing natural gas pipeline infrastructure, which has a large storage capacity, and can be

utilized for a multitude of purposes. Figure 1.1 compares the characteristics of P2G to methane or hydrogen and shows that it can compete on scale with pumped hydro and compressed air without their limitation of being site specific.

Thus, the P2G is a promising new concept in grid energy storage in which H₂ produced via water electrolysis is used for energy storage either directly or further converted into CH₄ via the Sabatier process, as shown in Figure 1.3. The P2G technology is being implemented in Europe (Jentsch et al., 2014), and California is also now exploring this option (California Hydrogen Business Council, 2015). The current efficiency of the P2G process is, however, around 40%, which is less than pumped hydro or battery storage. Alternately, all steps in the dashed box in Figure 1.3 can be combined into a single electrochemical reduction (*eRedux*) step to produce methane directly.

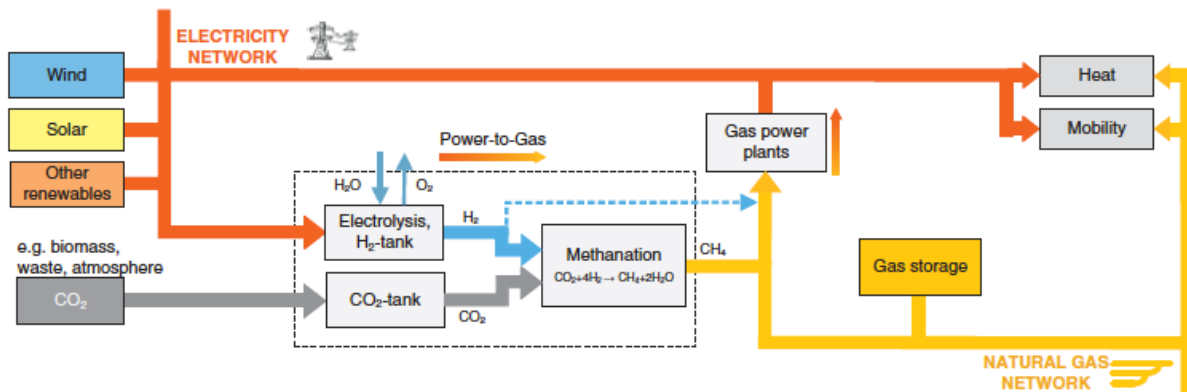


Figure 1.3. The grid storage concept power-to-gas (P2G) (Jentsch et al., 2014).

In the *eRedux* of CO₂ (Figure 1.3) the hydrogen is produced from the electrolysis of water, utilizing the excess energy from the grid. The methane produced can be injected back into existing gas infrastructure, which typically has a reserve of one or two years of natural gas storage capacity. This “renewable” methane can then be used on demand to generate electricity (CHP) either in conventional natural-gas fed power plants or in MCFC or SOFC. Especially, if this process is

implemented in conjunction with a methane-fed power plant, it also provides a ready source of CO₂ in its stack for direct recycle using excess electrons from the grid.

1.1.3 Hydrogen Economy

A clean energy vector proposed by Bockris (1975) is hydrogen. In this vision, the hydrogen is produced via the electrolysis of water using solar electricity. The use of hydrogen as a fuel or to produce electricity in a fuel cell produces only water as the product of combustion. Thus, it could greatly reduce environmental pollution and emission of greenhouse gases. However, this vision has some drawbacks. Being the lightest element, it is difficult to distribute and store, requiring either very high pressure or liquefied hydrogen, both of which are challenging. Widespread distribution would also require a new hydrogen infrastructure requiring a huge investment.

1.1.4 Methanol Economy

An alternate and more recent vision of a future sustainable energy scenario is the so-called “methanol economy,” proposed by Olah and coworkers (Olah, 2005; Olah et al., 2008; Olah et al., 2011), which advocates renewable methanol (CH₃OH) produced from CO₂ as the energy vector (Figure 1.4). Methanol is a liquid so that it is much easier to store and transport than hydrogen, and has 12.6% by wt. hydrogen rich. It is also a fuel for direct methanol fuel cell (DMFC) (Rosenthal et al., 2012), and as a platform chemical can be converted into various chemicals and fuels (Figure 1.4). A disadvantage is that it is a toxic chemical, and can cause blindness and death if ingested in larger amounts (30-100 mL).

The key step in this scenario involves generation of hydrogen from electrolysis of water using solar electricity or from other renewable sources such as geothermal, hydro, and wind, which is then used to reduce CO₂ into methanol. This route is being developed by Mitsui Chemicals, Inc., and by Carbon Recycling International, Inc. (Ganesh, 2014).

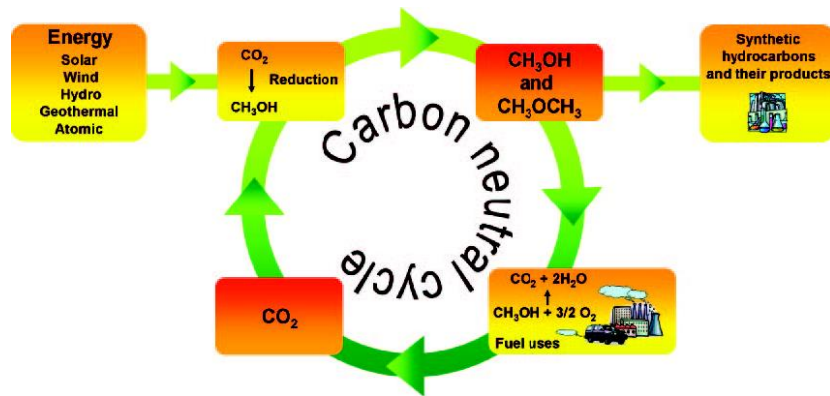
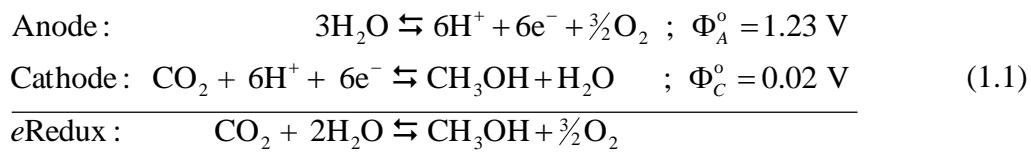


Figure 1.4. Carbon neutral cycle of methanol produced from CO₂ as a common energy vector

(Olah et al., 2008).

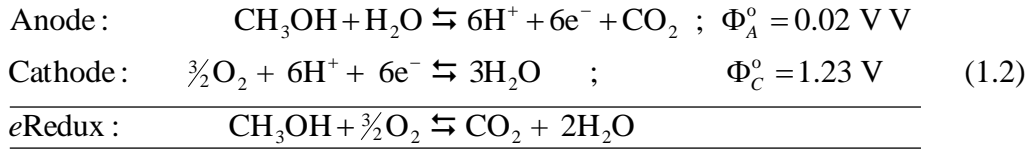
1.1.5 eRedux of CO₂ to Methanol

An alternate route being considered involves direct electrochemical reduction (*eRedux*) of CO₂ using the protons generated from the electrolysis of water (Albo et al., 2015)



which overall is simply the reverse of methanol combustion, and may be considered as artificial photosynthesis. Thus, it provides a means of storing the excess electricity on a grid as the energy dense fuel methanol. This process is being investigated at the moment to improve efficiency and selectivity so that it is a practically attractive route. Hydrogen evolution reaction (HER) competes with the CO₂ reduction reaction at the cathode. Note that the standard electrode potential of HER ($\Phi_{\text{HER}}^{\circ} = 0.00 \text{ V}$) is very close to that of the CO₂ reduction. The selectivity for CO₂ reduction can be improved by picking cathode catalysts that are poor catalysts for the HER. However, this also reduces the activity toward the desired reaction. Work on this is ongoing.

Nonetheless, assuming that electroreduction of anthropogenic CO₂ would one day be feasible, a global vision of coupling grid storage leading to renewable methanol as a convenient hydrogen/energy carrier is depicted in Figure 1.5. The stored methanol may be used directly in a DMFC to produce power

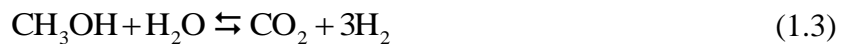


which is simply the reverse of the CO₂ *e*Redux process discussed above, so that the cycle is complete. However, DMFCs in general perform poorly (< 100 mW/cm²), requiring a large unit, with an order of magnitude higher catalyst loading coupled with low efficiencies (< 20%) due to methanol crossover and its polarization of *both* the anode and the cathode (Rosenthal et al., 2012). Alternately, as depicted in Figure 1.5, the methanol may be used to first release its hydrogen, followed by its use in a PEM fuel cell.

Finally, it can be seen that the cycle in Figure 1.5 is closed, with solar energy eventually resulting in electricity produced by the fuel cell on demand.

1.1.6 Hydrogen from Methanol

Hydrogen from methanol (Stephan, 2013) can, in principle, be produced via catalytic decomposition (Vilekar et al., 2007), methanol steam reforming, or via electrochemical reforming (*e*Reform) as shown in Figure 1.5. The methanol reforming (MeOHRef)



can be conducted at moderate temperatures (~350 °C) (Iulianelli et al., 2014), but still requires complex and/or expensive (e.g., a Pd membrane) cleansing steps (Palo et al., 2007) to reduce the CO level to less than 5 ppm required for using hydrogen in a PEM fuel cell (Zhang et al., 2002). Thus, even though methanol as a hydrogen carrier has a higher hydrogen density than compressed

or liquefied hydrogen, the advantage is largely dissipated by the bulk of the on-board reformer needed to convert it into hydrogen (Palo et al., 2007).

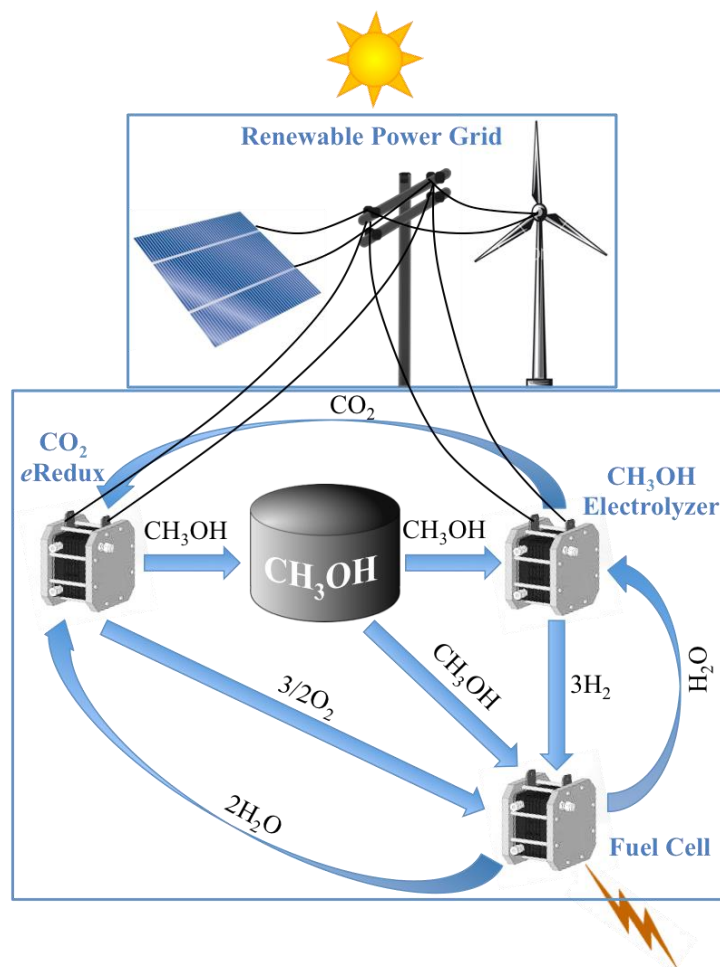
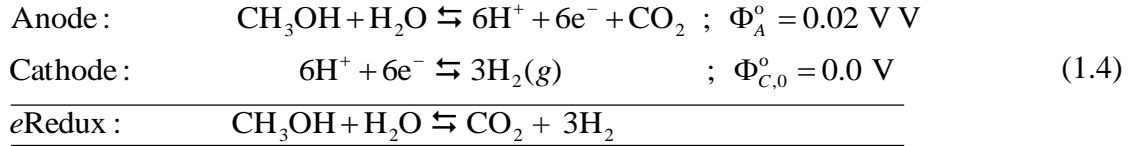


Figure 1.5. Schematic of a renewable methanol economy, wherein excess grid energy is used to electrochemically convert anthropogenic CO₂ into methanol, which can be stored, and utilized when needed for producing electricity either directly in a DMFC, or first in an electrolyzer to produce H₂ on demand which is then used in a fuel cell.

1.1.7 Hydrogen from Methanol Electrolysis

An alternative being considered more recently (e.g., Sasikumar et al., 2008) is to do *electrochemical* reforming of methanol (*eMeOHRef*) in a PEM electrolyzer (Figure 1.5).



This can directly produce pure hydrogen under mild conditions and significant amounts (two molecules of hydrogen per molecule of methanol, including one from a water molecule) in a compact and a light unit. In other words, the PEM unit acts as a reactor-separator with the PEM effectively separating the CO_2 and H_2 without requiring an external separator such as a Pd membrane. Further, compressing H_2 to a high pressure within the methanol electrolyzer stack is inherently more efficient than in a PEM water electrolyzer (Datta et al., 2015), because there is no unnecessary generation of oxygen with its large overpotential and efficiency loss. It is also inherently safer there is no oxygen that can diffuse across the PEM and mix with the hydrogen product, potentially creating a safety hazard.

Current work is investigating the feasibility of coupling a methanol electrolyzer with a hydrogen proton exchange membrane fuel cell (H_2 -PEMFC). This technology is thought to have a possible application in small scale portable electronics. This coupling is similar to direct methanol fuel cells (DMFCs), however offer better power efficiency (Halme et al. 2016). This work, however, still needs further development, though shows much promise as a viable technology.

This study is concerned with methanol electrolysis. Despite the attractive features of methanol electrolysis to produce hydrogen as compared to water electrolysis, it has not been extensively investigated in the literature. Thus, although, the first report on methanol electrolysis was published in 2002 by researchers at JPL (Jeffries-Nakamura et al., 2002; Narayanan et al., 2002), there were no further studies reported in the literature then until 2007 (Take et al., 2007; Hu et al., 2007), even though during this period the research on fuel cells grew exponentially. Even

thereafter, it has received only scant attention in the literature (Sasikumar et al., 2008; Cloutier and Wilkinson, 2010).

1.2 Summary of Work Accomplished

In order to further explore the possibilities of methanol electrolysis, experiments were performed to evaluate the performance of a Nafion[®] 212 membrane. These tests consisted of varying the operating conditions of electrolysis, focusing mainly on the effect of concentration and operating temperature. By using polarization plots, voltage losses could be evaluated to see which condition was most efficient at producing hydrogen.

In order to create a fully renewable system, a photovoltaic panel was coupled with the methanol electrolyzer. This system shows the viability of using solar power to produce hydrogen that can then be stored and used in any process that requires hydrogen such as a fuel cell.

The next chapter of this paper goes into detail on the background and overall vision of this project. Chapter 3 then describes all the experimental setups that were used throughout the duration of this project, as well as the methods that were followed to perform experiments and acquire data. Next, Chapter 4 discusses the results that were gathered during the experiments that were performed. Chapter 5 goes over the conclusions and recommendations that resulted from the experiments. Finally, an appendix and references are provided to show further details on various parts of the project.

Chapter 2. Background and Vision

2.1. Energy Storage and Energy Vectors

There are a lot of different types of fuels being used for energy sources in the world today including fossil fuels such as coal, oil, and natural gas. Alternative energies such as solar panels, wind turbines, nuclear fusion and fuel cells are also becoming more widely used with today's increase in global climate awareness. One problem that has yet to be overcome, however, is energy storage (USDOE, 2013). The renewable sources such as wind and solar power, are intermittent, and peak generation, e.g., at midday, does not generally coincide with peak demand, generally in early evening. Electric power systems must match generation and demand in real time, with tight tolerances (EIA, 2011), as there is little storage capacity in the power grid. These demands are usually the lowest throughout the night and early morning hours because most people are asleep and many companies aren't in operation. Energy demands primarily peak around 6 p.m. when most citizens are awake and returning from work. At these peak demand-points in time, electricity is at its highest price and energy producers are at their highest stress. In order to account for these peaks, the energy demand is usually predicted or forecasted days in advance in order to help the energy producers account for these demands. Besides from having to be generated on demand with small margins of error, there are many other technical hoops to jump through to supply the current grid's energy demands.

The intermittent nature of these renewable sources, thus, calls for efficient, locally deployable, cost-effective, and reliable electrical energy storage (EES) systems that have the potential to become an integral part of the U.S. grid to make it more robust (USDOE, 2013). Thus, one scenario envisions as much as 20% of U.S. electric power generation from wind by 2030

(USDOE, 2008). The various alternate electrical energy storage (EES) technologies are mentioned in Figure 2.1, along with their estimated costs.

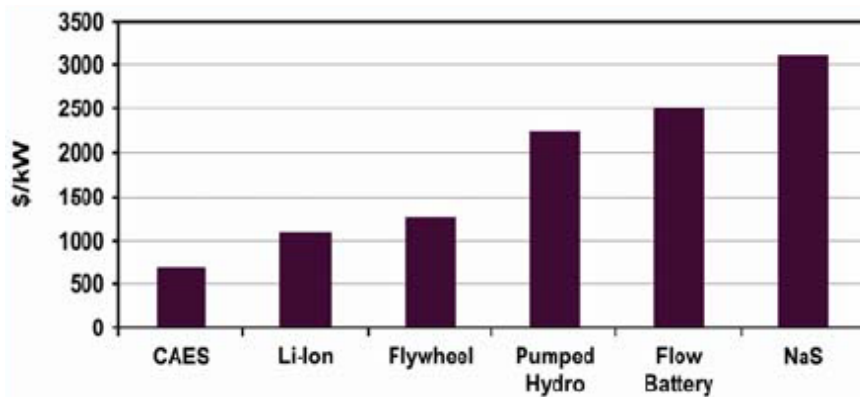


Figure 2.1. Current cost estimates for alternate electrical energy storage technologies (DOE, 2008).

Pumped hydro power is currently the most mature EES technology, but it is highly terrain specific. Thus, innovative new EES systems are needed. Electrochemical energy storage, including batteries (Dunn et al., 2011) and regenerative (reversible) fuel cells (Mitlitsky et al., 1998), is of the foremost interest. Examples include (Figure 2.2): 1) secondary batteries, i.e., the sodium-sulfur battery, the lead-acid battery, the Ni-Cd battery; 2) flow batteries such as the zinc bromine battery; and 3) regenerative H₂-O₂ proton-exchange membrane (PEM) fuel cells. However, none of these yet approach the cost and cycle life of pumped hydropower. For instance, the Zn-Br₂ cell has an energy density of ~50 Wh/kg, a cycle efficiency of ~70%, and a durability of 2,000 cycles.

An alternate possibility is to use regenerative fuel cells for electrolysis and store the excess grid energy as common gaseous and liquid fuels (Centi and Perathoner, 2011), which have much higher energy densities than batteries. An evident example is hydrogen produced from electrolysis of water. The volumetric and gravimetric energy densities of various chemicals are summarized in Figure 2.3.

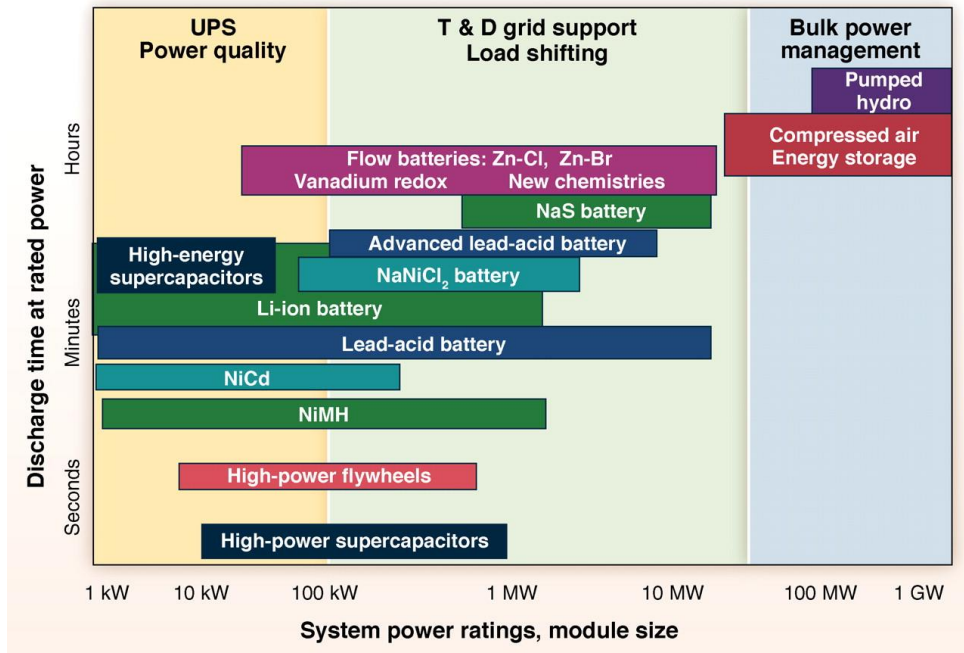


Figure 2.2. Discharge times and power ratings for different electrochemical energy storage technologies (Dunn et al., 2011).

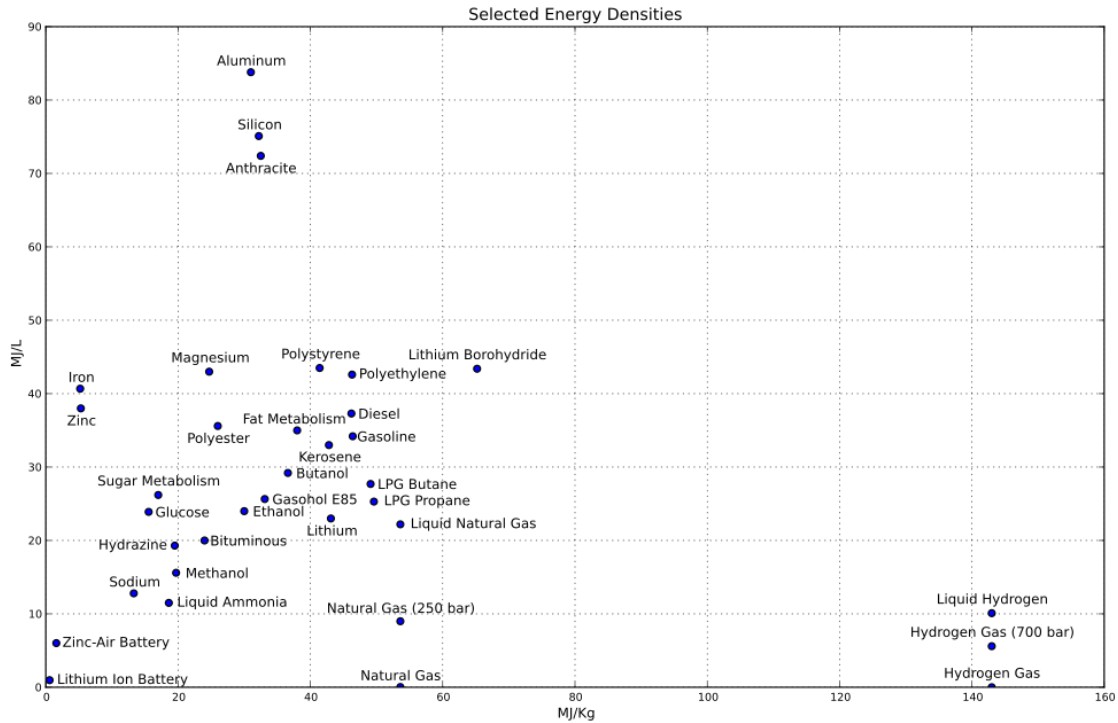


Figure 2.3. Volumetric versus gravimetric energy densities of selected chemical and batteries (Wikipedia, 2016).

2.2. Hydrogen Economy

The hydrogen economy (Bockris, 1975; Crabtree et al., 2004) is the idea that the conventional hydrocarbon fuels that exacerbate greenhouse gas emissions can be largely replaced with hydrogen. For example, hydrogen may be used as fuel for a fuel cell or to power a car instead of gasoline. Another possible use of hydrogen could be having a fuel cell in a home for power and heat. Using hydrogen for these tasks is beneficial because the combustion of hydrogen only produces water as a byproduct, instead of carbon dioxide and other emissions, ultimately making it a cleaner fuel.

One major problem with hydrogen, however, is that it is not naturally found on Earth in a usable form and has to be produced from another source. Further, as seen in Figure 2.3, hydrogen

has a very low volumetric energy density and cannot readily stored or transported. Fortunately, there are many hydrogen carriers that are abundant in the world including water, methanol, ethanol, biomass and methane. Methane may be considered as the most used hydrogen carrier. It is usually converted to hydrogen through steam reforming (Rostrup-Nielsen, 2005)



While steam reforming is currently the most efficient industrial scale method to make hydrogen, it is still not cheaper than using conventional fuels for energy. This is because of the high energy and capital costs of steam reforming and the relatively cheap cost of conventional fuels. Furthermore, a side product of steam reforming is CO₂, so that fossil methane contributes to greenhouse emissions.

Another method to produce hydrogen is through electrolysis. Electrolysis is where direct current is sent through a molecule to produce a chemical reaction. This is a particularly clean way to produce hydrogen on site when renewable electricity is used for electrolyzing water. However, it is not especially efficient, as it has a high thermodynamic potential requirement and large overpotentials, or potential losses, in particular at the oxygen electrode, where it produces pure oxygen as a side product. However, other hydrogen containing substances can be used in electrolysis, especially if they are sustainable. Electrolysis occurs in an electrolyzer and can allow for the separation of both gas products, such as hydrogen and oxygen for easy collection in water electrolysis.

In recent years methanol has been considered as a source of hydrogen via electrolysis (Sasikumar et al., 2008), and offers many advantages over water electrolysis. Methanol differs from water during electrolysis in the following main ways. One way is it needs a much lower amount of energy expended in the electrolysis step needed to break apart the molecule. The other

difference is that the electrolysis of methanol creates carbon dioxide gas instead of oxygen as a byproduct. In particular, if methanol could be produced from renewable resources such as biomass or by recycling anthropogenic CO₂, it could be an attractive energy vector, which can readily produce hydrogen via relatively efficient electrolysis. Finally, a molecule of methanol produces three molecules of hydrogen, one of these coming from a water molecule. Hydrogen produced can in turn be used in fuel cells to efficiently produce electrical energy on demand. Fuel cells provide energy using only hydrogen and oxygen from air with water as a byproduct. The current limiting factor for fuel cells is the low availability of hydrogen due to issues of storage and transportation of scalable quantities (Marbán, et al., 2007) and hence the need for onsite production (Brown, L. F., 2001)

As society becomes more Earth conscious about our carbon footprint as humans, we are moving more towards the idea of renewable and cleaner energy sources. Besides having to be generated on demand and creating pollution there is another downfall of oil and gas energy. The highest efficiency a gas turbine engine can achieve is around 60% and that is with the capturing of the heat it produces, while the electrical efficiency is only 30%. Solar panels and wind turbines also have low efficiencies and come with their own host of problems, but at least the source of energy is free and does not cause pollution. A key advantage is that when used as a fuel, hydrogen only gives off water and heat as byproducts. Hydrogen can be derived from abundant renewable resources, as opposed to finite fossil fuels. When paired with a renewable energy source, hydrogen can be used to produce clean and storable energy that is safe and will not harm the environment. Figure 2.4 schematically shows hydrogen as an energy vector used for storing solar electricity, and used to produce electricity on demand in a fuel cell.

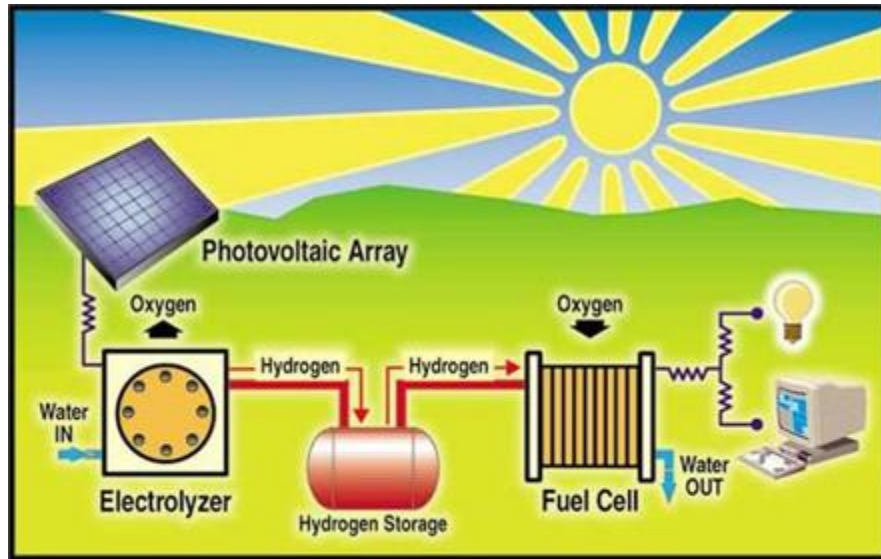


Figure 2.4. Solar derived hydrogen fuel for producing electricity on demand with a fuel cell.

Figure 2.4 depicts the overall role of a solar powered electrolyzer, and also displays the ability to store the hydrogen as well be able to call upon it in the future for later use. However, water electrolysis is inherently inefficient due to thermodynamic and kinetic reasons. On the other hand, by using other hydrogen carriers or fuels other than water in the electrolyzer, better efficiencies and outputs can be generated.

2.3 Hydrogen Generation

Since hydrogen does not occur in nature in uncombined form, in order to use hydrogen as an energy vector, it has to be produced from another fuel or energy source. There are many alternate ways to produce hydrogen as shown in Figure 2.5 (Florida Solar Energy Center).

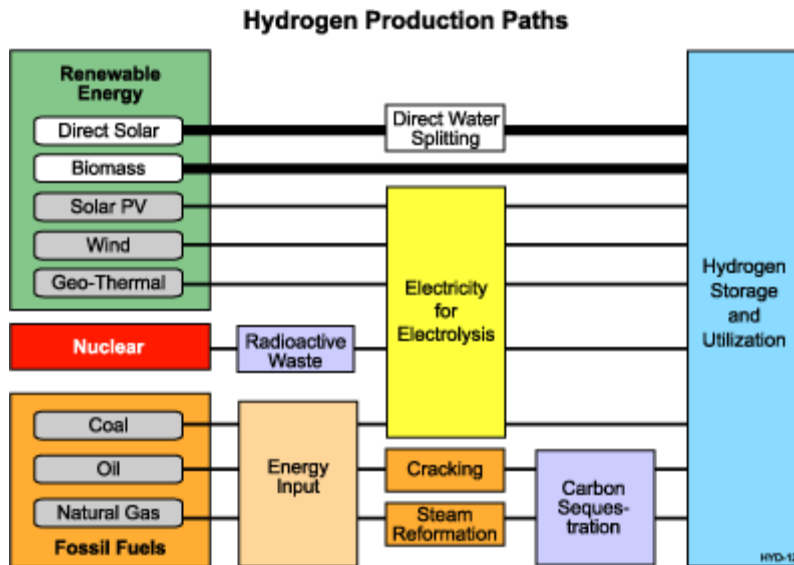


Figure 2.5. Alternate pathways to produce hydrogen from renewable, nuclear, and fossil resources (Florida Solar Energy Center).

The two main methods of hydrogen production are steam reforming and electrolysis. Steam reforming is currently the most common industrial method of generating hydrogen from another fuel, typically methane, which accounts for about 95% (US DOE, 2004) of all hydrogen production. Electrolysis is the use of electrical energy in order to split apart a molecule into hydrogen and the compound's counterpart, e.g., oxygen in the case of water. Electrolysis is typically done with water, but can be done with other alcohols such as methanol, ethanol, and glycerol (Lucas-Consuegra et al., 2014 & Lamy, C et al., 2014). The problem with many of the pathways to produce hydrogen is the sheer amount of energy that must be expended in order to generate hydrogen, and whether there is generation of CO₂ in the process.

2.3.1 Steam Reforming

Steam reforming of methane above 700 °C is currently the most commonly used industrial method of hydrogen production (Rostrup-Nielsen and Rostrup-Nielsen, 2002) because it is the most economical method for large-scale production (Figure 2.6). Hydrogen is used in large

quantities in the upgrading of fuels (hydrotreating) in a refinery, and in the production of ammonia and methanol. The worldwide total production of hydrogen in 1998 was 500 billion Nm³/y. (Elam, C. 2001)

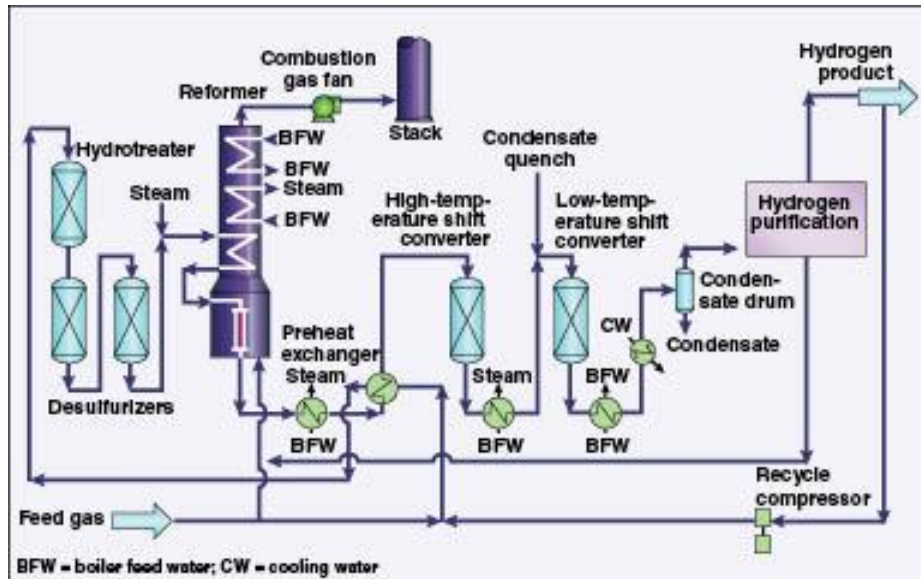
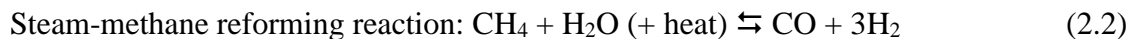


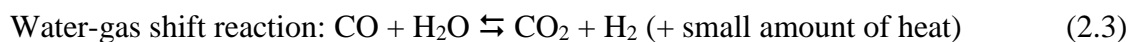
Figure 2.6. A typical steam reforming diagram (Gumilar, 2010).

The first step of steam reforming, after desulfurization, involves reacting methane with steam at temperatures between 750 and 1000 °C to make syngas, which is a mix of hydrogen, carbon monoxide, and some carbon dioxide. The equation for this reaction is:



This is a reversible reaction that is highly endothermic and so it must be carried out at very high temperatures to promote thermodynamics as well as kinetics.

The next step in the process is the water gas shift reaction where carbon monoxide resulting from the first step is reacted further with steam to form hydrogen and carbon dioxide:



The gas is then scrubbed to remove impurities such as sulfur and chloride. Finally the gas is separated from the CO₂ and traces of CO via methanation to make it pure hydrogen. (NYSERDA,

2005) As Figure 2.6 shows there are many different unit operations that are needed in order to create hydrogen via steam reformation. Because of this, creating hydrogen with this method proves to be costly and energy intensive. In order to produce one cubic meter of hydrogen, 0.46 cubic meters of methane must be reformed. The energy requirement of steam reforming in ideal circumstances is 0.78 kWh/Nm³ of H₂ production, but in actual processes, it is 2-2.5 kWh/Nm³. The cost of producing hydrogen is about three times the cost of the methane that is used to create it. (Florida Solar Energy Center, 2007) Including the utilities, annuity, maintenance, interest rates, and water costs, when generating 50 cubic meters/hour of H₂, it would cost \$0.3 million/year (Stoll, R. E. 2000). The total investment to build a small scale plant (10.6 lb/hr H₂ production) is estimated at \$0.39 million and for a large scale plant (101,885 lb/hr H₂ production) the estimated cost is \$368.5 million (Office of Energy Efficiency & Renewable Energy, 2006) Even though hydrogen generation in large-scale industrial facilities such as those described above is routine, transportation and storage of hydrogen for distributed applications is challenging due to the light nature of hydrogen. Thus, as shown in Figure 2.7, very high pressures are required to store enough hydrogen on board a fuel cell driven vehicle to go 300 miles between refills. Other hydrogen storage options are compared in Figure 2.8.



Figure 2.7. Tank volumes for various storage options for 4 kg of hydrogen on board a car (Schlapbach and Züttel, 2001).

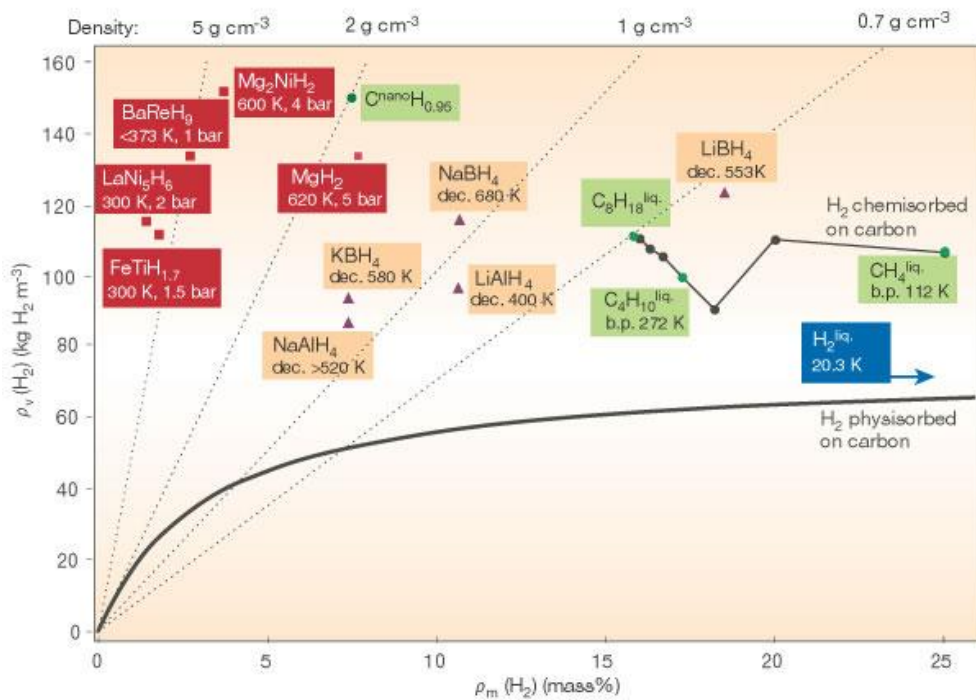


Figure 2.8. Comparison of various hydrogen storage options (Schlapbach and Züttel, 2001).

Given the storage challenges of hydrogen, the best option is to generate hydrogen on demand locally.

2.3.2 Hydrogen from Electrolysis

Steam reforming is not the most ideal method for smaller-scale onsite hydrogen production however. This is because of the necessary carbon monoxide removal as well as the startup times of the reformers. Steam reforming also requires large pieces of equipment, meaning large starting capital needed, and large amounts of energy needed to produce hydrogen. Electrolysis, on the other hand, is much better for on-site and instantaneous hydrogen production because it doesn't have much of a startup time. With electrolysis hydrogen can be produced with less parts and energy being put into the system. In addition, electrolysis also produces very pure carbon-free hydrogen gas (99.999%), which is much better for use in fuel cells because it reduces the amount of impurities in the system, leading to longer system life (Hydrogenics, 2013). Electrolyzers also have the ability to pressurize hydrogen without the need of a compressor. There are two different low temperature ways to create hydrogen through electrolysis (Hydrogenics, 2013). These two are through Alkaline and Proton Exchange Membrane (PEM) electrolysis. In alkaline electrolysis an alkaline water solution is created with either NaOH or KOH and does not use a PEM, and for PEM electrolysis water and/or alcohols can be used.

The main components of a PEM electrolytic cell are the anode, cathode, membrane, gas diffusion layers, and flow channel plates. In both the anode and cathode there is a catalyst made of a precious metal, normally platinum, which is usually coated on the gas diffusion layer of each side. This platinum is often supported with carbon or Ru, but can also be Pd, Ir, or other platinum group metals. A basic electrolytic cell is shown in the Figure 2.9.

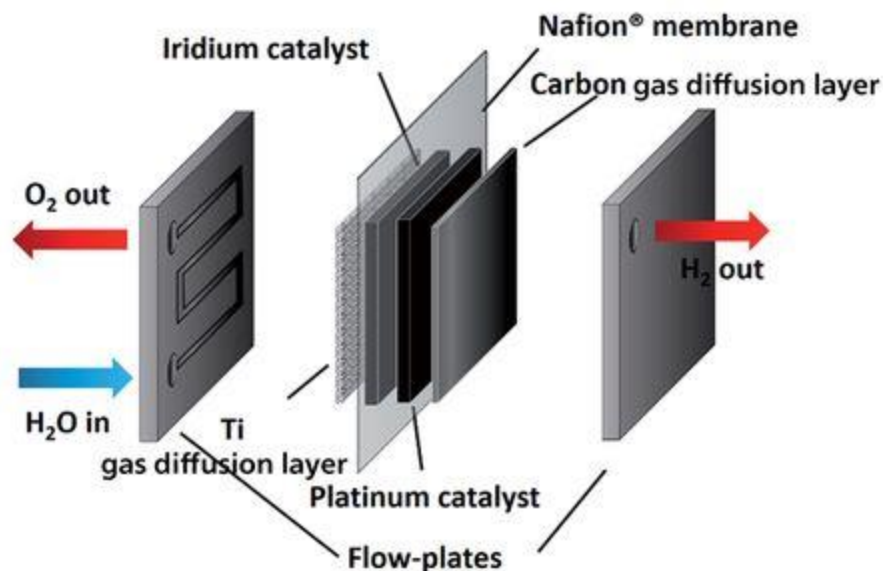


Figure 2.9. A typical electrolyzer cell.

The most common method for electrolysis is with water, however alcohols such as methanol, provide advantages that cannot be found by using water. When using water as the feed for electrolysis, the water goes to the anode and is oxidized to produce oxygen, hydrogen, and protons, as described in the equation below

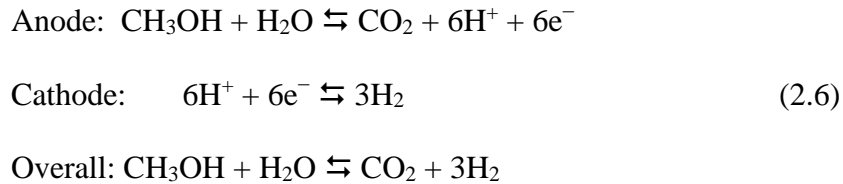


The oxygen is disposed to the atmosphere as the proton travels through the membrane to the cathode, as the electrons are passed through an external circuit. The protons then react with the electrons at the anode, which is shown in equation 2.5:



This process is similar to the electrolysis of methanol. In it, the methanol is split into carbon dioxide at the anode. As in the water electrolytic cell, the protons travel through the membrane, and the electrons through an external circuit to react at the cathode to produce hydrogen. The

equations at the anode, cathode, and the overall equation for the electrolysis of methanol are: (Take, et al. 2007)



One of the largest advantages of using methanol instead of water for hydrogen production is the operating voltage required for electrolysis. In the case of water electrolysis, 1.23V are required while methanol only needs 0.02V (Mazloomi, et al 2012). This saves a lot of power and makes the methanol more efficient and more competitive than other fuels. Hydrogen produced via methanol electrolysis is estimated to be 50% cheaper than water electrolysis, even after including the cost of methanol. (Uhm et al, 2012). While methanol electrolysis produces CO₂ as a byproduct, it is a relatively small amount, is concentrated to one area of the cell, and is therefore may be captured and sequestered.

2.4 Electrolyzer Anatomy

The basic components of the electrolyzer are the membrane, the catalyst, gas diffusion layer, and the bipolar plates (Figure 2.9). Fusing together the catalyst and the membrane results in the so-called membrane electrolyte assembly, or MEA. In the center of the MEA is the proton-exchange membrane. Sandwiching the membrane are the catalysts, which are embedded in the anode and cathode. By having these layers together, a three-phase contact is formed among the gases, membrane, and catalyst. This is the point where the reaction occurs, and the hydrogen is produced. There are a few different ways of assembling the MEA's as well. The most common method of assembly starts with a technique known as catalyst coated substrates by direct spray, which is then hot pressed. This method is used for mass produced MEA's and large MEA's as it

is the easiest method of manufacturing in this method, the catalyst ink is coated onto the diffusion media and then pressed into a polymer membrane. A disadvantage to catalyst coated substrates is that excess catalyst can be absorbed by the carbon cloth used in the MEA. This excess catalyst will then be wasted when the layers are hot pressed together. (Thanasilp, S., & Hunsom, M. 2010). Other techniques include catalyst coated membrane by direct spray or decal transfer. In catalyst coated membranes the catalyst ink is coated directly onto the membrane, and in decal transfer, the electrodes are temporarily put onto a film such as Teflon and then hot pressed onto the membrane. The catalyst coated membrane method performs the best out of the three and catalyst coated substrate performs the worst, however it is currently the easiest method and involves the least amount of steps. (Koraishy, et al. 2009)

2.4.1 Membrane

A common membrane that is used in both electrolyzers and PEM fuel cells is Nafion[®]. Nafion[®] is a polymer that was developed by DuPont and NASA during the 1960's. Nafion[®] is very well known for its proton transfer abilities as well as being extremely chemically and thermally resistant. Nafion[®] is a copolymer of tetrafluoroethylene, also known as Teflon, and perfluoro-3,6-dioxa-4-methyl-7-octene-sulfonic acid. The Teflon portion of the polymer adds chemical resistance, while the sulfonic acid portion adds the ability to absorb water as well as transfer protons across the membrane (Perma Pure.n.d.). Nafion[®] membranes come in different thicknesses and can have different characteristics. The name of a membrane is usually based off of its thickness. For example Nafion[®] 117 is 183 microns (.007 inches thick), Nafion[®] 115 is 127 microns (.005 inches thick), and Nafion[®] 212 is 51 microns (.002 inches thick) (Fuel Cell Etc., n.d.). Another style of Nafion[®] membrane is Nafion[®] XL. This membrane is chemically cross

linked which provides mechanical reinforcement for a longer operating life, while still being half the thickness of a Nafion[®] 212 membrane. Below is a picture of an MEA with a Nafion[®] membrane that has two catalyst coated carbon gas diffusion layers hot-pressed onto it.

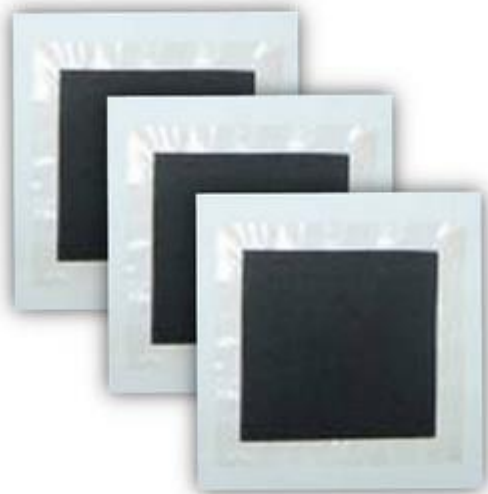


Figure 2.10. Nafion[®] Membranes with Carbon Cloth GDL.

Because Nafion[®] has a Teflon backbone, it displays some of its hydrophobic qualities and keeps water away from the electrodes. However, the Nafion[®] also has sulfonated side chains that are hydrophilic and attract water. The side chains are not as strong as the hydrophobic chains. Because of this, the water that is attracted to the side chains cannot go through the membrane, however the protons that are attracted can. Nafion[®] is one of the great proton exchange membranes, because it limits the amount of water crossover and promotes proton exchange.

The membrane has to have a balance of the amount of liquid in it, or else it will flood. The flooding then causes the three phase contact sites to be blocked which leads to mass transfer limitations, limiting the ability of the cell to operate. As protons move through the membrane, water molecules can be dragged with them through a phenomenon known as electro-osmotic drag. This can cause one side of the cell to dry out while the other is still hydrated. The cell may also

not hydrate evenly, which will cause additional problems within the cell. (Larminie, J., & Dicks, A., 2003).

2.4.2 Catalyst

The catalysts for electrolyzers are typically made with Pt supported on carbon and Pt supported on Ru. Other catalysts are used, however these are the most common. These catalysts come at different loadings, depending on what characteristics and lifespan are desired. Platinum is used because it increases the rate at which the methanol can be electrolyzed. It is supported on carbon so that there is a higher surface area. This allows for more active sites for reactions to occur. Ru is used as a catalyst on the anode to stop carbon monoxide poisoning that can be caused during the methanol oxidation. When the methanol is oxidized, carbon monoxide can be absorbed onto the Pt catalyst and reduce cell performance. By having Ru, water is oxidized which then oxidizes the CO to make CO₂ (Pham, A. et al., 2013). Carbon Monoxide poisoning can be a very large cause of problems within a cell and limiting as much CO production as possible is extremely important.

2.4.3 Gas Diffusion Layer

Another part of the cell is the gas diffusion layer. This layer is located on the outside of the catalysts. The gas diffusion layer (GDL) helps pass the reactants to the catalyst and also removes the product on the other side of the cell. The GDL is typically made of a carbon paper or carbon cloth, and can have PTFE as well as a hydrophobic component. The gas will diffuse through the carbon paper because it is a porous material. There is also sometimes a microporous layer, which consists of a high surface area carbon and PTFE to balance water levels in the layer. Balancing the water level in the cell is a very important aspect in improving the performance and longevity of

the cell and the hydrophobic and hydrophilic regions of the GDL help prevent the cell from flooding or dehydrating. (Yu, S., et al 2013)

2.4.4 Bipolar Plates

The outermost layer of the cell are the bipolar plates. The plates allow the reactants to reach their respective electrodes. These plates are used as a current collector and provides an electrical conduction between the cell. A flow field will be made in the plates to allow for the gases and liquids to move through the cell and over the membrane. The thickness of the plate also contributes to the resistance in the cell. These plates are made from materials such as carbon, metals, or composites. Graphite composite plates are beneficial because they have a high corrosion resistance and good surface contact resistance. The downsides of this material however is that it does not have as good manufacturability, permeability, or shock and vibration resistance as metal plates do. Metal plates corrode more than graphite and t have a passive layer that reduces contact resistance and possible fouling of the ionomer and catalyst. (Tawfik, et al, 2007) Contrary to intuition rougher surface topography, to a degree, bipolar plats actually give lower surface resistance and there for yield lower resistance across the cell. (Avasarala, B., & Haldar, P. 2009).

2.5 Cell Polarization

A polarization curve plots current density vs voltage, as shown in Figure 2.10 (Datta et al., 2015), which also schematically provides the various overpotential losses in the different components of the electrolyzer. It is seen that the oxygen electrode has the largest losses associate with it. This is an issue with water electrolysis, as oxygen evolution in a PEM water electrolyzer produces a side product often just discarded. Further, it is seen that the thermodynamic voltage of water electrolysis is high, i.e., 1.23 V.

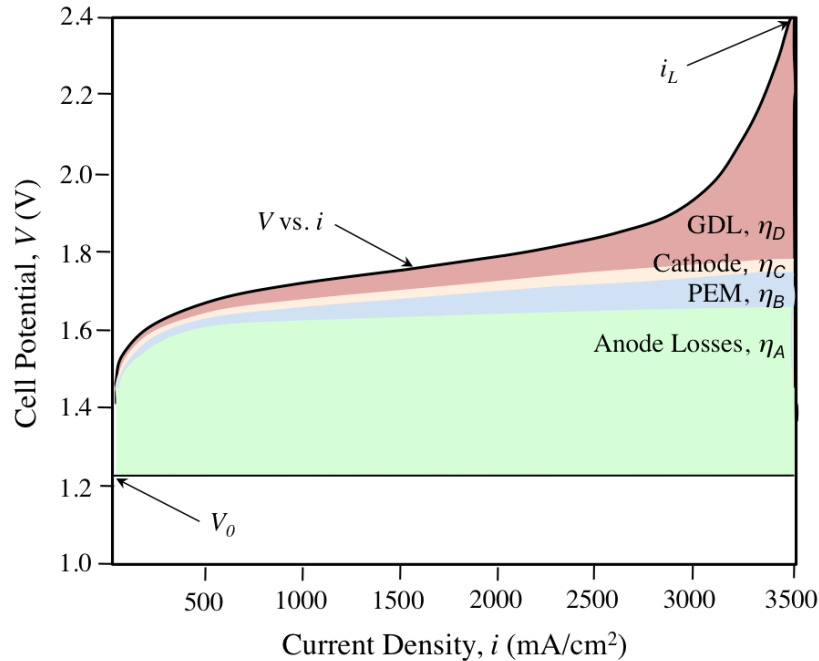


Figure 2.11. A schematic polarization plot and the various overpotentials within the PEM-water electrolyzer (Datta et al., 2015).

Such curves can be used to evaluate the performance of an electrolytic cell. The curve represents the power per active square centimeter that is needed to generate hydrogen. When comparing an electrolyzer polarization curve and a fuel cell polarization curve, you will see that they display opposite trends, which is expected since they perform opposite duties. The lower the cell voltage at a given current density, the better the electrolyzer. This is because the electrolytic cell will need less overall driving force at a set current. The increases of voltages on the cell are typically caused by Ohmic losses, activation losses, and mass transport losses (Figure 2.10). Ohmic losses are due to resistance by the internal parts of the cell. This loss of energy is normally caused by heat, and then requires more voltage to make up for the loss. Ohmic losses can also be caused by the different resistances of the materials that are used in the makeup of the cell. Activation losses, account for the energy that is required to transfer an electron to from the anode. At low

currents, the reaction has to be forced to completion and this takes additional energy. (Rayment intro to fuel cells) Mass transport losses are caused by the membrane not being able to diffuse everything through it at once. With more mass coming into the system at the same time the membrane will essentially become clogged and a loss in performance will occur. When comparing the polarization plot from a water electrolyzer and a methanol electrolyzer, it is clear that the methanol electrolyzer is much more efficient.

The electrolyzer polarization plot can be modeled via (Datta et al. 2015)

$$V = V_0 + \frac{RT}{\beta_A \nu_{Ae}^* F} \sinh^{-1} \left\{ \frac{1}{2} \left(\frac{i/i_{A,0}}{1 - i/i_{A,L}} \right) \right\} - \frac{RT}{\beta_C \nu_{Ce}^* F} \sinh^{-1} \left\{ \frac{1}{2} \left(\frac{i/i_{C,0}}{1 - i/i_{C,L}} \right) \right\} + i \left(\frac{L_B}{\sigma_B} \right) \quad (2.7)$$

where V is the cell voltage, i is the current density, V_0 is the thermodynamic potential (1.23 for water electrolysis), β_A is the symmetry factor while ν_{Ae}^* is the stoichiometric coefficient of electrons in the rate-determining step of the electrode reaction, $i_{A,0}$ is the exchange current density for the anode, and $i_{A,L}$ is limiting current density for the anode. The corresponding quantities for the cathode are distinguished by the subscript C replacing the subscript A for anode. Further, σ_B is the conductivity of the membrane and L_B is its thickness.

A comparison of the theoretical model with experiments for PEM water electrolysis (PEM-WE) is shown in Figure 2.12.

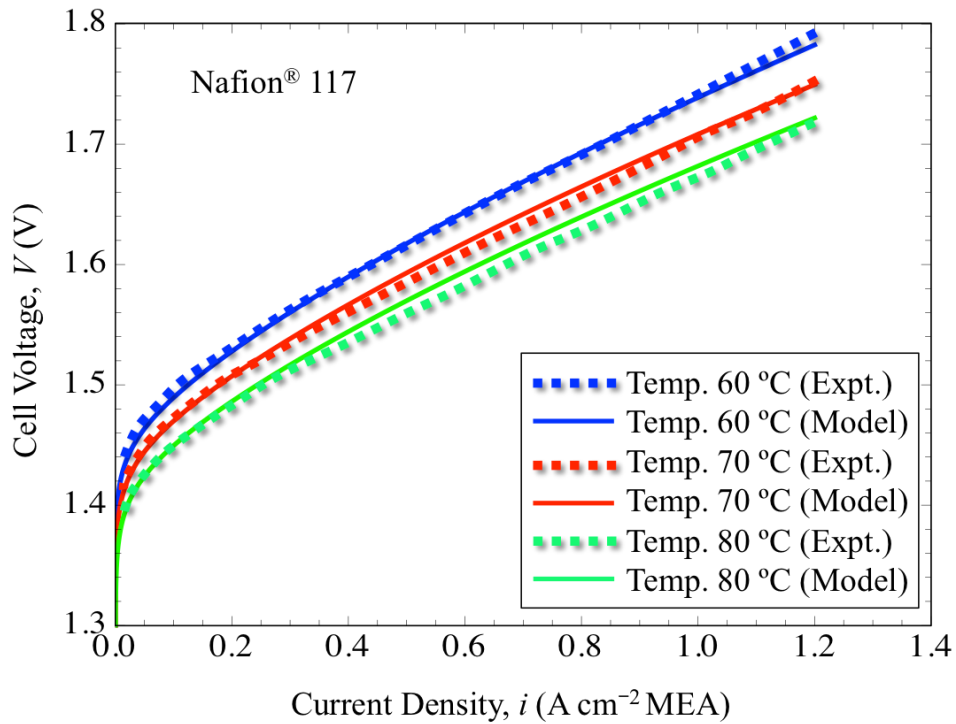


Figure 2.12 Comparison of prediction with experiments for polarization plot of a PEM-WE based on Nafion® 117 at different temperatures.

2.6 Degradation

Degradation of the Electrolyzer components is one of the biggest obstacles to electrolysis becoming more viable. There are many ways that degradation occurs, including thermal, chemical, and physical manners. Defects can occur during the manufacturing process that can lead to an increase in degradation. These defects include small tears, foreign objects getting in the parts, or cracks forming. When the system is run outside of its operating conditions, then the parts can fail as well.

2.6.1 Membrane degradation

One of the main causes of electrolyzer failure is degradation to the membrane. Extreme conditions such as high temperature and methanol concentration can cause degradation. Nafion

begins to lose its thermal resistance above 80 °C and then more so above 150 °C. Studies have shown that degradation begins at the ends of the chains, and the Nafion loses fluoride ions as well as repeat units.(Tang, 2007) The loss of these units is thought to be caused by radicals such as OH and OOH. Degradation of the membrane can also occur due to mechanical failure. For example tears can form where the membrane meets the flow field channels when the membrane is pressed together. Also if any debris is in the assembly, tears can be formed. (Tang, 2007)

2.6.2 Catalyst Degradation

Degradation of the catalysts is another problem that is faced by electrolyzers. One way that the catalyst can be degraded is by dissolution of the platinum. The Pt particles are then deposited in the cathode. The particles can also be diffused into the membrane (Bi, W., & Fuller, T. F, 2008).. A high voltage also leads to Pt degradation. The Pt particles then diffuse into the membrane and form a Pt band. These particles change the molecular makeup of whatever it is deposited on, and affects performance of the cell. High temperatures, low pH, and other side reactions also cause Pt degradation in the cell. These failures can be caused by faults in the Pt while it is being manufactured before it is out in the cell. Additionally Ruthenium also degrades in the cell. The Ru degrades from the anode and is then deposited on the cathode.

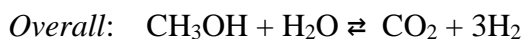
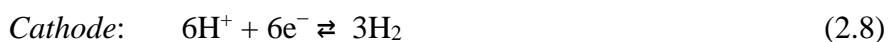
2.6.3 Gas Diffusion Layer Degradation

Performance of electrolyzers is also affected by the degradation of the GDL. As degradation occurs in the GDL, the hydrophobicity decreases, allowing water to move through easier. This decreases the performance of the cell greatly. (Yu, et al. 2008) The loss of hydrophobicity of the GDL increases the mass transfer limitations, and increases voltage losses.

2.7 Methanol Electrolysis Literature Review

Electrolysis is the electrochemical process of using direct current to drive an endergonic chemical reaction. The opposite reaction that occurs in fuels cells, where chemical combination reactions drive a direct current. On the molecular level, in a PEM electrolyzer cell, protons and electrons are produced at one electrode, the protons pass through the membrane while the electrons are directed to the outer circuit, and arrive at the opposite electrode to recombine with electrons and other species and protons to form molecules. In methanol electrolysis, the protons are hydrated 'H⁺' ions, that recombine with other protons and electrons supplied by the direct current applied to the cell to produce hydrogen.

Despite the existence of an early US patent describing hydrogen being produced from the electrolysis of aqueous organic solutions in 2001 (Narayanan et al. 2001), there are only a handful of technical reports on methanol electrolysis (Jeffries-Nakamura et al., 2002; Narayanan et al., 2002; Take et al., 2007; Hu et al., 2007; Sasikumar et al., 2008; Cloutier and Wilkinson, 2010; Uhm et al., 2012; Guenot et al., 2015; Lamy et al., 2015a). The electrode and overall reactions that govern methanol electrolysis are (Take et al. 2007)



Note that the overall reaction is comprised of two half-cell reactions, representing the anode and cathode, which are the two electrocatalyst sides of the electrolysis cell separated by the membrane. At the anode (positive pole of the electrolysis cell, where the electrons are produced), methanol is oxidized on the anode catalyst (usually Pt–Ru/C), producing carbon dioxide and protons. Then, the protons, after crossing through the proton-exchange membrane (PEM) which precludes

electrons, reach the cathode side (the negative pole of the electrolysis cell, where the electrons are consumed) where they are reduced, with electrons provided by the DC power, to molecular hydrogen (H_2), on the Pt/C or PtB catalyst (Guenot et al. 2015). A schematic of the methanol electrolyzer is provided in Figure 2.13 (Jefferies-Nakamura et al., 2002). This is similar to the setup that is described in Chapter 3, where CO_2 produced at the anode is collected in a reservoir/separator with unconverted methanol recirculating with a pump and separated in the reservoir and released at a desired pressure with a back-pressure regulator.

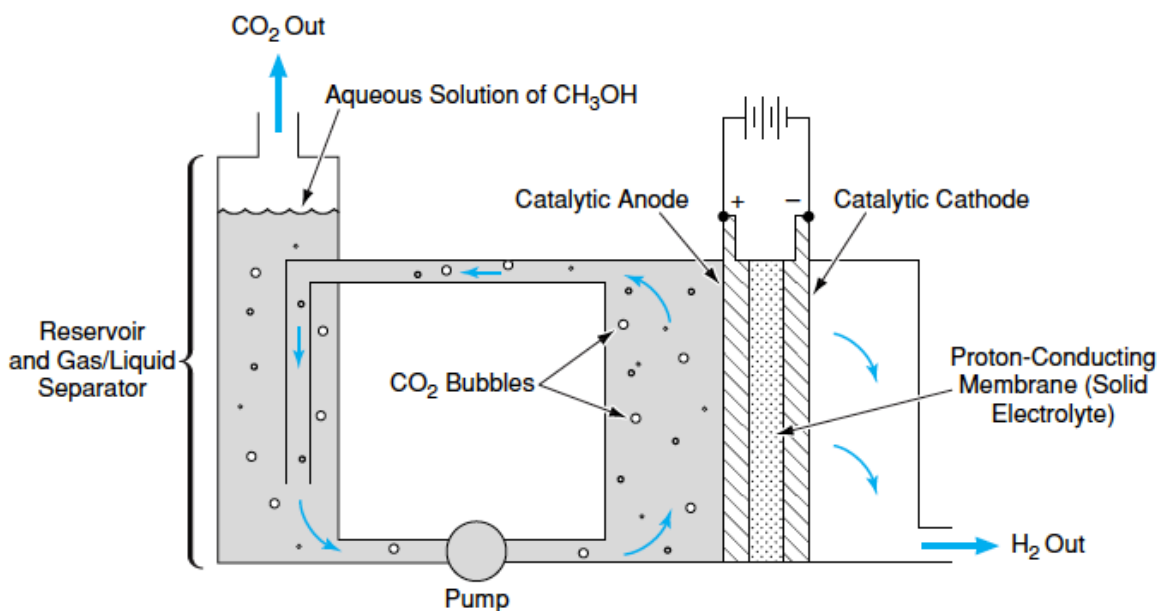


Figure. 2.13. Schematic of methanol electrolyzer developed by NASA's Jet Propulsion Laboratory (Jefferies-Nakamura et al., 2002).

2.7.1 Methanol Electrolyzer Performance

The state-of-the-art MEA for methanol electrolyzer comprises of a 2-4 mg/cm^2 Pt-Ru/C anode, 0.5-2 mg/cm^2 Pt/C, or Pt black, cathode, and Nafion[®] 117 as the PEM, along with carbon paper as the GDL. The voltage vs. the current density at 90 °C for a 2 M methanol feed is shown

in Figure 2.15 for 2.5 mg/cm² Pt-Ru/C anode, 1.5 mg/cm² Pt/C cathode, as well as a tungsten carbide promoted Pt (Pt-WC/C) cathode (Hu et al., 2007).

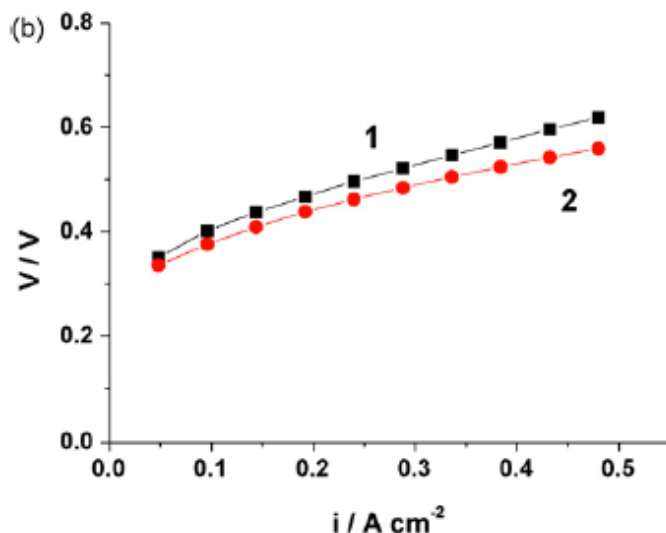


Figure 2.14. Polarization plots at 90 °C for a 2 M methanol feed for 2.5 mg/cm² Pt-Ru/C anode, and 1.5 mg/cm² Pt/C (1), and Pt-WC/C (2) cathode (Hu et al., 2007).

Initially, there is a sharp increase in voltage due to activation overpotential of the methanol oxidation reaction (MOR), followed by a more gradual increase, in accordance with the Butler-Volmer equation. It is, further, noteworthy that the cell potential is low enough even for the possibility of using solar cells to power it (Jeffries-Nakamura et al., 2002; Hu et al., 2007). Alternately, it may use a part of the energy produced by a subsequent H₂ fueled PEM fuel cell. The MEA with Pt-WC/C cathode gives a somewhat better performance (Figure 2.14). Further, Hu et al. (2007) found that increasing the methanol concentration higher than 2 M had only a small effect on the potential. On the other hand, at concentrations less than 1 M, there is a step increase in polarization at higher current densities, and sometimes instability, when methanol becomes depleted and water electrolysis is needed to maintain a current. On the other hand, Take et al.

(2007) used Pt for both anode and cathode, with the result that their cell voltages were high (> 1.0 V). They also found that the cell performance was insensitive to methanol concentration.

Cloutier and Wilkinson (2010), investigated acidified methanol electrolysis in a batch mode using a two-compartment Pyrex[®] glass cells as anode and cathode chambers, rather than the usual flow-through chambers, with an MEA based on Nafion[®] 117 and 4 mg/cm^2 Pt-Ru/C anode and a 2 mg/cm^2 Pt black cathode, and sandwiched in between. They determined anodic and cathodic voltages using the standard hydrogen electrode (SHE) as a reference electrode. They found that the anode overpotential due to MOR is dominant, while the cathodes overpotential is relatively small, indicating little MOR occurring at the cathode from the methanol crossing over. In fact, higher methanol concentrations appear to reduce anode overpotential.

2.7.2 Methanol Electrolyzer Application Potential

Methanol electrolysis can be more attractive than water electrolysis mainly because of the significantly larger electricity power requirement for water electrolysis (Hu et al., 2007), in addition to potential cheaper and more durable components because of its lower operating potentials. Despite the limited literature and experimental work reported in the literature so far, researchers have already discussed its superiority to water electrolysis, and speculate about its potential applications.

Some of the advantages of methanol electrolysis as compared to water-alkaline electrolysis, are low ecological impact, and increased safety, because of the lack of oxygen produced by the reaction, as it is in water electrolysis (Grigoriev, 2006). As a further advantage, the cost of production of hydrogen from methanol, including the cost of buying the methanol and the power required, is less than half that of water electrolysis (Jeffries-Nakamura et al., 2002). A comparison of the power requirement of water and methanol electrolysis is evident in the

polarization plot for the two shown in Figure 2.15 (Uhm et al., 2012). One disadvantage is that methanol is currently derived from fossil resources, mainly natural gas. Eventually, of course, it may be possible to produce methanol from recycled CO₂, as described in Chapter 1, making it a sustainable process.

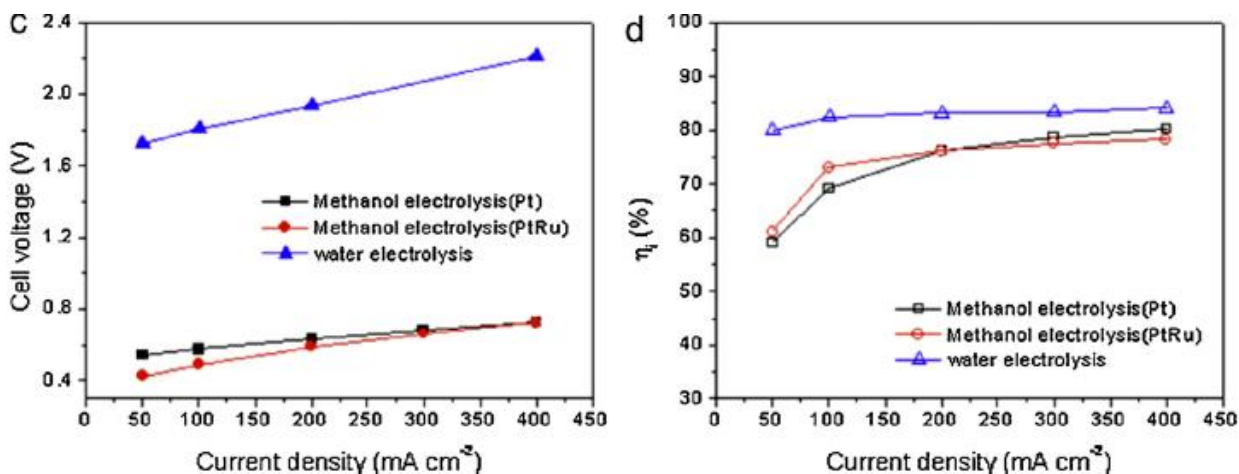


Figure 2.15. A comparison of the polarization and current efficiency of methanol and water electrolysis (Uhm et al., 2012).

The relatively low operating potentials in methanol electrolyzer (Figures 2.14 and 2.15) can be very beneficial as at higher potentials Ru can dissolve ($\text{Ru} \rightleftharpoons \text{Ru}^{2+} + 2\text{e}^-$) and can be leached from the anode catalyst. At even higher voltages (>1.8 V), carbon support corrosion ($\text{C} + 2\text{H}_2\text{O} \rightleftharpoons \text{CO}_2 + 4\text{H}^+ + 4\text{e}^-$) can occur. Clearly absence of higher voltages in a methanol electrolyzer as compared with water electrolyzer means that the methanol electrolyzer durability is longer, and cheaper catalysts and GDLs can be employed. The PEM water electrolyzer (Grigoriev et al., 2006) is typically based on the Nafion[®] 115 or 117 membrane, flanked on either side by porous electrodes comprising a gas diffusion electrode (sintered porous titanium at the anode and/or porous graphite at the cathode), and with Pt-B or Pt/C cathode and Ir-B-based anode (Datta et al., 2015).

Even with the additional cost of producing methanol, estimates are that it is between 50% less costly per unit volumetric production of hydrogen gas and roughly 70% less in energy costs vs. pure water electrolysis (Tuomi et al, 2014). Figure 2.15 illustrates this point with the large difference in voltage (V) needed to ultimately drive the reaction, the rate of which is proportional to current, since two electrons are needed for every H₂ molecule produced. Thus, the volume of generated hydrogen is a linear function of the electrolysis time and current intensity, i.e., of the quantity of electricity involved in the electrochemical process according to Faraday's law (Guenot et al. 2015) and therefore the more the current passed through the cell, the more electrolysis takes place and more fuel is reacted. The higher the voltage requirement for a given current (Figure 2.15), the larger the power requirement is, as power is simply the product of voltage and current. Polarization plots as in Figure 2.14 and 2.15 are an important tool for evaluating the performance of a cell because the current density correlates with the hydrogen production and the voltage is marker of the power requirement.

Hydrogen production by electrolysis of a methanol water mixture consumes approximately 1.89 kWh (kiloWatt hour) per standard (normal) cubic meter (Nm⁻³), which is much less than that required for water electrolysis. The energy consumption of commercial water electrolyzers (4.5-5 kWh Nm⁻³) (Sethu et al., 2014) compared with methanol electrolysis (2.03 kWh Nm⁻³) (Sasikumar et al., 2008) is clearly less energy intensive. From the calculations of Sethu et al. (2014), the energy required for methanol electrolysis is 42% of the energy required per Nm⁻³ of hydrogen produced, vs. commercial water electrolysis. Others have achieved even lower energy consumption, 1.2 kWh Nm⁻³ operating at 0.55 V, which is roughly less than a quarter of the electrical demand for commercial water electrolysis (Guenot et al. 2015).

The safety of methanol electrolysis is also attractive. Methanol electrolysis produces hydrogen gas and carbon dioxide, whereas water electrolysis produces hydrogen and oxygen. The potential safety hazard is of their mixing, as hydrogen and oxygen are the main components in the rocket fuel. These gases, when exposed to an ignition source, react explosively to form water. A down side to methanol electrolysis is that methanol is poisonous to humans and the majority of it is currently manufactured from nonrenewable fossil fuels. These negatives are, however, overcome by the lower cost and energy required to electrolyze and potential green energy advantages.

2.7.3 Optimizing Operating Conditions and Electrolyzer Design

In spite of increased recent research activity in methanol electrolysis, much work remains to be done to design and develop a high performance membrane-electrode assembly (MEA) for methanol electrolysis that is low cost and durable, and to optimize the operating conditions in terms of methanol concentration and operating temperature. These aspects are discussed in further detail below. In recent research, specifically by Sasikumar et al. (2008), and later by Uhm et al. (2012) as well as by Guenot et al. (2015) and Lamy et al. (2015a), experiments were conducted to optimize operating conditions for methanol electrolysis. Temperature, methanol concentration and MEA (Membrane Electrode Assembly) membrane thickness were varied and performance investigated. There have been several more experimental studies conducted on these topics. Separated in different sections below are provided the salient literature results on these aspects of methanol electrolyzer operation and design.

2.7.4 Effect of Temperature on Methanol Electrolysis Performance

In much of the literature, operating temperature typically ranges from 20 °C (~room temperature) to 80 °C for methanol electrolysis. The working temperature has a great effect on

performance and energy consumption (Guenot et al. 2015), because the governing reaction in methanol electrolysis is the methanol oxidation reaction (MOR), where the rate of reaction is increased as the temperature is increased, as per Arrhenius equation for the rate constant. This has been shown recently in papers by Uhm et al. 2012 as well as Guenot et al. 2015. In fact, the rate constants of the electrochemical reactions are not only determined by temperature, as given by Arrhenius equation, but also by overpotential η_ρ , as described by the Butler-Volmer equation

$$k_\rho = A_\rho \exp\left(-\frac{E_{\rho,\Phi_0}}{RT}\right) \exp\left(\frac{\alpha_\rho F \eta_\rho}{RT}\right) \quad (2.9)$$

so that at a higher temperature of operation, lower overpotential are required for a given rate of reaction or current density. An electrocatalytic activation energy for MOR $E_{\rho,\Phi_0} = 50 - 60 \text{ kJ mol}^{-1}$ (Guenot et al., 2015), which means that kinetics are significantly improved with higher operating temperatures at the anode. Of course, a key advantage of methanol electrolysis is that the thermodynamic potential for the process is very low as compared to that for water electrolysis, although overpotential η_ρ for MOR must still be sacrificed at the anode. However, the overpotential for the hydrogen evolution reaction at the cathode is very small. Sasikumar et al. (2008) had also earlier found that increasing the temperature reduced the voltage needed for a given current density or hydrogen production rate, as shown in Figure 2.16.

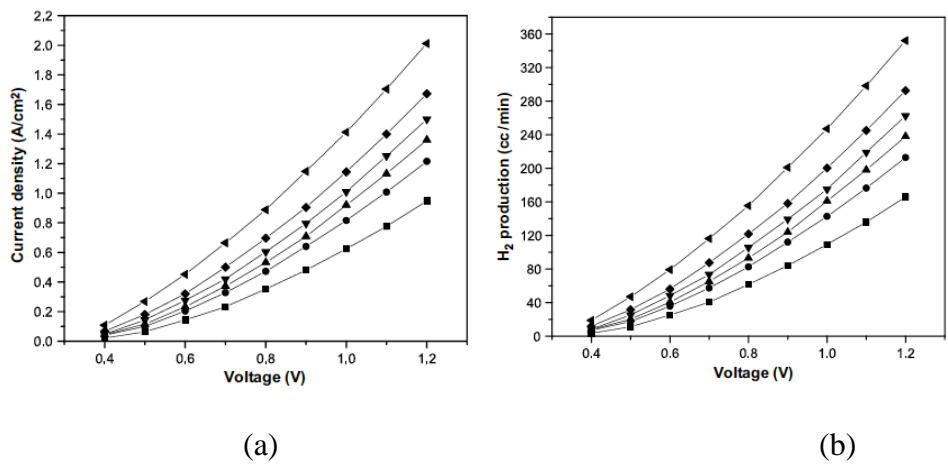


Figure 2.16 Effect of operating temperature on current density (a) and on hydrogen production rate (b) by methanol electrolyzer with Nafion-117 and 4 M methanol, at 30 °C (lowest curve), 40 °C, 50 °C, 60 °C, 70 °C and 80 °C (highest curve) (Sasikumar et al. 2008).

It is also clear from Figure 2.16 that the current and hydrogen production rate are proportional. This direct correspondence is confirmed in Figure 2.17 (Guenot et al., 2015).

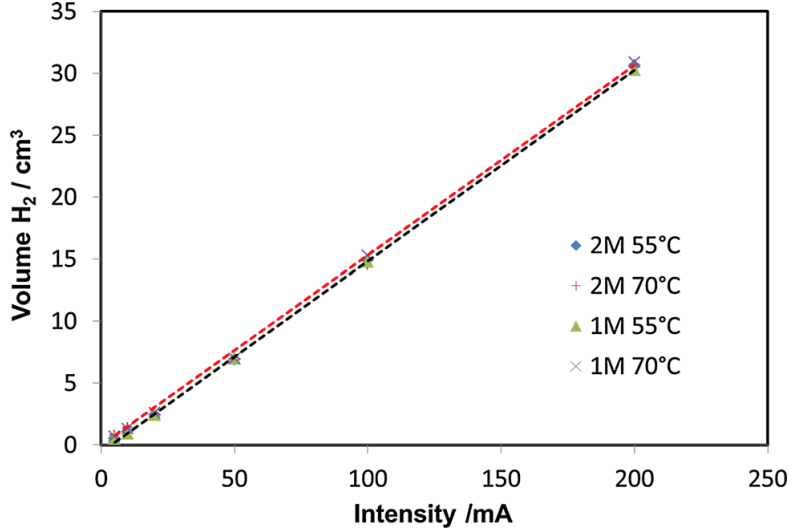


Figure 2.17: Volume of evolved hydrogen after 20 min of electrolysis as a function of the current intensity I for two methanol concentrations and two working temperatures (Guenot et al., 2015).

Cell efficiency can, however, decrease with increase of cell temperature. Operating conditions of the electrolytic hydrogen production by electrochemical reforming of methanol–water solutions need to be optimized in terms of current efficiency, catalyst stability, and energy requirements (both thermal and electrical) when compared with conventional water electrolysis. Electrical efficiency increases with current density, while external energy expenditure as well as catalyst degradation increases with increased cell temperature. This is due largely to the mechanism of methanol electrooxidation on Pt-based catalysts (Uhm et al. 2012). MOR overpotential can be decreased with the addition of Ru to Pt in anodic catalyst layer. Thus, Sasikumar et al. (2008) utilized MEAs fabricated from 3 mg/cm² Pt-Ru/C anode, and 0.5 mg/cm² Pt/C cathode, and were able to obtain excellent performance as shown in Figure 2.17. However, Ru in the anode catalyst is not as stable as Pt and tends to dissolve at higher operating potentials, which must consequently be avoided in methanol electrolysis.

2.7.5 Effect of Methanol Concentration

Like temperature, concentration or aqueous methanol molarity of the solution, is often a key variable in experiments. Unlike the case for direct methanol fuel cell (DMFC) where the performance and efficiency declines with increasing methanol concentration due to anode catalyst poisoning and methanol crossover that increase with concentration, the consensus in the literature (Uhm et al., 2012; Lamy et al., 2015a; Lamy et al., 2015b) on methanol electrolysis appears to be that increasing concentration in general improves performance (Figure 2.18). At least it does not have the strongly deleterious effect it does in DMFC. That said, some researchers have found limitations to this, with very strong solutions (12M +) did not continue to improve the MEA performance. This is because the reaction depends on the permeation of methanol and water at the

anode, where water is constant regardless of the concentration so therefore it becomes the limiting reactant at higher methanol concentrations Take et al. (2007.)

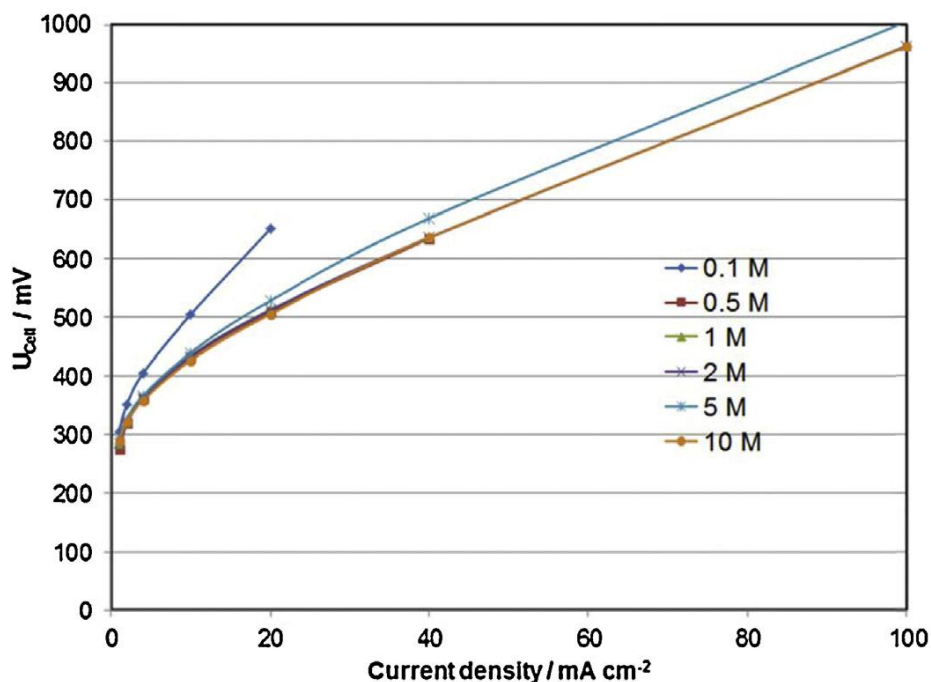


Figure 2.18. Polarization plots for methanol electrolysis at different temperatures for different methanol feed concentrations (Lamy et al., 2015a).

2.7.6 Performance of Different Anode Catalysts

Platinum (Pt) and Ruthenium (Ru) are both platinum group metals and have good electrocatalytic properties for a broad a range of chemical reactions. They have been time tested with a Pt to Ru atomic ratio of 1 to 1, and have been recognized as the best anode electrocatalysts at room temperature for proton exchange membrane fuel cells with reformed hydrogen feed (H₂ + CO₂ ,along with traces of CO) or for direct methanol feed as well as methanol electrolyzers alike (Uhm et al. 2012.) One of the reasons Ru is used as a cocatalyst with Pt at the anode when carbon monoxide can be formed from methanol as an intermediate or is present in the hydrogen feed is

because it is more effective than Pt in dissociating water to OH intermediates at lower overpotentials, which is an excellent oxidant and oxidizes CO intermediate in MOR to CO₂ (Halme et al. 2016). Through extensive experimentation, it has been found that PtRu catalysts are better than just Pt for methanol oxidation in alkaline as well as acidic electrolysis cell in low potential region <1.2 V, which is the methanol region (Tuomi et al. 2015). The way these catalysts are supported inside the MEAs are as nanoparticles on carbon particles to increase their surface area and in turn their effectiveness. In literature, the catalyst loading will often be shortened to “4mg Pt/C” which translates to 4 milligrams of Pt supported on carbon. The supported catalysts allow them to have excellent reactivity and longevity. The stability of the platinum catalyzed membrane was studied at intermittent discharge rate for 2500 hours, and show excellent degradation resistance (Sethu et al. 2014).

2.7.7 Performance of Different Membranes

2.7.7.1 Nafion® Membranes

One membrane that is used most commonly in both electrolyzers and PEM fuel cells is Nafion®. Nafion® is a polymer that was developed by DuPont and NASA during the 1960's. Nafion® is very well known for its excellent proton transfer abilities, as well as being extremely chemically and thermally resistant. Nafion® is a copolymer of tetrafluoroethylene, also known as Teflon®, and perfluoro-3,6-dioxo-4-methyl-7-octene-sulfonic acid as shown in Figure 2.19.

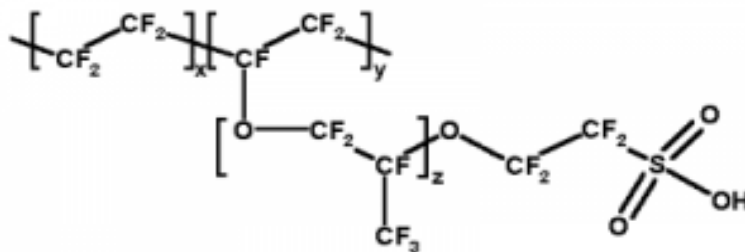


Figure 2.19. The polymer structure of Nafion[®].

The Teflon[®] portion of the polymer adds chemical resistance and hydrophobicity, while the sulfonic acid portion adds the hydrophilicity and dissociates in the presence of water to transfer protons across the membrane. Nafion[®] membranes come in different thicknesses and can have different characteristics. The name of a membrane is usually based on its equivalent weight (the first two numbers) plus its thickness (the last digit). For example, Nafion[®] 117 has an equivalent weight of 1,100 and is 183 microns (or 0.007 inches thick), Nafion[®] 115 is 127 microns (0.005 inches thick), and Nafion[®] 212 is 51 microns (0.002 inches thick). Another style of Nafion[®] membrane is Nafion[®] XL. This membrane is chemically cross linked which provides mechanical reinforcement for a longer operating life, while still being half the thickness of a Nafion[®] 212 membrane. Below is a picture of an MEA with a Nafion[®] membrane that has two catalyst coated carbon gas diffusion layers hot-pressed onto it.

Because Nafion[®] has a Teflon[®] ($-CF_2$) backbone, it displays its hydrophobic qualities and keeps water away from the pore surface. However, the Nafion[®] also has sulfonated side chains that are hydrophilic and attract water. The side chains are not as strong as the hydrophobic chains. Because of this, the water that is attracted forms water clusters that when interconnected form a percolation pore network within Nafion[®] for the dissociated protons to diffuse via both Grotthuss and vehicle mechanism. Nafion[®] is one of the great proton exchange membranes, because it limits the amount of water absorbed but promotes proton exchange.

Sasikumar et al. (2008) experimented with Nafion[®] thickness and found that for 4 M methanol at 30 °C, the cell performance followed the order: Nafion[®] 112 > Nafion[®] 115 > Nafion[®] 117. There are two competing factors that are affected by membrane thickness. The proton conduction resistance increases in proportion to thickness while methanol crossover flux is inversely proportional to membrane thickness. In other words, methanol crossover was also found to increase with thinner membranes. Overall, in view of lower methanol crossover and better mechanical stability, they found that Nafion[®] 117 was preferable.

2.7.7.2 Alkaline Anion Exchange Membranes (AEM)

A recent study has shown that methanol electrolysis can take place using electrolytes other than acidic proton-exchange membranes (PEMs) such as Nafion[®]. In fact, alkaline electrolytes have been shown to work. Thus, Tuomi et al. (2013) used the anion exchange membrane (AEM) Fumapem FAA-2 (FuMa-Tech, Germany) as the solid electrolyte sandwiched between a Pt/C cathode and a Pt–Ru/C anode, both with a 0.5 mg/cm² metal loading, as shown schematically in Figure 2.20. Performances at 70 °C of ca 50 mA/cm² and 100 /cm² were obtained at cell voltages of ca 1.0 V and 1.2 V, respectively which is much lower than those obtained with acidic Nafion[®] membranes. Even with lower performances the cost and crossover was lower and required much lower amounts of the Pt catalysts. An example of better crossover performance is the Fumapem FAA-2 membrane has a crossover rate only 16% of that of the Nafion-115 membrane (Tuomi et al, 2015.)

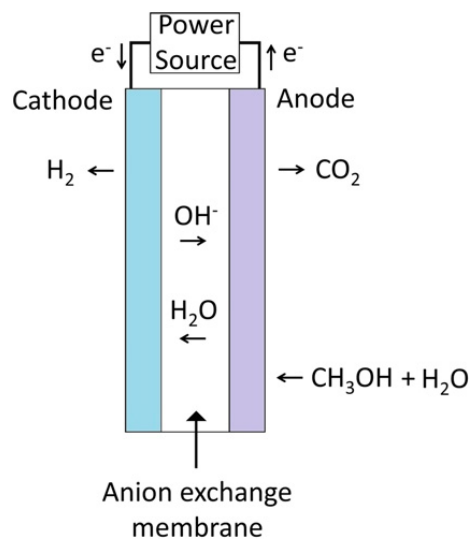


Figure 2.20. Schematic of methanol electrolyzer based on an anion-exchange membrane (AEM)

(Tuomi et al., 2013).

Some of the alkaline membrane electrolyzer qualities make it good candidate for further research in methanol electrolysis. Low-cost membrane materials coupled with lower catalyst loadings and the possibility of using non-precious metal catalysts offers potential savings with material expenses. At the caveat increasing methanol concentration resulted in decreased performance in the electrolysis due to morphological changes in the membrane structure resulting in a decreased ion conductivity and overall performance. (Tuomi et al., 2015).

2.7.7.3 Sulfonated Polyetherersulfone (SPES)

Another solid polymer electrolyte that has been recently used in methanol electrolysis is Sulfonated Polyetherersulfone (SPES). These polymers do not contain any perfluorosulfonate repeats and still have sulfonated side chains allowing for the specific qualities of a proton exchange membrane. Below in Figure 2.21 is a structure of the precursor polymer, Poly ether sulfone (PES) and SPES (Muthumeenal et al. 2016).

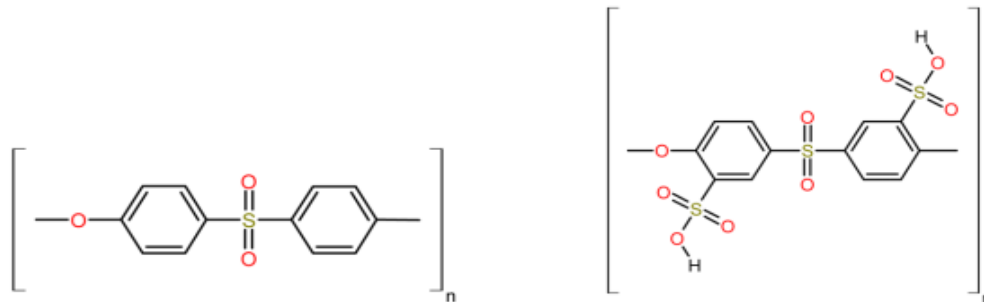


Figure 2.21. Chemical structure of polyethersulfone (PES) and sulfonated polyethersulfone (SPES, right) (Muthumeenal et al. 2016).

The reason these new polymer membranes were experimented with is they are far cheaper than their perfluorosulfonate counterparts. They also have good mechanical attributes, with a higher tensile strength, better high temperature performance and reduced methanol permeability than Nafion[®] 117. The drawbacks are a proton conductivity is about a third of Nafion[®] 117, and the high methanol concentrations can degrade the membrane relatively fast. The performance was confirmed by the electrolyzer cell test at 80 °C with the current density of 0.806 A/cm² at a cell voltage of 1.2 V, which is good considering the proton conductivity of SPES is about a third only of Nafion[®] (Muthumeenal et al. 2016). For comparison, Sethu et al. (2014) achieved 2.75A/cm² @1.2 Volts @ 80°C with Nafion[®]. A caveat is with more methanol cross over, the consumption of fuel rises and the hydrogen gas purity goes down (Tuomi et al. 2015.)

2.7.8 Advanced Methanol Electrolysis Systems

Multiple-cell stack systems have proven interesting for larger hydrogen production systems via methanol electrolysis. They are attractive because a stack vs. a cell can have a larger MEA area, a more compact package, and fewer end plates. The compromise is the advanced planning and cell design that are needed as well as a larger voltage power source. Sethu et al. (2014) developed a 5 cell stack that was able to produce 102 L h⁻¹ of hydrogen using 50 cm² active MEA

area, Nafion[®] 117 membranes, operating at 50 A and 3.95 V across the stack. Also reported was the electrolyzer, running at its highest current density, while still not electrolyzing water, produced close to 300 L h⁻¹ (Sethu et al. 2014).

Recently a novel concept has appeared in the literature that combines a methanol electrolyzer and a hydrogen Proton Exchange Membrane Fuel Cell (H₂-PEMFC) to a power source for small scale applications, e.g., portable electronics. This team of researchers experimented with a single fuel cell linked to a single electrolyzer cell. This unit was successful in producing between 1.26 Wh/mL-1.39Wh/mL of methanol (Halme et al. 2016). Therefore, the researchers aim to scale up the experiment, and calculated that an electrolyzer stack with 11 cells and a PEM fuel cell with 18 cells (smaller active area per cell than the electrolyzer) will produce more power. While successful in producing more overall power the team fell short in the efficiency of the system vs. that of the 1 to 1 cell system. With the 11 to 18 cell system, the electrical efficiency at this point (net power/FC power) is 37% instead of 40% in the single cell experiment (Halme et al. 2016).

2.7.9 Conclusions on Methanol Electrolysis Literature

With the further global awareness of the environmental damage and their finite nature of fossil fuels, the search for new renewable technologies, more efficient and less costly to traditional energy source is underway. Methanol electrolysis could be implemented as a part of this cleaner energy strategy. First investigated in 2001, although the pace of research seems to have picked up a bit in the last couple of years, much further research and development work is needed to advance the technology. Theoretical modeling could predict the optimal operating temperatures and concentrations in regards to overall energy consumption. Degradation experiments would be crucial as other applications of methanol electrolysis are considered. More advanced systems where electrolyzers are combined with fuel cells, allow for high efficiency energy storage. Along

the same line, possible development of a dual function electrolyzer/fuel cell could be proves less costly option. While this promising technology is still in early stages of development, the possibilities are many and hence the need for further research and development.

2.8 Solar Panels

The first solar panel was made in Bell labs in 1954 and had an efficiency of 4%. Over time the photovoltaic cell has made advances and has had breakthroughs thanks to years of research and the need to develop a clean method to create energy. (Dhar, B. M., 2013) In order for a solar panel to create electricity, photons have to hit the photovoltaic cell. The photovoltaic cell is made out of semiconducting material, most often silicon. These semiconducting plates are coated with other materials such as phosphorus and boron. The phosphorus doped silicon, known as n-type, is the negative plate. The addition of the phosphorus atoms allow for more electrons to be transferred. This is because the phosphorus atoms can break free from the silicon lattice and bring electrons along with it. Adding boron to the silicon makes it positive, and it is known as the P-type. Because the Boron has three instead of four electrons in its outer shell, it can easily accept another electron. These elements help create an electric field for electrons to flow through. By attaching metal plates and wires to the cell, the electrons can flow to an external source. By bringing the two silicon plates together, a diode is formed and an electric field is made, pushing electrons from the P side to the N side. When photons from light hit the silicon, electrons are freed and can flow, providing a current and the electric field provides voltage to the system.

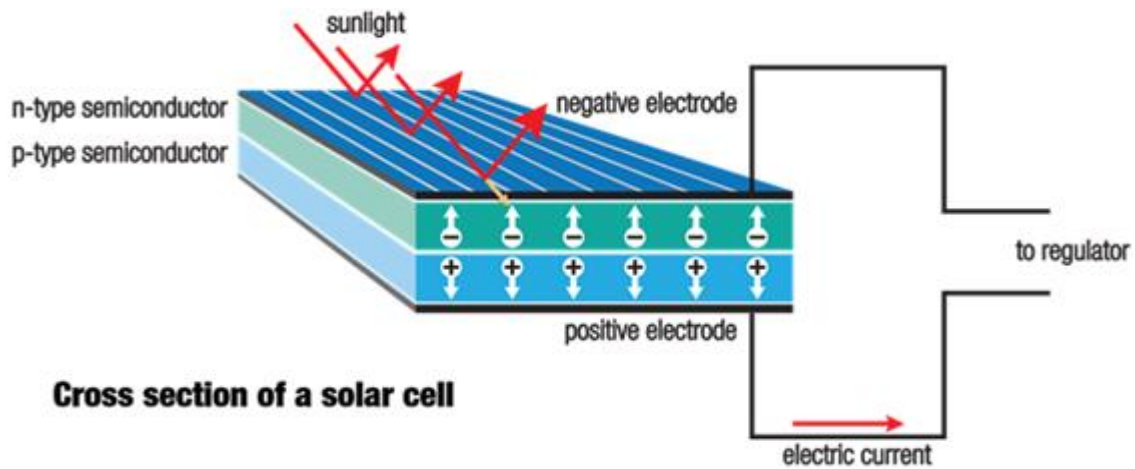


Figure 2.22. A typical solar panel schematic.

2.8.1 Solar Power Issues

The largest problem facing solar power is that solar energy is intermittent. The sun doesn't shine evenly everywhere around the world. This makes solar a poor choice for places like the Arctic Circle where half the year there is very little sun, or cities like Seattle that are very cloudy. Because there are roughly six hours of usable sunlight for solar power during the day, solar panels need to be able to make 24 hours of power in those six hours, and be able to store it in order to be able to eliminate conventional fuels. (Lee, 2015) With enough panels any house can be powered throughout the day with solar panels and the proper sunlight. However, since the batteries needed to store the electricity that is produced from the solar panels are rather expensive and not widely used most house or businesses choose to stay on the grid for those hours without sunlight. Additionally excess power that is produced can be bought by power companies. (Jones, et al., 2012)

Another problem with solar power is the efficiency of photovoltaic cells. Commercial solar panels can only get to around 35% efficiency and theoretically can only reach 85% efficiency. One reason for the loss of efficiency is heat. A portion of the energy that comes from the sun is lost as

heat on the panel, and is not absorbed. Additionally, the panel can only absorb certain light frequencies, and the rest is wasted (Forbes, 2013.) Another way to lose energy from a solar panel is for it not to be facing the right way. Most solar panels are set up on houses facing south because that angle will accumulate the most sun throughout the day. Many commercial solar farms however will use solar trackers that use various techniques to follow the sun throughout the day. Solar trackers are expensive and can cost up to \$7000 for a full size solar panel, but it is estimated that panels become around 25% to 35% more efficient (Perma Pure. n.d.) Because of these disadvantages solar farms need to be fitted with more or less solar panels depending on the cost and type of panel that is chosen to be used.

Chapter 3. Methodology

The purpose of this project was to design and construct a solar powered methanol electrolyzer system to produce hydrogen gas. As this is relatively uncharted territory, a sharp learning curve was called for in order to understand the basics of PEM electrolyzers including stack design, effect of altering operating conditions, system design, hardware, and data acquisition. Tests were thus initially carried out on a single cell PEM methanol electrolyzer at Enviowerks by altering operating temperature and methanol concentration in order to gain a basic understanding of the system. Further tests were subsequently conducted with a single cell in the Fuel Cell Center (FCC) located in Goddard Hall at WPI in order to obtain more detailed polarization plots on methanol electrolysis under a broad range of conditions. In parallel, a four-cell test stand was designed and assembled to run more in-depth performance and durability tests simultaneously with different MEAs in the future. Finally, a stand-alone solar powered methanol electrolyzer system was constructed including a data acquisition system for analysis, and tested on sunny days, which were few and far between over the winter season.

3.1 Single Cell Test Stand at Enviowerks

In order to gain basic experience using the electrolyzer test stand provided by Enviowerks, experiments were conducted to test the performance of a patented MEA stack design. The related patent application by Enviowerks included claims of increased performance and longevity based upon the assembly of the electrolyzer stack. Familiarity with the stack design, mechanical system and control system had to be first accomplished in order to be able to perform these tests. Figure 3.1 is a labeled picture of the single cell test stand at Enviowerks that was used to perform these initial tests.

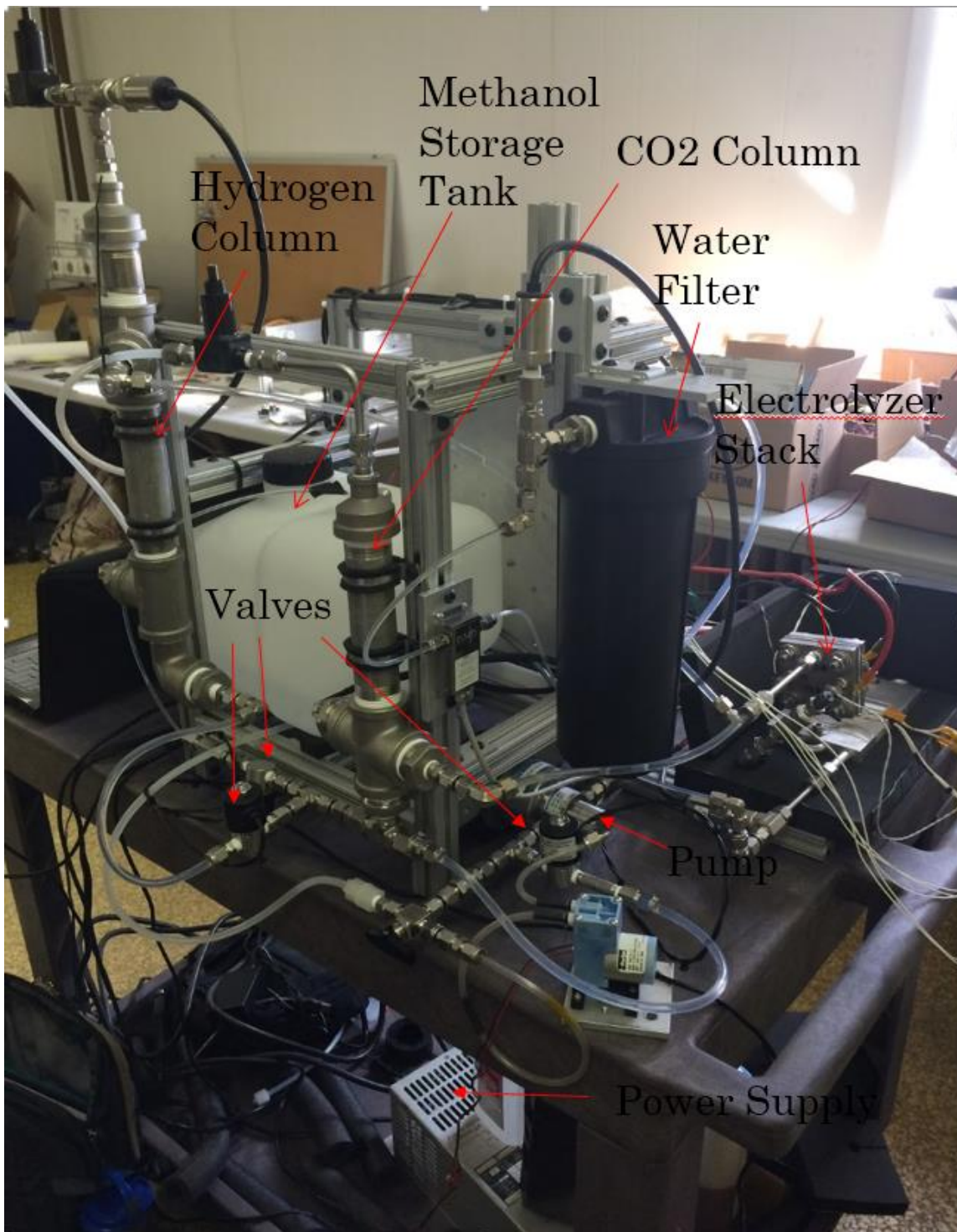


Figure 3.1: Envirowerks Original Single Cell Test Stand.

The 12 V Deltron power supply provided the needed power to operate all of the necessary actuation (valves, pumps, etc.), and also to provide power to the electrolyzer. A pre-measured concentration of methanol would be loaded into the Methanol Storage Tank for use in experiments. With control of the inlet valve and the pump, the methanol solution would make its way through the system and into the deionizing filter, as ions can deactivate the polymer electrolyte membrane (PEM). After deionization filter, the solution would then go via a methanol concentration sensor into the pre-stack solution heater, DBK HP 06. The heated solution would be then fed into the electrolyzer stack with CO₂ and H₂ being generated. The sealing system in the stack was designed so that the two gases would always be separated and returned to their specific columns. Depleted methanol solution and CO₂ would travel back to the CO₂ column, while H₂ along with some methanol solution that had crossed over across the MEA would move on to the H₂ column. Level sensors in the two columns would register when the methanol solution level was too high, triggering the appropriate valves sending the solution back into the feed loop. Back-pressure regulators were placed at the top of each column to allow for gases to be released at a specific pressure. Once the columns reached the set pressure both gases were combined and escaped through a flow meter. Mass flow rates would be calculated, and the gas would be released into the atmosphere.

This system, however, did not run completely autonomously, and because of this a computer control system was needed. The entire control and data acquisition system was coded by our corporate sponsor Patrick Emerick in C Sharp (C#). The Graphical User Interface (GUI) for this system is displayed in Figure 3.2 and is further described below.

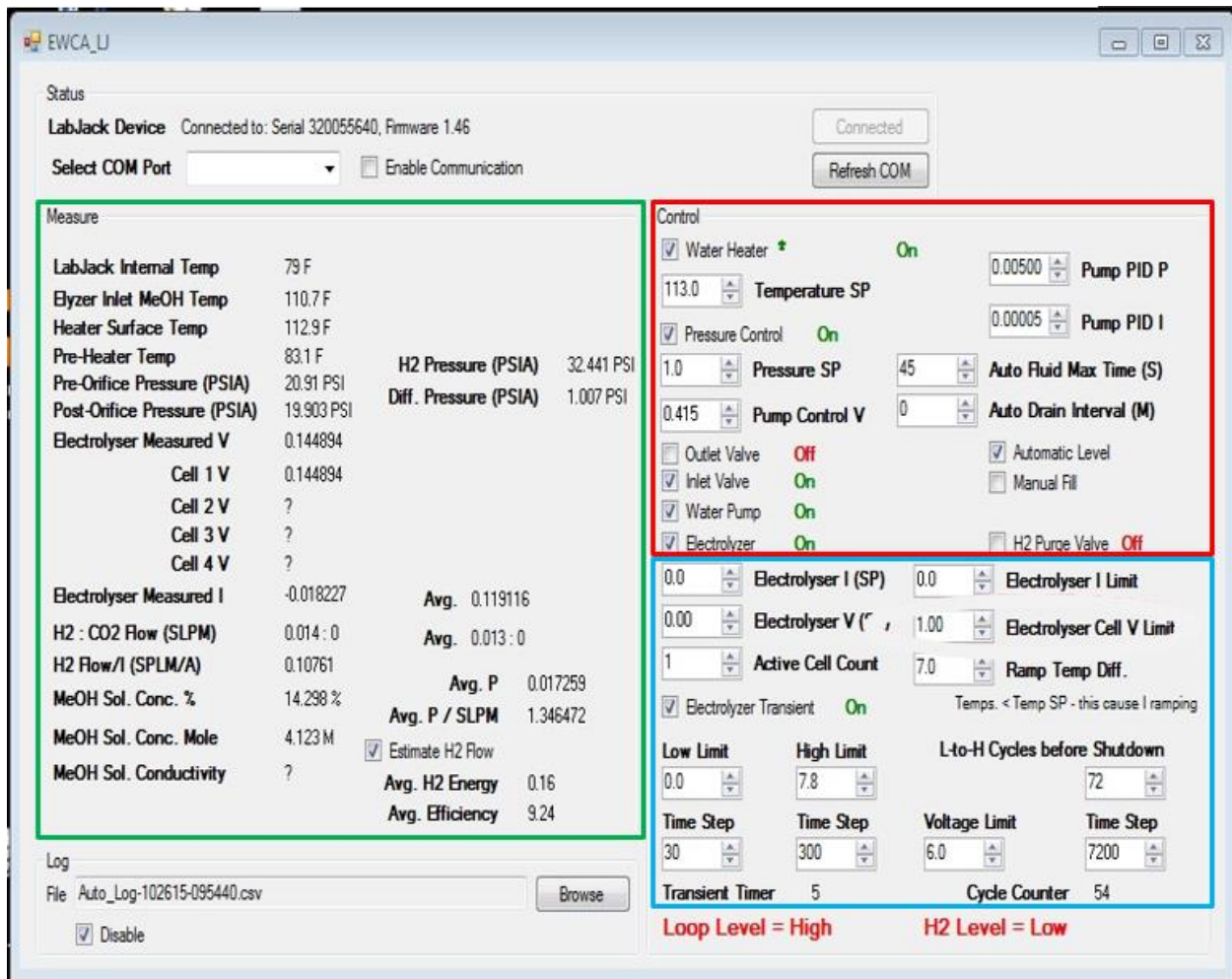


Figure 3.2: Control System for Envirowerks Test Stand.

On the left side of the GUI, outlined in green, is the data that was constantly measured by the data acquisition system. This data was measured constantly at ten times a second while the system was running. Temperature readings were acquired through the use of various thermistors placed throughout the system. These thermistors were located before the 24V heater (Pre-Heater Temp), on the heater surface plate (Heater Surface Temp), and at the inlet to the electrolyzer stack (Elyzer Inlet MeOH Temp). Pressure sensors also played an important role in this test setup. By controlling the difference between Pre-Orifice Pressure (PSIA) and the Post-Orifice Pressure (PSIA), the speed of the pump could be controlled. A pressure sensor was also placed in the H₂

column. Once this pressure stabilized the back-pressure regulator could be adjusted in order to raise or lower the pressure in the column. Cell 1 Voltage was measured through the use of an operational amplifier, which read a difference in voltage across the cell. Current was set and measured through a simple calculation found in the datasheet of the DC-DC converter, which was used to send the desired power to the stack. As previously stated, H₂ and CO₂ flow rates were measured with a mass flow meter, and finally the methanol concentration was measured through the use of an ISSYS Methanol Concentration Sensor (MCS) SN: 201357.

On the right side of the GUI, the control side, everything that could be actuated in the system was displayed. In the top right, outlined in red, was the controls for specific units such as valves and heaters. Check boxes could be operated manually, for actions such as introducing more solution into the system loop, or automatically during events such as an Automatic Level Control. The bottom right blue box was more closely related to running the electrolyzer. Voltage and Current set points could be established to run the electrolyzer at various operating conditions. Also, corresponding set points would be put in place to prevent the cell from going above a certain amount of power. Finally, there were also controls put in place to set how long the cell would run for before shutting down, as well as how long it would shut down for. This was to prevent excess CO₂ from building up in the stack and potentially degrading the membrane.

3.1.1 Design and Assembly of the Cell

A well thought out design and assembly of an electrolyzer stack is imperative to the performance and longevity of the cell. Patrick Emerick's stack design takes into consideration everything from support of the MEA, to the isolation of the anode and cathode for complete gas separation. A cross-sectional view of the implemented stack design is provided in Figure 3.3 below.

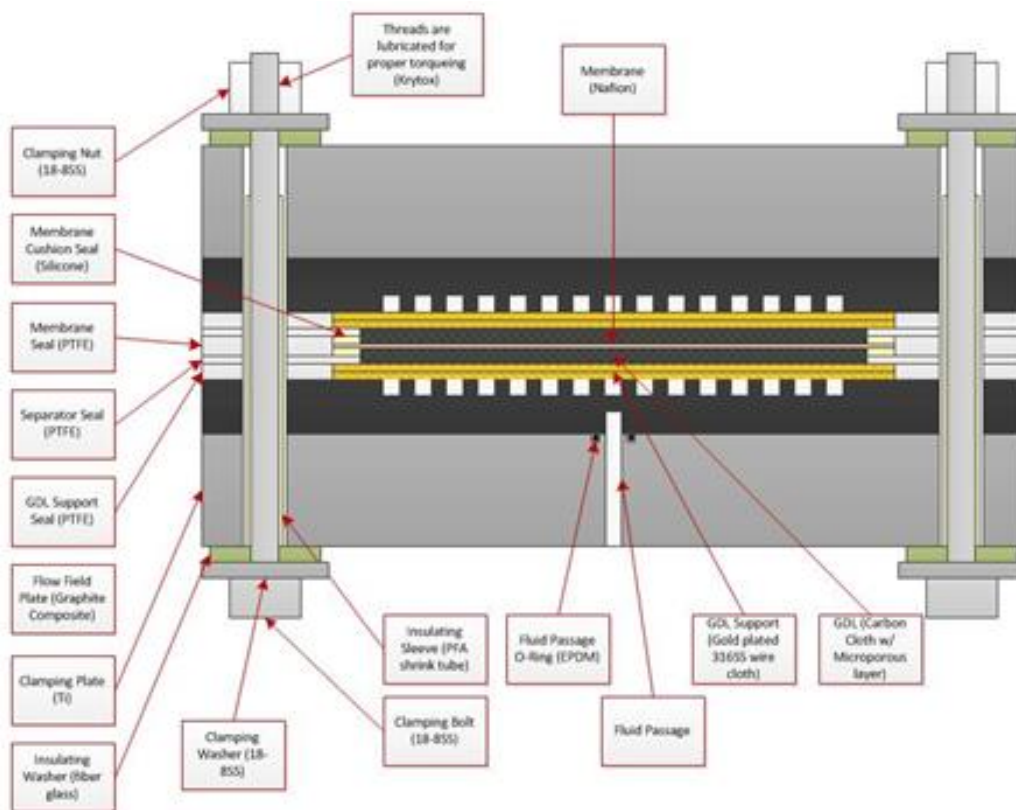


Figure 3.3: Cell Design & Assembly Used Throughout Entire Project.

This cell configuration was successful in providing the best results for Envirowerks, to date, and was used throughout the duration of this project. Clamping plates made of Titanium were used, because of its good conductive properties. Quarter inch bolts were used to hold together the entire stack, and each was insulated to prevent shorting. Each bipolar plate is made of a graphite and polymer resin combination. These plates have parallel flow channels as shown in the Figure 3.4 below. Also displayed in Figure 3.4 is the opposite side of the flow plate with four circles milled into the surface. These spaces hold EPDM O-Rings, which are used to seal the fluid passageways into and out of the stack. Gold plated wire mesh is used to support the GDL of the MEA in order to prevent it from being pressed into and ultimately blocking the flow channels

under high compression. With the gold mesh support, the entirety of the GDL will be available for mass transfer, serving a double purpose.

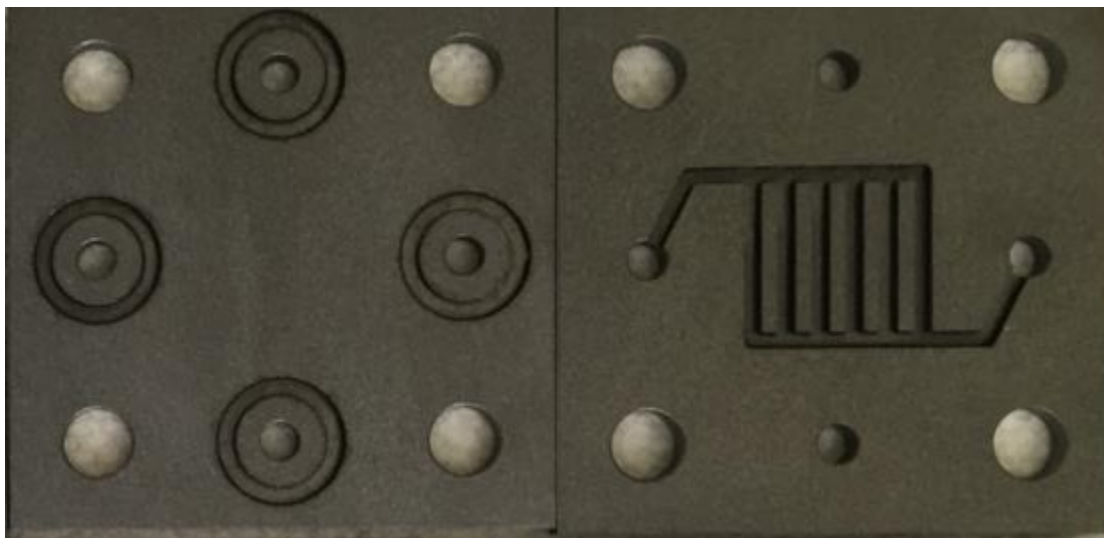


Figure 3.4: Carbon bipolar plates used throughout the project.

Silicone gaskets were used as a cushion during the compression of the stack and also help prevent any tearing of the MEA by providing a softer layer between it and the PTFE gaskets. PTFE gaskets of various thicknesses are used strategically to seal everything as well as allow for a certain amount of compression. While sometimes varied, the GDL was usually compressed to 7.5 thousandths of an inch thick (50% its original size). Calculations were done to find the torque required on each bolt to provide 50% compression, and were found to be around 100 inch pounds per bolt. A fully assembled electrolyzer stack is shown in Figure 3.5.

3.1.2 Experimental Procedure

In the beginning of the project, the single cell at Envirowerks was already setup for running. All that was done was to learn the GUI of the system and assemble a stack with a new MEA. To not damage the new MEA during the learning phase, a previously operating cell was used for practice. Once adequate learning proficiency was achieved, tests were carried out to validate

results. It was decided to complete tests at four varying temperatures as well as five different methanol concentrations in order to cover a broad range of different operating conditions.

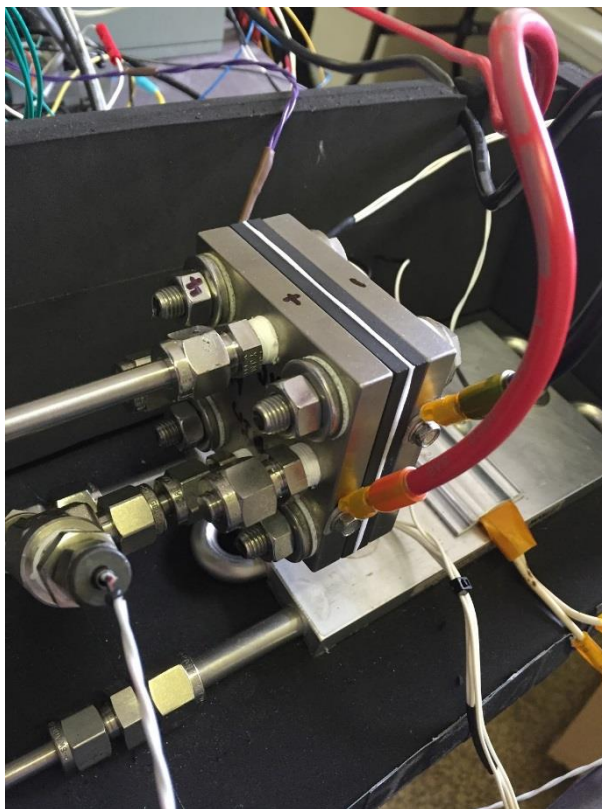


Figure 3.5. A fully assembled single cell electrolyzer.

The temperatures chosen for these experiments were: 45 °C, 55 °C, 65 °C and 75 °C, while the concentrations chosen were: 1.25 M (5 wt. %), 3.7 M (15 wt. %), 6.19 M (25 wt. %), 11.14 M (45 wt. %), and 16.09 M (65 wt. %). An MEA based on Nafion[®] 212 membrane with an active area of 6.25 cm² was chosen to be used based on its lower price compared to thicker membranes, and lower resistivity. This MEA obtained from Fuel Cell Etc. had a carbon cloth GDL hot-pressed on both sides, with a 4 mg Pt-Ru anode and a 2 mg PtB (platinum black) cathode catalyst loading. To test the performance of the cell under these various conditions, polarization plots were to be created with the data acquired, plotting voltage (V) vs. current density (A/cm²). For each test, the

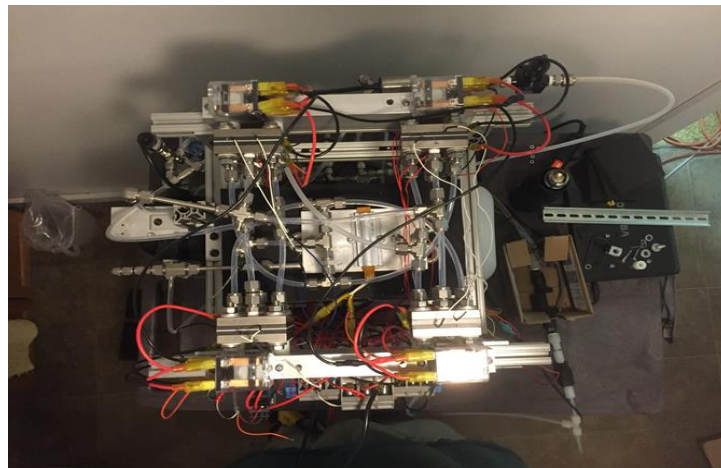
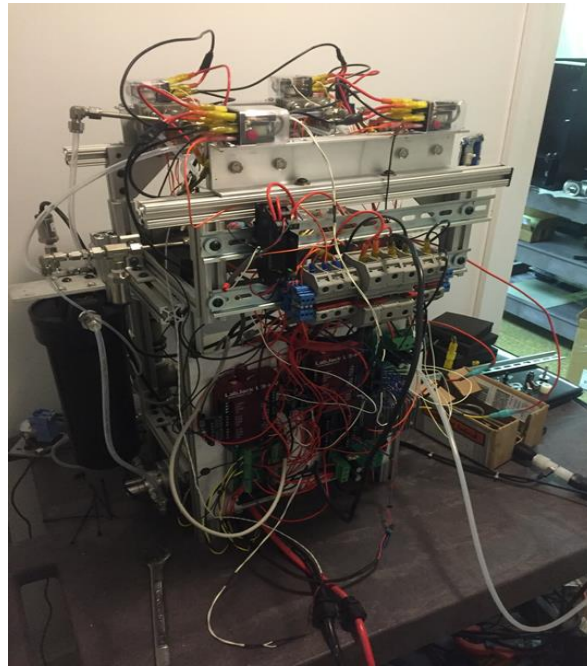
concentration was set as close to the predetermined point as possible and the corresponding temperature was set to 45 °C. This was done because of the ease to raise the temperature over time compared to varying the concentration or lowering the temperature each time. From there, tests were run starting at 1.25 A (0.2 A/cm²) and ramped 1.25 A every five minutes, with a 30 second rest in between to eliminate CO₂ build up, until approximately 1.2 V was reached, since water electrolysis can occur above this voltage. At this point, thus, the system would stop supplying power to the electrolyzer and the next test could be run. Because temperature was easier to set up than concentration, the concentration was held constant until data for all four temperatures were obtained. These steps were followed until every concentration and temperature was completed. The data was then imported into Microsoft Excel, where voltage and current were averaged for each step and then plotted into a polarization plot.

3.2 Four-Cell Performance and Durability Testing

A setup was designed and fabricated for the simultaneous performance and degradation testing of four different MEAs, each with a different membrane different thickness. Tests of varying concentration and temperature were chosen to be performed simultaneously in order to determine the difference in performance of the four electrolyzers at different conditions. If a membrane failed it would be replaced and tests would restart at the conditions under which the previous membrane had failed. Each membrane was allowed to have approximately a 2 hour break-in period, in order to fully rehydrate the MEA. After this period, tests could be run on a membrane in order to acquire the sought after results. The experiment was planned to be conducted at four different methanol concentrations and five different temperatures. The current density was to be increased every five minutes until a limiting current is found for each membrane at each temperature and concentration or until a voltage of 1.2 V was achieved.

3.2.1 Setup

In order to conduct these in-depth performance and degradation experiments, a new test stand had to be designed and constructed. Using the existing test stand at Envirowerks as a basis, the four-cell set up was engineered. Figure 3.6 & 3.7.



Figures 3.6 & 3.7: Modified Test Stand at Envirowerks.

The earlier test stand at Envirowerks, shown in Figure 3.1, to test single-cell methanol electrolyzer, was substantially modified to fit the four cell testing rig. The electronics were taken apart and

rewired in order to accommodate the need for additional data acquisition. This setup has the ability to test four cells at once, with each stack experiencing identical conditions. A flow schematic is provided below in Figure 3.8 for further description of the setup.

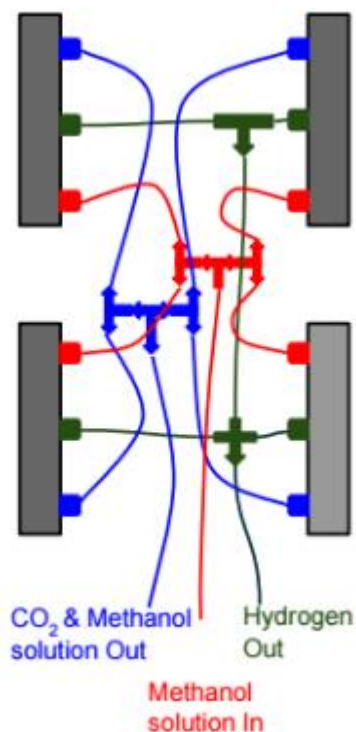


Figure 3.8. The flow schematic of the four cell test stand.

In order to keep the feed solution at an elevated temperature, the feed is initially heated before the entering the cells, each cell is also fitted with two 1" x 1" electric heaters in order to further control the temperature. A 24 V pump, Micropump P/N: 83273-1199, was used to draw the methanol solution from the methanol reservoir tank and then circulate the solution through the entire system. The pump flow rate was gauged by a pre- and post-orifice pressure sensor. This could then be adjusted accordingly to change solution flow rate. To connect all the cells in series, a circuit was wired using four twelve-volt double pole double throw relays, presented in Figure 3.9.

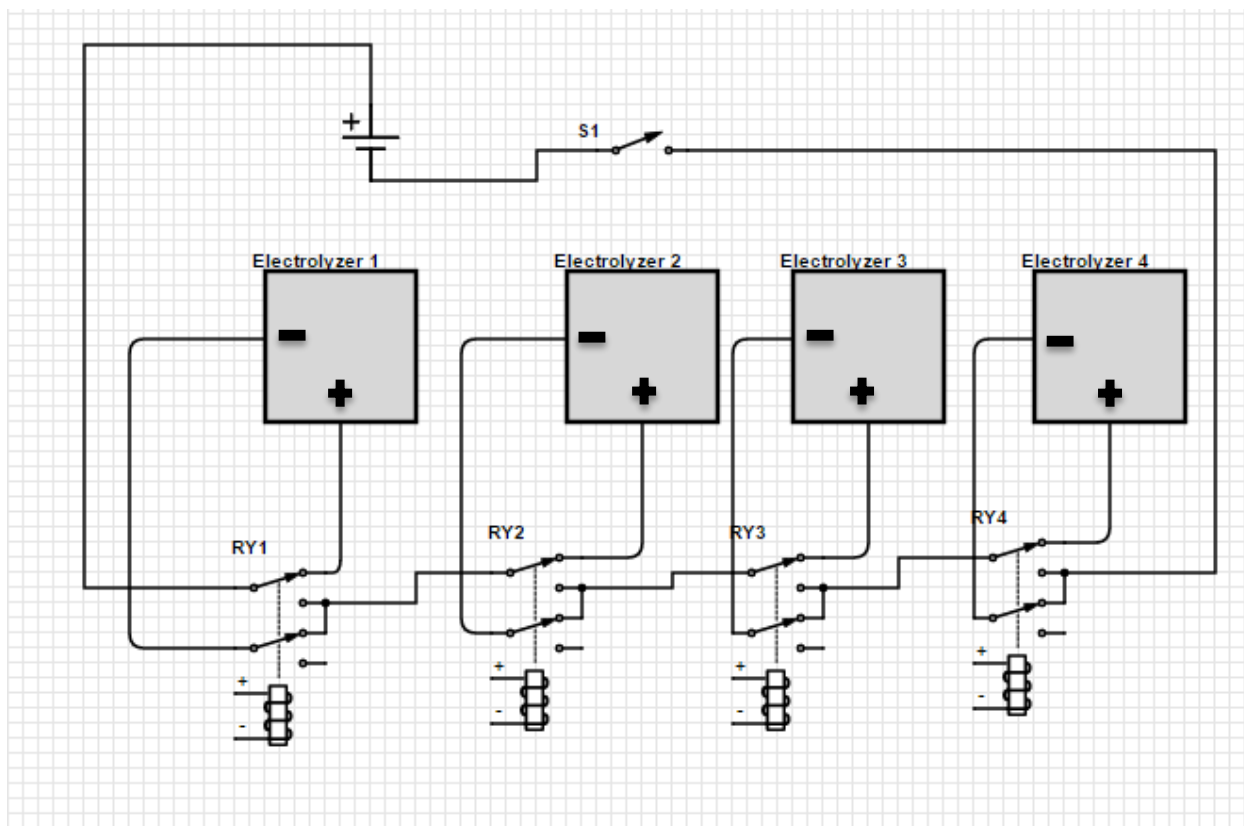


Figure 3.9. Schematic of the four cell test stand relay circuit.

With this circuit in place all cells can be powered at once, and if one membrane fails the relay bypasses that cell to power the others. The rest of the system uses the previously described single cell test stand components with no other modification.

3.2.2 Data Acquisition

Data acquisition is vital in any scientific experiment. The four-cell setup was designed with various different sensors to acquire a wide range of relevant data. Each of the four cells was fitted with a thermistor in each carbon plate in the stack. The temperature could then be accurately displayed and recorded in real time. With two sensors in each stack, any inconsistencies in temperature could be observed as well as any temperature ramp up lags. Feed temperature was also measured and used as a reference point for the actual stack temperature. Voltage across the

stack was measured and an automatic shutdown was programmed so that if the voltage rose above 1.2 V in a stack, it would be shut off to avoid water electrolysis. The current being sent to the system was measured and recorded for each cell. This allowed for simultaneous polarization curves to be created for all four cells. Further, this allows for a direct analysis of the any differences in performance and efficiency of each cell under identical operating conditions. Many other analog inputs are recorded but do not necessarily play any role in the evaluation of the four different cells. These data collections include the hydrogen column pressure, pre- and post-orifice pressure, methanol concentration, pump speed, hydrogen gas mass flow rate, electrolyzer current and voltage set points, and H₂ column and CO₂ column liquid levels.

3.2.2 Experimental Procedure

For this experiment, different Nafion[®] membranes, namely, Nafion[®] 212, 115, 117 and XL were to be used in MEAs to compare the performances of these different membranes in methanol electrolysis. The MEAs were otherwise identical, using the same catalyst loadings at the anode and the cathode, only differing in membrane thickness as above. The electrolyzers were powered by a 12 V DC power supply and power was regulated by two DC-DC converters. This provided the voltage needed for the electrolyzers themselves, as well as the 24 V needed for the heaters and pump.

The tests were supposed to be started at 1 M methanol concentration and 25 °C. A current of 0.1 A was to be applied to the cells for five minutes while data recording software was being used to track the voltage output. The current density would then be increased in 0.1 A segments every five minutes until 1.2 A was reached. The five minute period allowed steady state to be reached after step change in current, and an average reading of voltage at each current could be taken. After 1.2 A was reached the test would be ramped up 1.2 A every five minutes. This pattern

was to increase until one of the cells reached a maximum current and/or the voltage reached 1.2 V, or the cell failed. The failed cell would automatically be turned off, and the tests continued on the remaining cells. After a max current was found for each cell, the test at those respective concentration and temperature would be deemed finished, the temperature would then be raised and the same test was repeated at 40 °C, 55 °C, 75 °C, and 85 °C. Once all of the polarization plots had been hence determined at each temperature, the test would be repeated at 3, 5, and 10 M, repeating the same testing procedure. If an MEA were to completely fail during the tests, the damaged MEA would be thrown out and all new MEAs would be put into all the other cells as well to maintain consistency. This protocol was also to be followed if one membrane was found or thought to be largely damaged in any way. Although good progress was made on the design and construction of the 4-cell setup, it could not be completed in time to obtain data for this report, and is planned to be used in the future.

3.3 Fuel Cell Center Lab Single Cell Testing

In order to get more in-depth and accurate polarization graphs of methanol electrolysis under a variety of conditions, tests on single cell were also run in the Fuel Cell Center (FCC) Lab in Goddard Hall. This setup allowed for controlled experiments to be performed on the single cell electrolyzer MEA. These experiments took place in lieu of using the four cell test stand, which could not be completed in time, as mentioned above. The experiments were run on a new Nafion[®] 212 membrane based MEA and consisted of methanol concentrations of 1, 3, 5 and 10 molar at room temperature as well as 30 °C, 40 °C, 50 °C, 60 °C, and 70°C. The catalyst loading on the anode of this membrane was 4 mg Pt-Ru and the cathode was 2 mg PtB (platinum black).

3.3.1 FCC Single Cell Setup

The majority of the equipment needed to run experiments was already present in the FCC, with the only thing missing being the electrolyzer cell. A cell that was originally intended for the 4-cell test stand was used to perform these experiments. A labeled picture of the FCC setup is provided below in Figure 3.10.

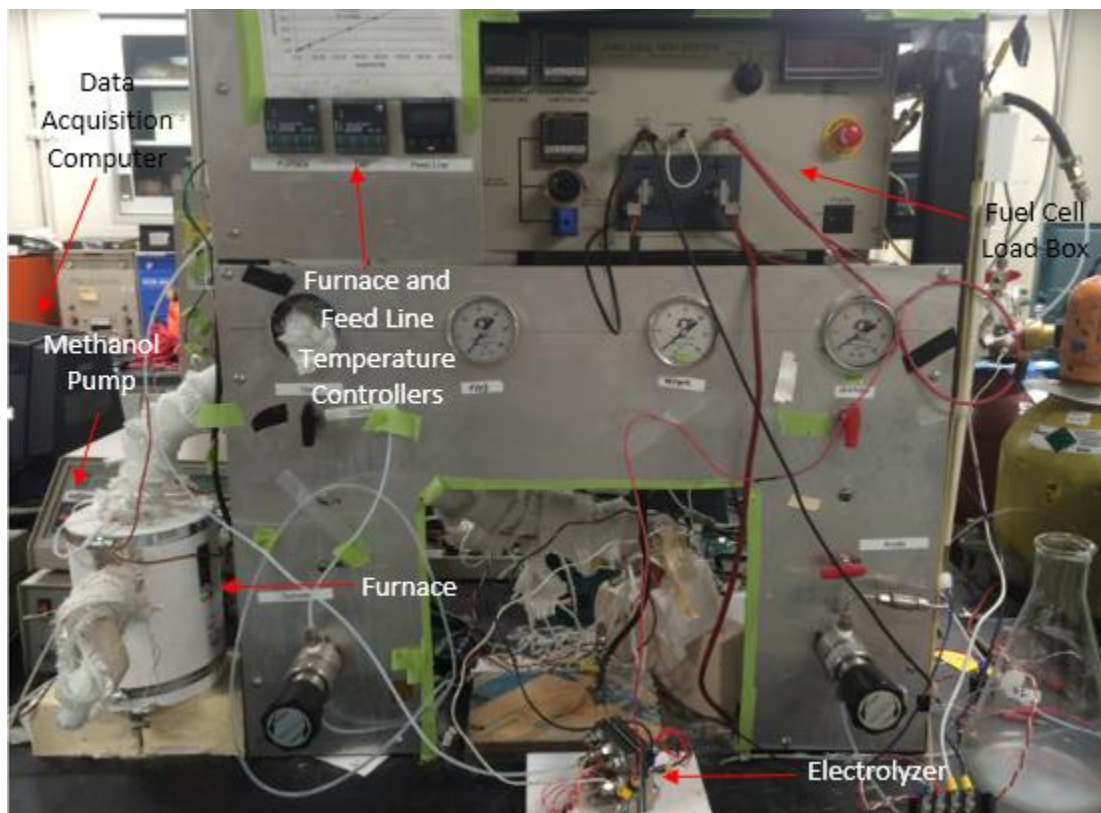


Figure 3.10: Single cell setup used for FCC testing.

The Fuel Cell Test System Series 890 B was the heart of this test set up. This load box, usually used for fuel cells, allowed for the gathering of important data from the tests that were run. By wiring the Fuel Cell Test System in series with the cell and power supply, voltage and current data could be gathered. Voltage across the stack was displayed on a screen on the load box. Data was also sent to a computer running the program FuelCell, the partner program to the Fuel

Cell Test System. From here, data was logged and saved into files that could later be extracted into Excel. These files could then be broken down and averaged allowing polarization plots to be created. Externally powering the electrolyzer was a Hewlett Packard 6651A power supply. This supply had a voltage range of 0-8 V and a 0-50 A current range, and is displayed below in Figure 3.11.



Figure 3.11: Power supply used during FCC testing.

A syringe pump, ISCO Series D Model 1000D, was used to send the methanol solution to the cell. Pump speed, in mL/min, could be manually controlled, however the solution could not be recirculated. Because of this, new solution had to be added to the pump after 1000 ml had been used, as this was the syringe pumps capacity. From there, a furnace was used to preheat the methanol solution going to the fuel cell. This furnace was only used for above room temperature tests. If the cell did not need to be heated, the solution was sent directly to the cell bypassing the furnace. The heated solution was sent through the cell to heat it to specific temperatures, which were monitored through a thermistor that was attached to an Arduino Uno. The thermistor values

were read and displayed by the Arduino through the usage of a voltage divider circuit. A schematic of the circuit is shown in Figure 3.12.

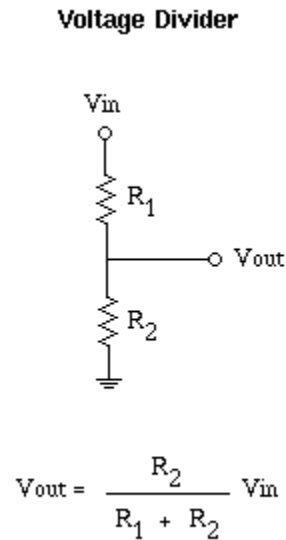


Figure 3.12: A version of a voltage divider circuit diagram, with Vout calculation.

Resistor 1 (R1) in this case was the thermistor, which varies resistance based off changes in temperature. These changes in resistance cause Vout to vary, which will in turn be picked up by the Arduino. As long as R2 stays constant (10 K Ohms), this variation in Vout can be calculated into a temperature by the Arduino code. Temperature controllers, Omega CN9000A, were used to set the temperature set points for the furnace as well as the feed line heater. Heat loss throughout the system required the set points to be set much higher than the test run temperature in order to achieve the desired temperature in the cell. The Arduino powered thermistors accurate reading of the cells internal temperature allowed experiments to be run at various temperatures with little error.

3.3.2 FCC Single Cell Tests

The set up in the FCC was used to perform similar experiments to the planned experiments for the four-cell test stand. Because of time constraints, not all of the experiments could be finished. Instead of testing four different membranes, only one, a Nafion[®] 212 membrane was experimented on. Additionally, only a few of the selected temperatures and methanol concentrations were used. The solution was pumped into the cell at 10 mL/min and the spent solution was collected in a 1 L bottle. Hydrogen produced was bubbled through water so that a visual observation could be made when the hydrogen was being produced. Initially the voltage was set to 0.1 V and it was held until steady state was reached and the resulting current was recorded. The voltage was increased by 0.1 V until 0.4 V was achieved, and the current was recorded repeatedly. The current was then limited and increased to get a corresponding voltage. The voltage was increased in steps as close to 0.05V as possible, until the voltage reached around 1V. Because of mass transfer limitations and a resulting voltage drop, the input voltage would have to be raised much more than 0.05V in order to see the desired increase across the cell. The Fuel Cell system could only handle 10 A going through it before an automatic shutdown would occur. This led to many tests at higher concentrations and temperatures maxing out the system before 1V could be achieved. This test procedure was used on the following tests to plot voltage and current density to create polarization plots.

3.3.2.1 Flow rate experiments

Tests were first conducted using a 5M solution to determine if flow rate had an effect on the performance of the electrolyzer. The methanol solution was fed to the electrolyzer at 1, 5, 10, and 15 mL/min and polarization plots were graphed using the testing procedure described above.

3.3.2.2 Temperature and Concentration experiments

Experiments were then conducted to determine the effect of temperature and concentration of the solution on the cell performance. Methanol concentrations of 1, 3, 5, and 10M were fed into the cell at 20, 30, 40, 50, 60, and 70 °C. All of these concentrations and temperatures were tested in the same procedure as described before, with the resulting voltage and current densities plotted. The same solution was used for each concentration throughout the various temperature tests. This eliminated any possible differences the making of another solution of the same concentration.

3.4 Solar Powered Methanol Electrolysis System

A solar powered methanol electrolyzer was designed and constructed in order to determine the feasibility of producing hydrogen on demand powered by the sun. This set-up was created as a proof of concept that methanol is an attractive hydrogen carrier and that on-site hydrogen production from it is a more efficient method to create hydrogen than other methods. A data acquisition system was also put into place in order to acquire vital information on the operation of the system. This information could then be used to evaluate the performance and efficiency of the solar powered methanol electrolysis prototype.

3.4.1 Designing the setup

A design was develop of the solar powered methanol electrolyzer prototype and was drawn using Solidworks as shown in Figure 3.13.

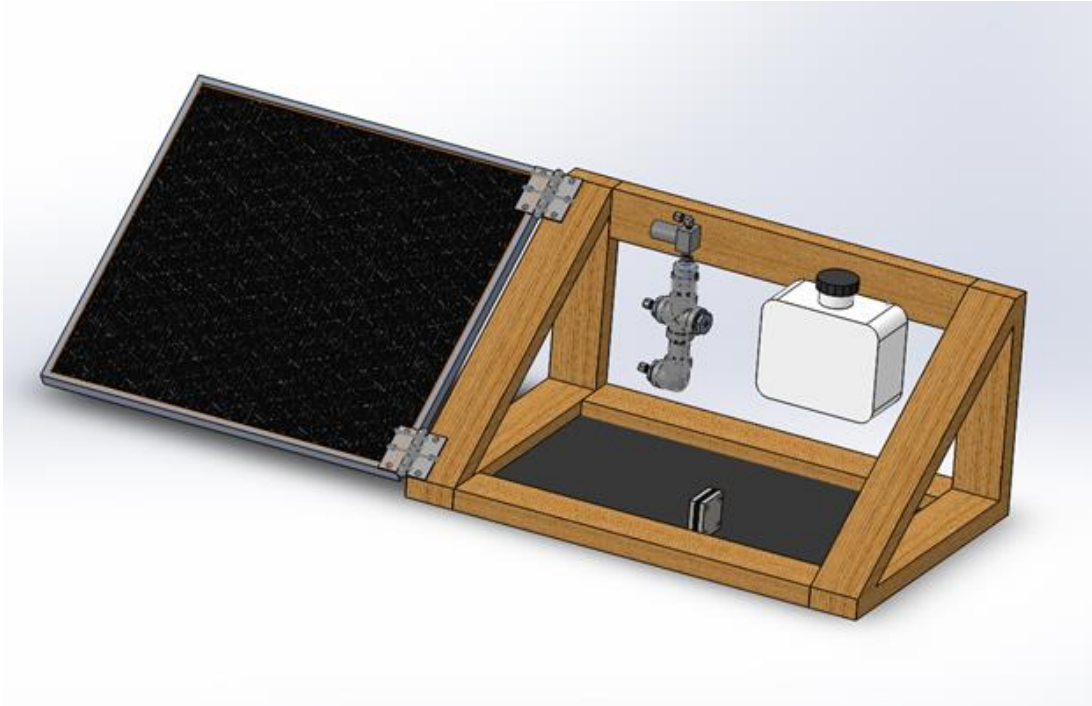


Figure 3.13: Solidworks Design of a Solar Methanol Electrolyzer.

The solar panel purchased to power this electrolyzer is an Aleko 60 W, 21.8 Open Circuit Voltage, Monocrystalline Solar Panel, shown in Figure 3.14.



Figure 3.14: The monocrystalline solar panel mounted on the stand alone system.

For optimal year round performance the solar panel was placed at a 35-degree angle, as shown in Figure 3.15. The solar panel was connected to the frame with hinges and also acts as a

cover, protecting the electronics and the cell placed in the box. Since for the single cell electrolyzer used in the prototype, the voltage cannot exceed 1.2 V, it was determined that the best way to step down the voltage from the panel, for the electrolysis, was to implement a DC-DC converter. The DC-DC converter allows the output current and voltage to be controlled. The converter was set so that its output voltage to the cell will be no higher than 1.2 volts, as opposed to the 20 volt open circuit voltage the panel will deliver at peak performance. This safety precaution ensures that the MEA will not be damaged by the accidental electrolysis of water. Current was also monitored through the IMon pin on the converter, providing information necessary for polarization plots.

A monocrystalline solar panel (Figure 3.14) was chosen because, although more expensive than a polycrystalline panel, it provides higher efficiency as well as a longer working life. One benefit of this is that the higher efficiency will deliver more power than a less efficient panel under the same solar conditions. This increase in power will in turn help create more hydrogen gas. Another benefit of the Monocrystalline Solar Panel is its longevity, this means that this project could be carried on for many years to come with future MQP teams investigating further improvements.

In order to keep the system simple to use and to operate, it was decided to make the system passive and avoid using pumps, heaters, and valves like in the four cell test setup. Instead the methanol solution is gravity fed, and will be heated by solar radiation as well as the heat generated by electrolysis/solar panel. The premise of a gravity fed system was tested and proven to work, on a previous test stand set up at Envirowerks, as long as the system feed tank is located at an appropriate level above the stack. Wired after the electrolyzer in series with the solar panel and DC/DC converter was a 30 Amp current sensor. This sensor reads the amount of current after the cell, allowing the calculation of the amount of current being consumed by the electrolyzer. Voltage

in the stack was measured with the use of a voltage sensing circuit, which was made up of two probes, an operational amplifier, and four resistors.

An Arduino Uno, supplied from Arduino.cc, was used as the brain of the data acquisition system. Current entering the Arduino had to be limited to 40 mA, otherwise damage could occur (arduino.com). In order to achieve this, a Texas Instruments operational amplifier (op amp) LM324AN was used with four resistors of the same strength; this set-up, a differential amplifier, has a 'gain' of one. This means that the amplifier does not amplify the voltage and the output voltage is the same as the input. The current sensor used one of the other op amps to create a voltage follower which doesn't change to voltage reading just buffers it and give a more steady reading. In the Stand Alone system and in the 4-cell test stand, 10K ohm $\pm 0.1\%$ resistors were used. Having both voltage and current data, allows for the plotting of polarization curves and analysis of the cells performance. Thermistors were also used in the cell to determine the temperature the single cell is operating at. Finally a pressure sensor was placed in the gas column in hopes that the gas could be pressurized from the stand-alone system.

The wooden frame, housing the electrolyzer and electronics, was constructed with slanted sides that the solar panel was then mounted on. The latitudinal location of the testing site was used to find the proper angle to suspend the solar panel so that it receives optimal sunlight. The frame of the system was created out of wooden 2x4s for cost efficiency and the walls were made of spare Plexiglas. Inside of the box can be found a solution tank to provide the cell with methanol, the electrolyzer stack, and the gas column all connected with clear PTFE tubing to make it a complete observable system. Also located inside of the frame is the Arduino and breadboard with all the various data acquisition system wires. Weatherproof stripping was used in attempt to seal the

system, and the all possible points of entry were caulked. The finished prototype is shown below in Figures 3.15 & 3.16.

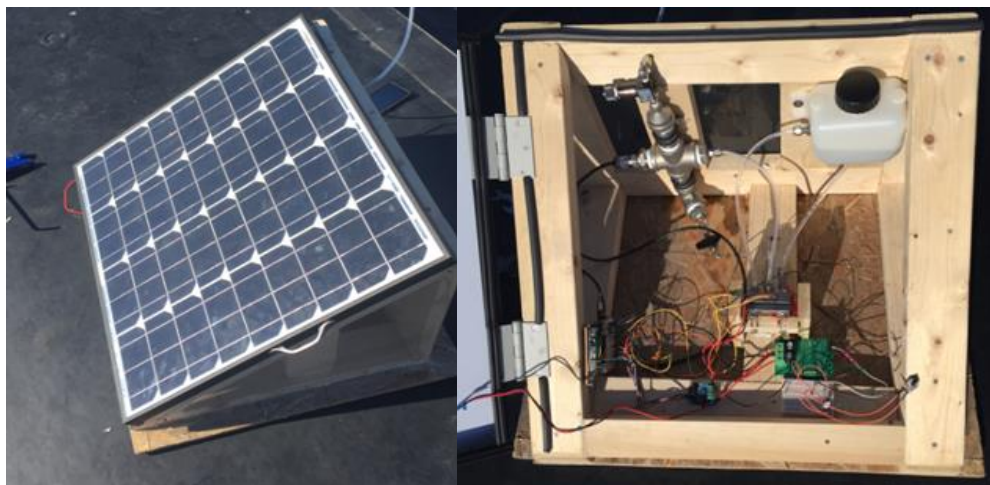


Figure 3.15 & 3.16: The solar powered methanol electrolyzer system prototype.

3.4.2 Test Procedure

An AC-DC power supply was used to debug the system; this eliminated the need for sunlight, in short supply during the winter months of testing, to operate the system. Testing and troubleshooting could be done at any time of the day, thus, allowing for easier and timely completion of the system testing and trouble-shooting. Once fully working, the stand alone system was left outside on a roof for four hours during a sunny day. A 25-foot USB cable ran from the roof into a room where it was connected to a computer. Data was collected every 1 second for each of the six readings. Leaving the system outside for extended amounts of time allowed for the performance to be evaluated under different weather conditions. For example, if the sun went behind clouds it would be seen in the data that the electrolyzer would not be performing as well as it was in direct sunlight. From here, comparison of solar powered electrolysis performance versus that of a wall powered system could also be made.

Chapter 4. Results and Discussion

The main objectives of this project were to investigate the characteristics of PEM methanol electrolysis, and to determine if solar powered methanol electrolysis is a feasible method of hydrogen generation. While not all of the originally planned tests could be performed, useful data were still obtained through the experiments that we were able to perform. Thus, while the 4 cell test stand could not be completed in time, data on the effects of flow rate, temperature, and methanol concentration were gathered on a single cell based on Nafion[®] 212 membrane. Additionally, tests run on the stand alone solar powered system that proved that solar powered methanol electrolysis is a viable method of hydrogen generation. These results are described here and discussed within the context of our goals.

4.1 FCC Single Cell Tests

Performance of the single cell methanol PEM electrolyzer was gauged via the polarization plots that were obtained from the data collected during the experiments under a variety of flows, temperatures, and feed concentrations. The main goal was to identify conditions that required less electric power, or voltage, input per unit hydrogen produced. Therefore, an operating condition that provides a similar current density, or hydrogen production rate, at a lower voltage than a different operating condition would be considered to have better performance.

Figure 4.1 provides a picture of the single cell electrolyzer used. The MEA used is a Nafion[®] 212 membrane with an active area of 6.25 cm² based on its lower thickness and higher conductivity. This MEA, obtained from Fuel Cells Etc., had a carbon cloth GDL hot-pressed on both sides, with a 4 mg/cm² Pt-Ru anode and a 2 mg/cm² PtB (platinum black) cathode catalyst loading. To evaluate the performance of the cell under these various conditions voltage (V) vs. current density (A/cm²) data was acquired, and polarization plots were graphed. These graphs, though very

detailed, do not begin with an origin of (0,0). This is because of a system offset of around 0.200 V at the beginning of each run. It is unknown why this offset occurred, however it is fairly consistent throughout every test.

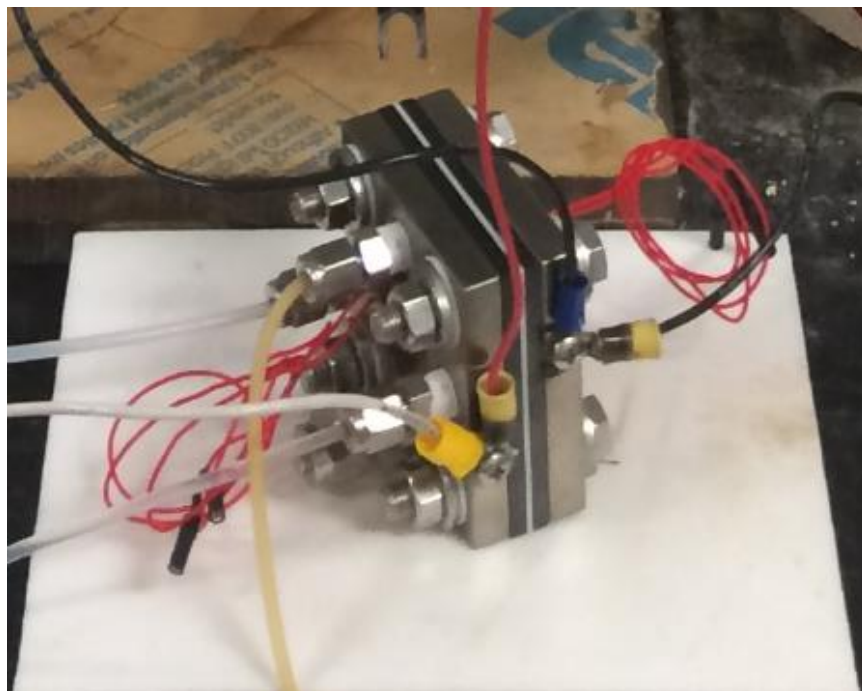


Figure 4.1. A picture of the single cell electrolyzer used in FCC.

4.1.1 Effect of Feed Flow Rate

The effects of feed flow rate at a fixed concentration and temperature were studied by altering the flow rate of the solution fed to the cell via a methanol syringe pump an ISCO Series D Model 1000D. Using a 5M solution of methanol, polarization plots were obtained using flow rates of 1 mL/min, 5 mL/min, 10 mL/min, and 15 mL/min. It was anticipated that the flow rate would not play much role in the performance of the electrolyzer, except at very small flow rates. This would be beneficial because more tests could be accomplished with the same amount of solution at a lower flow rate (pump reservoir capacity is 1000 mL). The polarization plots at different flow rates are displayed in Figure 4.2.

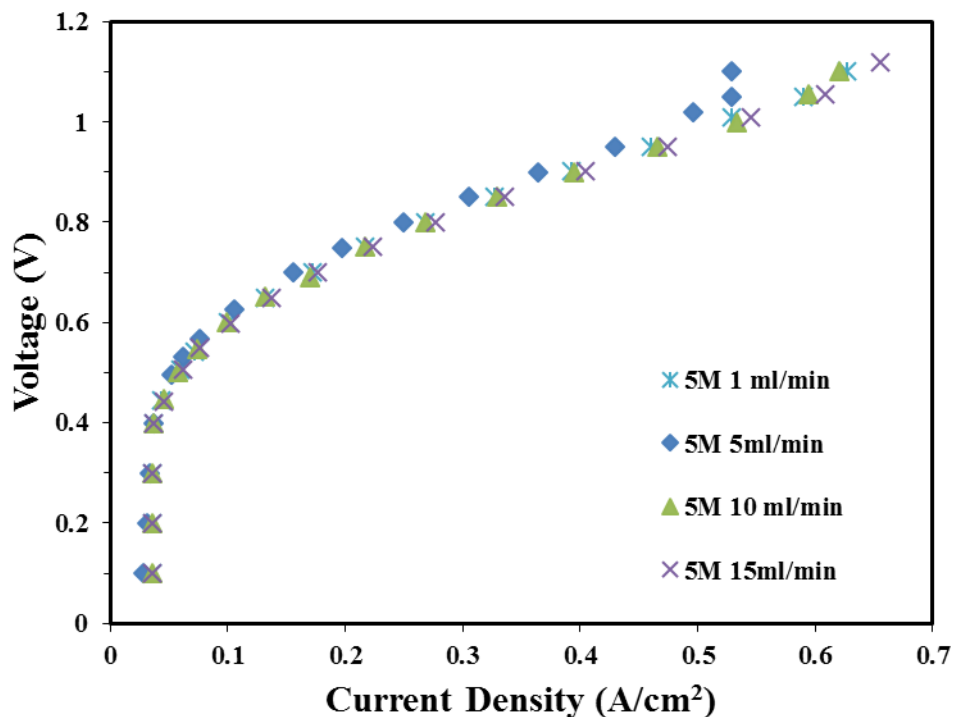


Figure 4.2: Effect of feed flow rate on the performance of the cell operating at 20 °C and a methanol concentration of 5 M.

As can be seen in the graph, the flow rate had very little effect on the overall performance of the cell. 1, 10, and 15 mL/min follow almost the same trend, however there were some differences, especially at the higher current densities, when at low flow rates methanol concentration can be depleted, as characterized by the S-shaped curve showing mass transfer limitations at higher current densities. Thus, the best performance was at the highest flow rate, 15 ml/min.

However, since these were the first set of experiments with a new MEA, and because the membrane was not fully “broken in,” the 5 mL/min test it was redone, and definitely an improvement in the performance was observed, as shown in Figure 4.3.

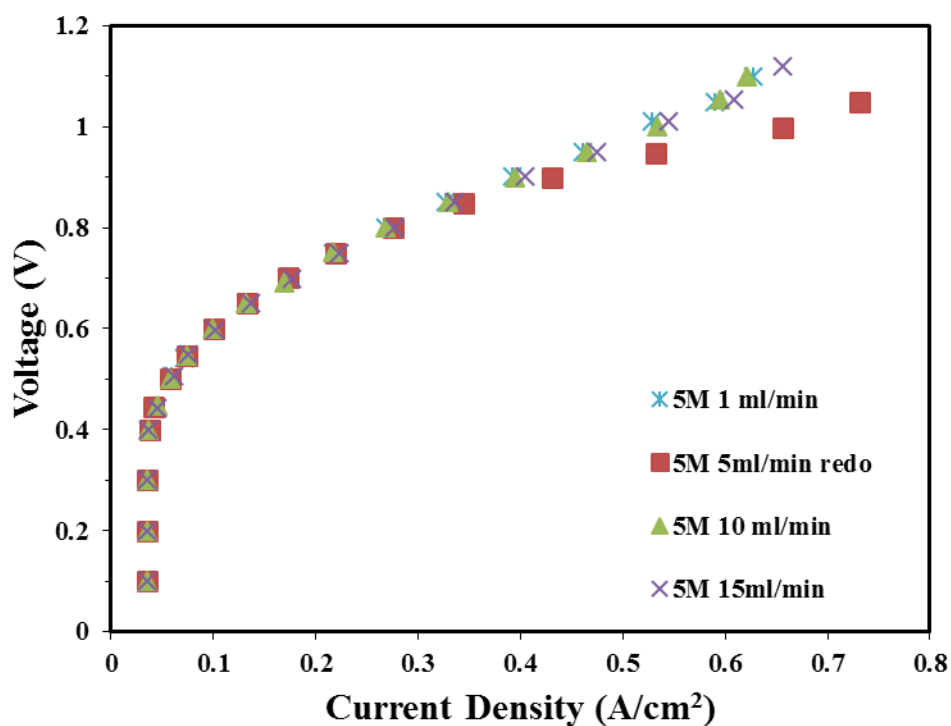


Figure 4.3: Repeat experiment of feed flow rate of 5mL/min on the performance of the cell operating at 20 °C and a methanol concentration of 5 M.

This occurred after multiple additional hours of testing, and shows the importance of fully preparing the membrane before accurate experiments can be conducted. It also shows how important it is to run all tests within the same time period or when the membrane is completely broken in. This avoids inevitable discrepancies and avoids additional uncertainty to the data sets.

4.1.2: Effect of Feed Concentration

In the literature on methanol electrolysis described in Chapter 2, concentration has been shown to be one a significant factor in affecting the performance of methanol electrolysis. Tests were thus conducted at various different concentrations in order to quantify this effect. Methanol

feed concentrations of 1M, 3M, 5M, and 10M were all first utilized at room temperature (20 °C) and a 10 ml/min flow rate. A polarization plot was created as shown in Figure 4.4.

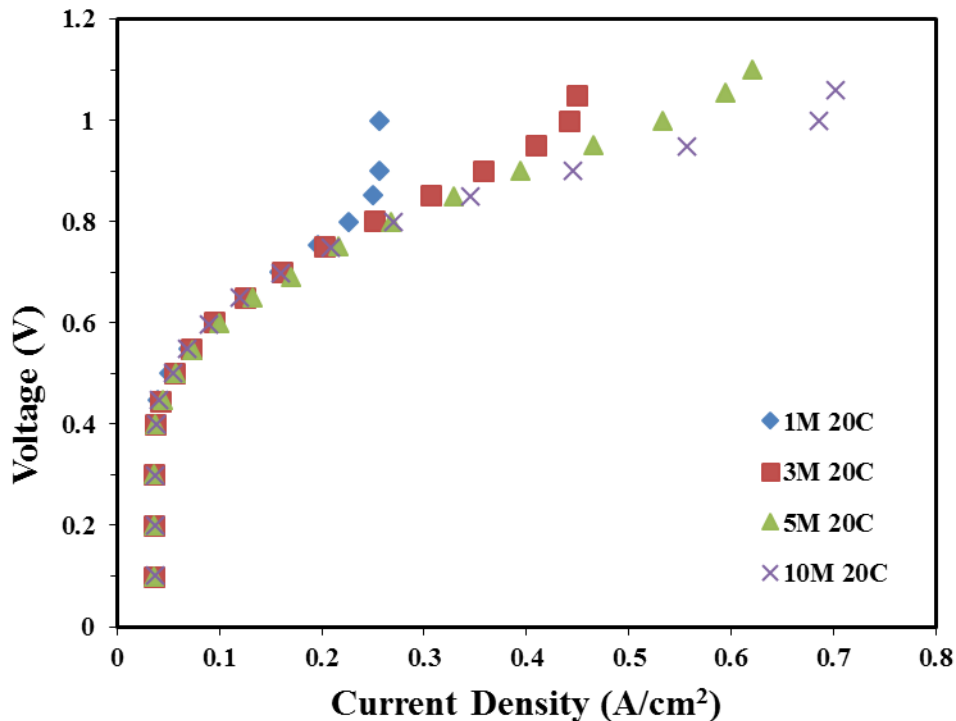


Figure 4.4: Effect of concentration at 20 °C and 10 ml/min flow rate.

Figure 4.4 shows that while the concentration has little effect at low current densities at 20 °C, the difference is significant at higher current densities. Thus, as the concentration increases, so does the highest current density for each run, correlating to more hydrogen being produced. At 1 V, thus, it can be seen that the 10M feed performance is almost 2 to 3 times better than the 1M solution. In part, this might be explained by a higher limiting current density (representing mass transfer limitations) at the higher concentrations. All the curves for the different concentrations eventually curve up, indicating transport limitations.

Based on these results, performance might have been expected to follow a similar trend at increased temperatures as well. However, this was not found to be the case, and performance differences at different feed concentrations followed various different trends as the operating temperature was gradually increased. Thus, provided in Figure 4.5 is a polarization plot displaying the effect of feed concentration at 30 °C.

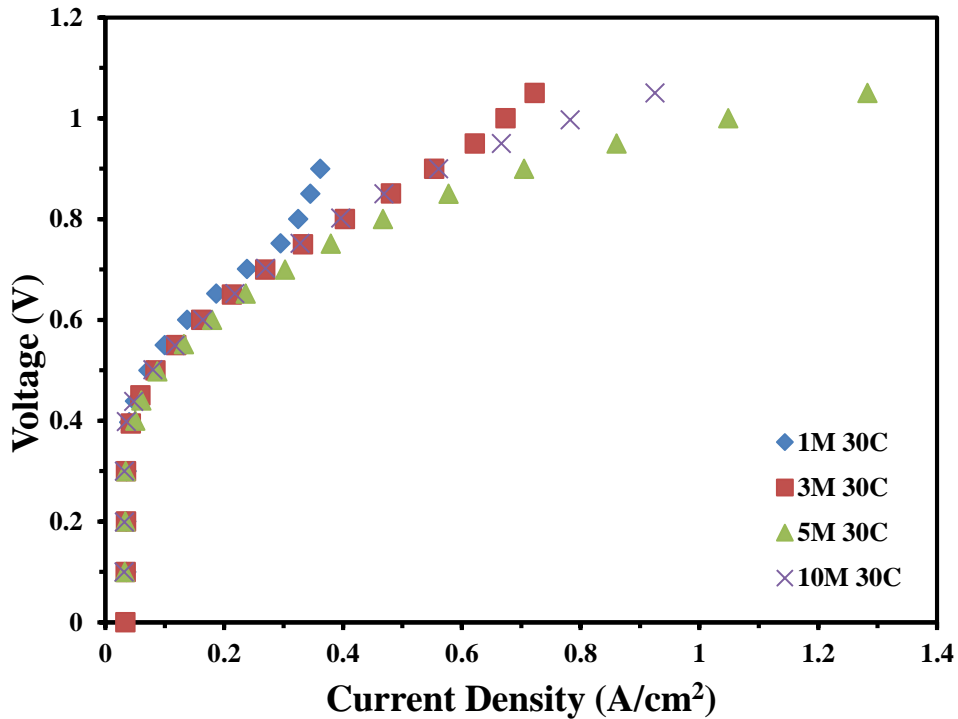


Figure 4.5: Effect of concentration at 30 °C and 10 ml/min flow rate.

Although this graph still shows rather similar trends as the previous one, it should be noted that in fact 5M performed much better than 10M at higher current densities at this temperature. The breaking in of the membrane can't be the presumed reason in this situation. This is because the 10M experiment was performed after the 5M run. Upon further investigation, these trends were also noticed in the Envirowerks tests, and alluded to in some of the literature as well. Take et.al.

(2007) proved that strong solutions (12M+) did not continue to prove the electrolyzers' performance. This is because the permeation of water becomes a mass transfer limitation in the cell. It could also be that depending on the temperature, beyond a certain concentration, kinetic considerations, e.g., anode self-poisoning through the intermediate CO, become more significant than any mass transfer limitations. Also, the 1M run was stopped early at 0.9 V because it was increasing in voltage without any gain in current density, i.e., it had reached a limiting current.

Next, each of the same feed concentrations were run at 40 °C and the polarization results are displayed in Figure 4.6.

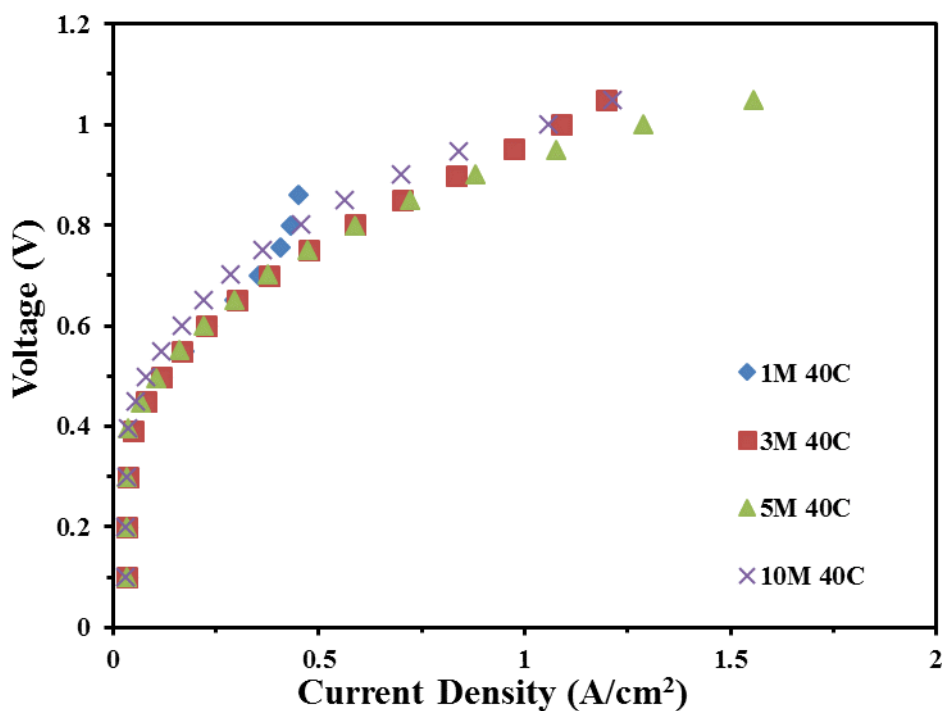


Figure 4.6: Effect of Concentration at 40 °C and 10 ml/min flow rate.

Again, as at 30 °C, the 5M feed still outperformed the 10M feed and even maxed out the testing system, limited to a total current of 10 A, at 1.05 V. In the absence of this instrumental limitation,

it is possible that the 5M experiment at 40 °C would have reached around 2 A/cm² at the upper operating voltage limit of 1.2 V (to avoid water electrolysis). It can also be seen that initially 3M starts off performing better than 10M, until at higher current densities where 10M performs slightly better than 3 M. It seems like 3M starts to curve upwards at around 0.95 V likely due to diffusion limitations, and it seems that if the experiments were carried out further 10M would provide a higher current density than the 3M feed. Nonetheless, almost equivalent performance for a much smaller methanol, makes 3M a better candidate than 10M feed at 40 °C. Following the 40 °C tests, the temperature was increased another ten degrees and the same experiments carried out. The results are shown in Figure 4.7.

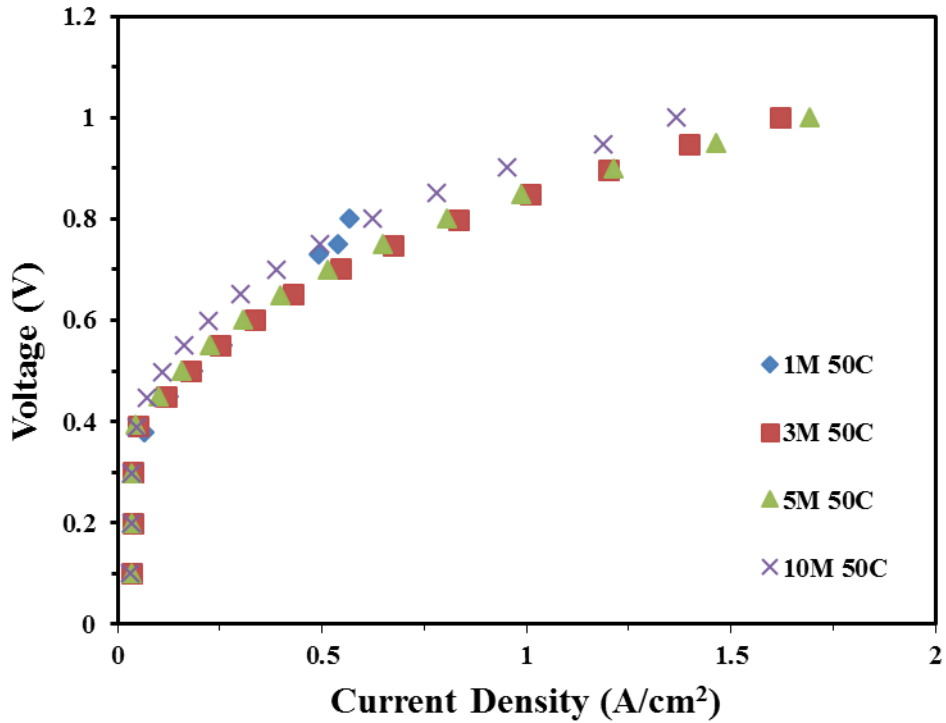


Figure 4.7: Effect of Concentration at 50 °C and 10 ml/min flow rate.

For this run 5M is still is the best concentration, maxing out the load box at 1 V. However, 3M feed showed the biggest gain in efficiency and performed almost the same as 5M for the majority of the run, with 10M not performing as well as either 3M or 5M. The 1M run again had to be stopped early again because of a max in current density again presumably because of transport limitations. The temperature of 60 °C was next tested with the same feed concentrations and the results are presented below in Figure 4.8.

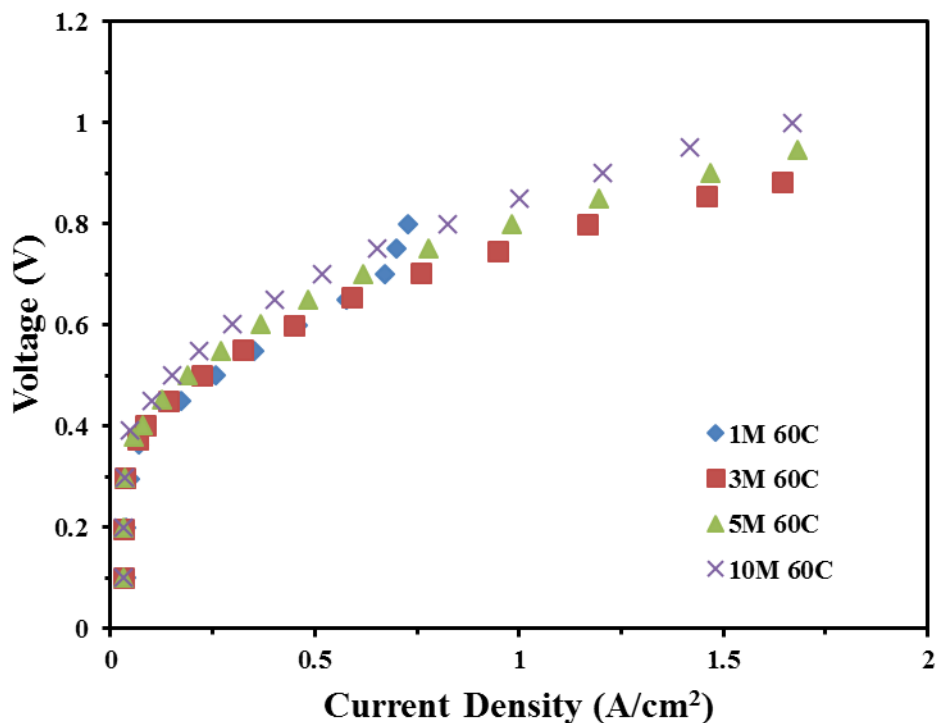


Figure 4.8: Effect of Concentration at 60 °C and 10 ml/min flow rate.

This graph presents a major turning point in the performance of the cell at varied concentrations. For this temperature, 3M proved to be the most efficient feed concentration and the most efficient run to this point. The 3M feed maxed out the load box at 0.882V for this run, while the 5M did that at 0.942 V. Although, 10M appears to perform better at 60 °C than at 50 °C, but it is still not the optimal feed concentration for this temperature. If 3M could be carried out all the way to 1.2V, the current density might have exceeded 2 A/cm². Because of this, it is believed that this is the most efficient temperature and concentration for the Nafion[®] 212 membrane based MEA. One last temperature, 70 °C, was finally tested for this system. The graph presented in Figure 1.9 shows the polarization data that was collected during the 70 °C run.

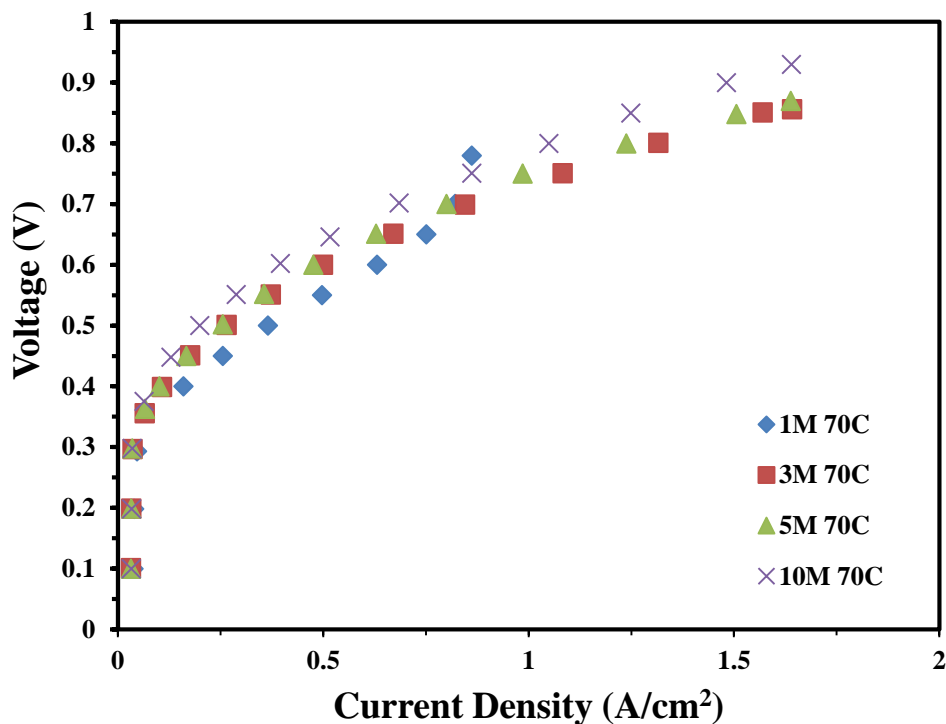


Figure 4.9: Effect of Concentration at 70 °C and 10 ml/min flow rate.

This final graph displays the same trends that were observed throughout these experiments. The 3M, 5M, and 10M feeds all showed slight increases in performance with an increase in temperature, with the best increase being 5M going from 0.942 to 0.87 V before the system current maxed out. Overall, it appears that a feed concentration of 3-5 M and an operating temperature of 60-70 °C are the best conditions to operate a methanol electrolyzer at.

4.1.2.1: Overall Discussion of the Effect of Feed Concentration

These non-intuitive effects observed on the performance of different feed concentrations at different temperatures in a methanol electrolyzer might be explicable based on an interplay between electrode kinetics (characterized exchange current density) and mass transfer limitations (characterized by limiting current density) and how they are individually affected by methanol

concentration and temperature. Let us try to explain the results with the help of some basic correlations in electrode kinetics.

The anode overpotential η_A may, e.g., be given by Rosenthal, N. S. et.al. (2012).

$$\eta_A = \frac{RT}{\alpha_A^* \nu_{A,e^-}^* F} \sinh^{-1} \left\{ \frac{1}{2} \left(\frac{i/i_{A,0}}{1 - i/i_{A,L}} \right) \right\} \quad (4.1)$$

where i is the current density, F is Faraday's constant, α_A^* is the symmetry factor and ν_{A,e^-}^* is the stoichiometric coefficient of electrons in the rate determining step in the MOR mechanism.

Further, in the above, the anode limiting current density depends on anode diffusion layer (ADL) effective permeability $P_{Me,D}^e$ and the methanol concentration in the bulk $c_{Me,b}$

$$i_{A,L} \equiv \left(\frac{\nu_{A,e^-}}{-\nu_{A,Me}} \right) F P_{Me,D}^e c_{Me,b} \quad (4.2)$$

corresponding to the maximum possible diffusion flux across the ADL, while the MOR exchange-current density that characterizes its kinetics

$$i_{A,0} = \gamma_{M,A} \frac{c_{Me,0}}{c_{Me,ref}} \left(\frac{1 - \theta_{CO \cdot S}}{1 - \theta_{CO \cdot S,ref}} \right) \exp \left[-\frac{E_{A,\Phi_0}}{R} \left(\frac{1}{T} - \frac{1}{T_{ref}} \right) \right] i_{A,0,ref}^* \quad (4.3)$$

where $c_{Me,0}$ is the anode catalyst layer concentration under equilibrium conditions, i.e.,

$c_{Me,0} = k_{Me,A} c_{Me,b}$, and the reference methanol concentration, $c_{Me,ref} = 1.0 \cdot 10^{-3}$ mol/cm³, or 1 M.

Assuming CO as the most abundant surface species on Pt, and its formation minimally affected by electrode potential, the fraction of Pt sites covered by CO, $q_{CO \cdot S}$, in the exchange-current density expression is assumed to be given by the Langmuir isotherm

$$q_{CO \cdot S} = \frac{K_{Me} c_{Me,0}}{1 + K_{Me} c_{Me,0}} \quad (4.4)$$

where the adsorption equilibrium constant is assumed to be that for CO adsorption on Pt

$$K_{\text{Me}} = 1.41 \times 10^{-8} \exp\left(\frac{130,000 \text{ J mol}^{-1}}{RT}\right) \quad (4.5)$$

Thus, on the whole, increasing methanol concentration at a given temperature positively impacts the limiting current density but may have an overall negative or effect on the exchange-current density depending on the temperature. Of course, it is also possible that the methanol crossover, which increases with methanol concentration, and its influence on cathode kinetics, may also be factor.

4.1.3 Effect of Temperature at a Given Concentration

The final aspect that was evaluated with single cell experiments was the effect of temperature on performance of the methanol electrolyzer at a given feed concentration. Previous literature has shown that an increase in temperature correlates to an increase in cell performance. The experiments done in this project follow the expected trend, and show sustained performance increasing with temperature at every feed concentration. For a 1M solution, thus, the peak current density increased from 0.26 A/cm² at 20 °C to 0.86 A/cm² at 70 °C, i.e., an enhancement of more than 3 times. At the upper limit of the applied voltages for low feed concentrations, the methanol depletion comes into play and the graphs curve sharply upward because of transport limitations. This can be clearly seen in the Figure 4.10, which shows all temperatures showing eventual diffusion limitation at this low concentration.

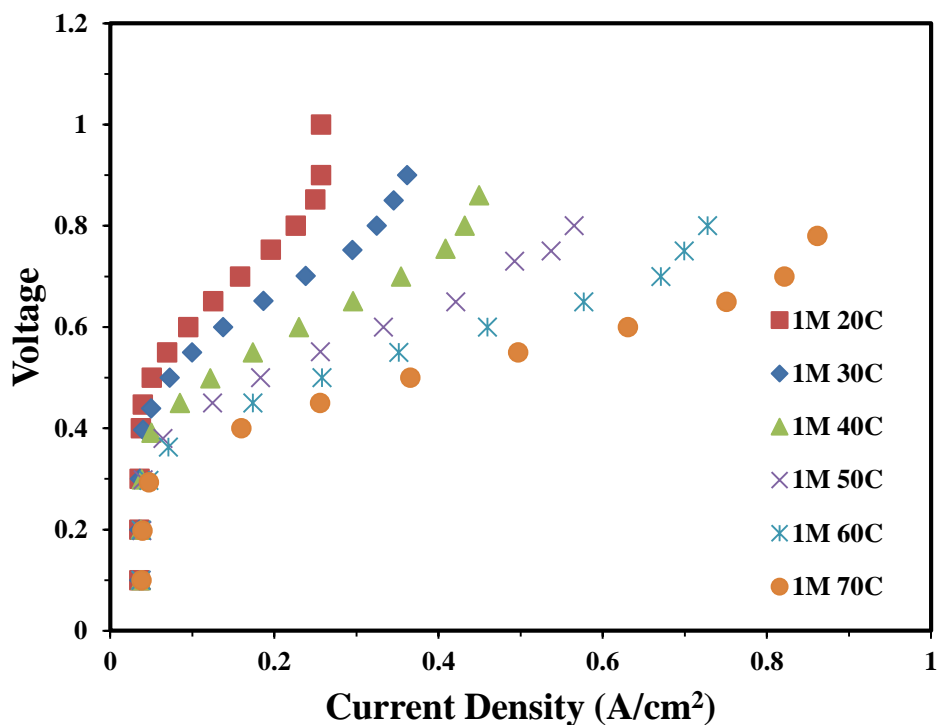


Figure 4.10: The effect of temperature on a 1M feed solution.

At the higher feed concentration of 3M, the current density increased from 0.305 to 1.64 A/cm² at a voltage of 0.85V. This is an increase of 1.335 A/cm² at the same voltage. Like in the 1 M solution, mass transfer limitations were evident at the lower temperatures, but had disappeared above 30 °C. In other words, feed concentrations above 3M are likely to be relatively free of transport limitations above 30 °C.

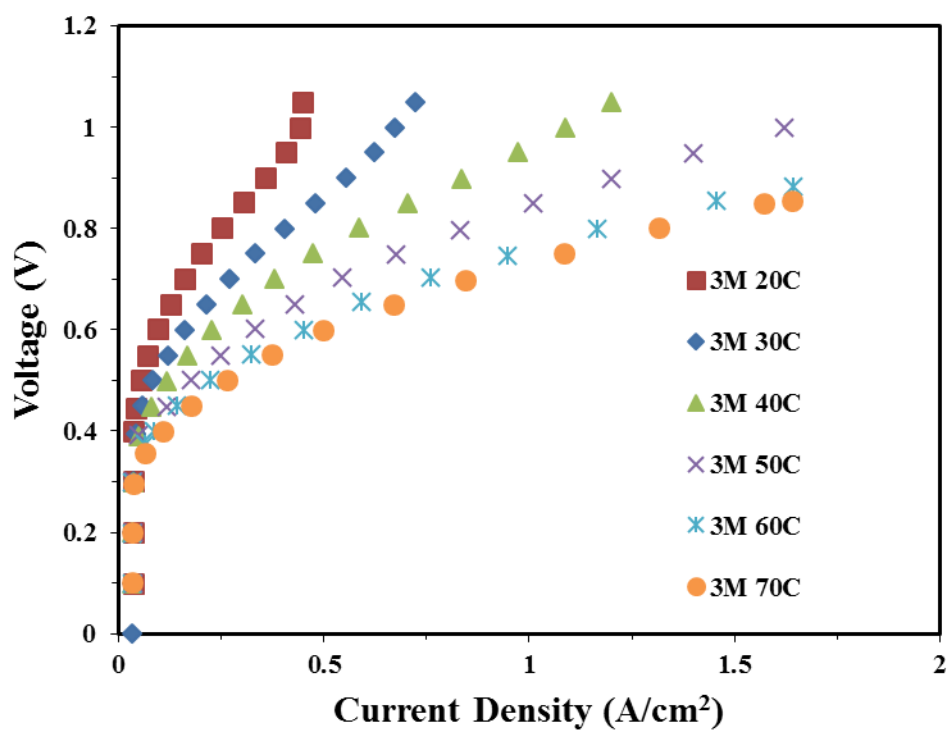


Figure 4.11: The effect of temperature on 3M solution.

Similarly, at 5 M feed concentration, the current density increased 1.331 A/cm^2 , from 0.33 A/cm^2 to 1.64 A/cm^2 at around $.85 \text{ V}$. The initial trial at $20 \text{ }^\circ\text{C}$ also experienced mass transfer limitations that were not seen at the higher temperatures.

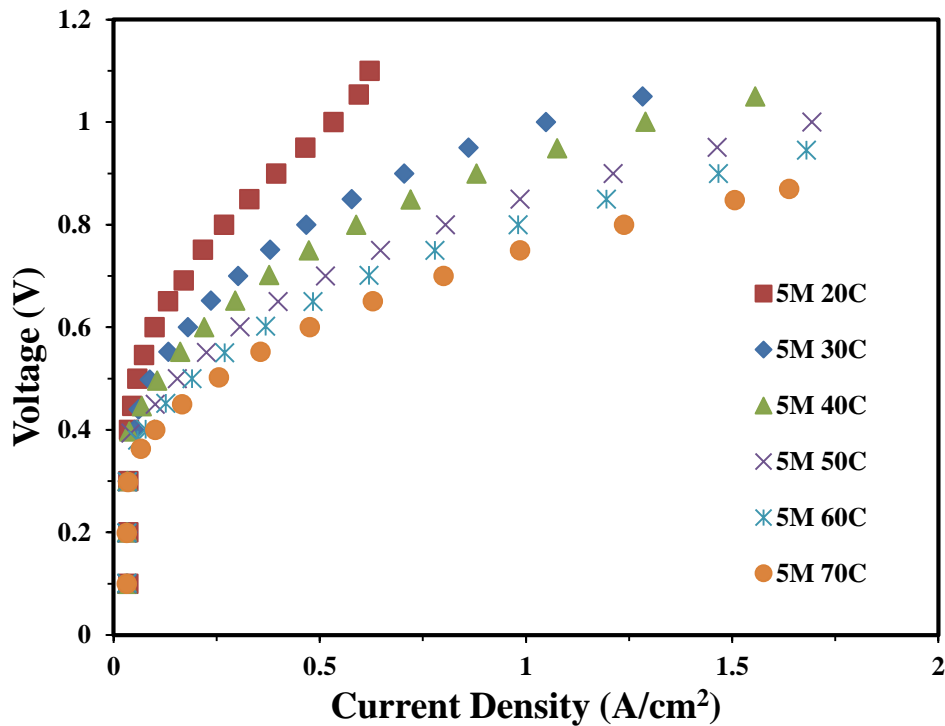


Figure 4.12: The effect of temperature on 5M solution.

Following the previous trend for other concentrations, the efficiency of the 10 M feed solution also increased monotonically as the temperature was increased. At 0.9 V, thus, the current density was recorded to be 0.45 A/cm² at 20 °C. At 70 °C, where the performance was the best, 0.9V produced 1.48 A/cm². This is an increase of 1.03 A/cm². It can also be seen that mass transfer limitations caused a sharp upward increase at the upper end of the voltage for the 20 °C test. This limitation is not seen at higher temperatures.

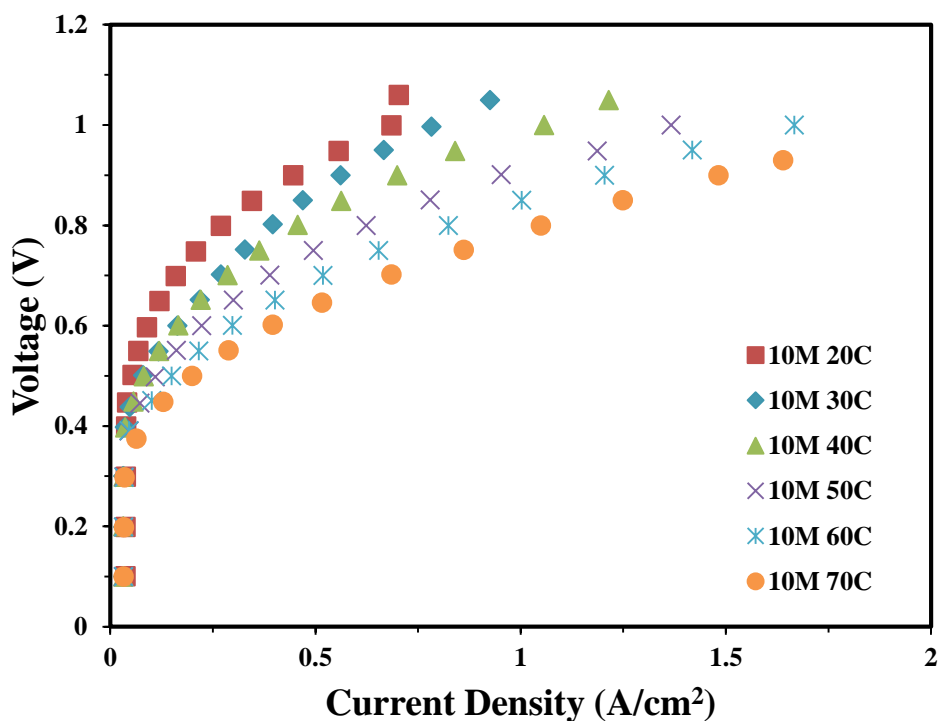


Figure 4.13: The effect of temperature on 10M solution.

Because of limitations of the testing set up, the maximum current of 10 A was reached at higher temperatures of the more concentrated solutions well below the upper voltage limit of 1.2V, not allowing for a determination of the highest current at the maximum voltage that can be utilized for methanol electrolysis. While the final current density at the limiting voltage could not be found for the more concentrated solutions, it can still be seen that temperature affects all of the solutions, with the largest impacts occurring in the 3M and 5M solutions.

While the increases in temperature from 20 °C to 70 °C were significant for all of the feed concentrations, the increases with temperatures were not all equal. For example in the 1M solution, at 0.8V the largest performance increase came by increasing the temperature from 50 °C to 60 °C, an increase of 0.16 A/cm². The smallest increase came from increasing from 20 °C to 30 °C with

an increase of 0.1 A/cm². This trend was repeated at 3M with the smallest increase being from 20 °C to 30 °C with an increase of 0.17 A/cm². The largest increase came again from 50 °C to 60 °C, with a current density increase of 0.45 A/cm². This trend varied slightly with the 5 M and 10 M experiments. In the 5 M tests, the largest increase in current density was from changing from 40 °C to 50 °C, with an increase of 0.33 A/cm². The smallest change came from increasing from 60 °C to 70 °C. This was a change of 0.174 A/cm². It should be noted however that while in 1M and 3 M the 20 °C to 30 °C increase was the smallest, it was the second largest increase for 5 M, being 0.309 A/cm². During the 10 M test, the largest increase was during the increase from 60-70 °C, with an increase of 0.277 A/cm². Like 1 M and 3 M feeds, the change from 20 °C to 30 °C had the least effect on the efficiency of the 10M feed with an increase of 0.115 A/cm².

4.1.3.1: Overall Discussion of the Effect of Operating Temperature

Understanding the effect of operating temperature on the performance of the methanol electrolyzer is more straightforward than that for the effect of feed concentration. With an activation energy of around $E_{A,\Phi_0} = 65$ kJ/mol (Rosenthal et al., 2013), the kinetics of the MOR, and hence its exchange current density (Eq. 4.3), rapidly improves with rising temperature. This is further abetted by a reduction in the fraction of Pt sites covered by CO, $q_{CO,S}$, with temperature, as indicated by Eqs. (4.4) and (4.5). Further, the ADL permeability improves with temperature and hence so does the limiting current density with temperature, although not quite as rapidly as the exchange current density. As a result for any given feed concentration, there is a monotonic increase in performance with temperature.

4.2 Performance of the Standalone Solar Powered System

Because of the cloudy nature of Worcester's weather during the winter months of early 2016, the standalone system could only be tested for a limited time. Once a suitably sunny day had

presented itself, the system was placed facing the sun and the data acquisition system was attached to a computer to log the data, tracking the cell voltage, current supplied, cell temperature, ambient temperature, and hydrogen column pressure. Over a three-hour span, this data was logged as hydrogen, had already been, and still was being produced.

4.2.1 System Pressure

As hydrogen was being produced and stored in the hydrogen column, pressure was being built. It quickly reached 42 psig before a leak sprung in the PTFE that sealed the column. This can be seen in Figure 4.14.

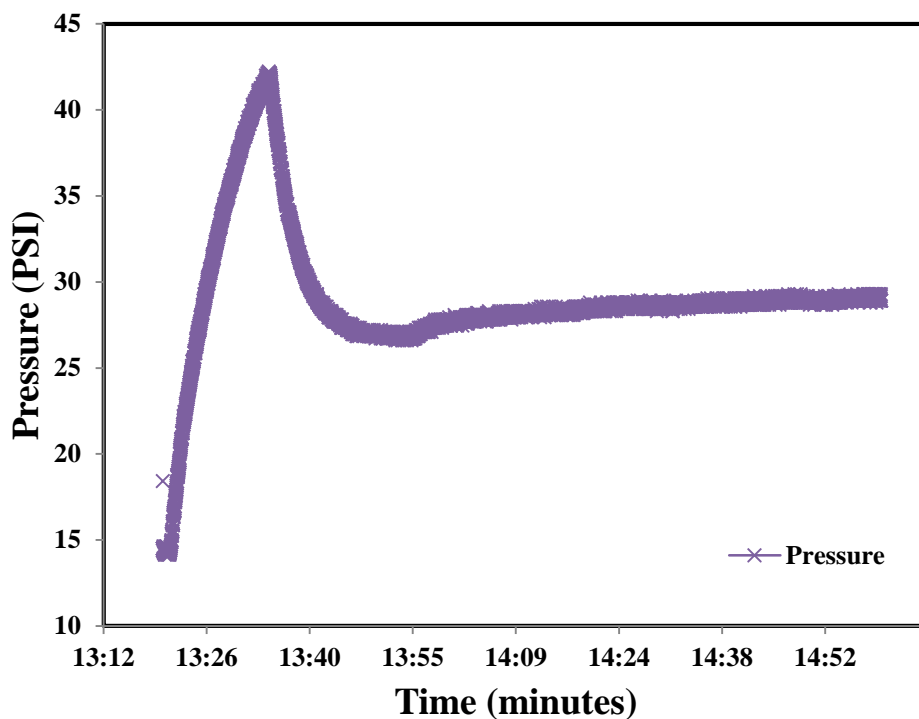


Figure 4.14: Column pressure as a function of time, before and after a leak.

Once the seal sprung the leak, the pressure rapidly dropped to under 27 Psig and slowly rose back up to 29 Psig where it leveled out, with the rate of leak and rate of production of hydrogen

balancing out. It is not known what the maximum pressure would have been with this single cell setup.

4.2.2 System Temperature

Throughout the course of these tests, the temperature of the cell and that of the surroundings was recorded. The cell was consistently at a somewhat higher temperature than the surroundings because the reaction is exothermic and therefore heated the cell. As the ambient temperature and the internal cell temperature increased, the rate of the reaction increased, in accordance with the single cell results. This in turn caused the cell to produce more heat, increasing the temperature difference between the cell and the surrounding environment. In the beginning of the test, the temperature difference was 6.6 °C, and as the time went on, it peaked at 14 °C. Averages of the internal cell temperature, the ambient temperature, and their temperature difference are plotted as a function of time in Figure 4.15.

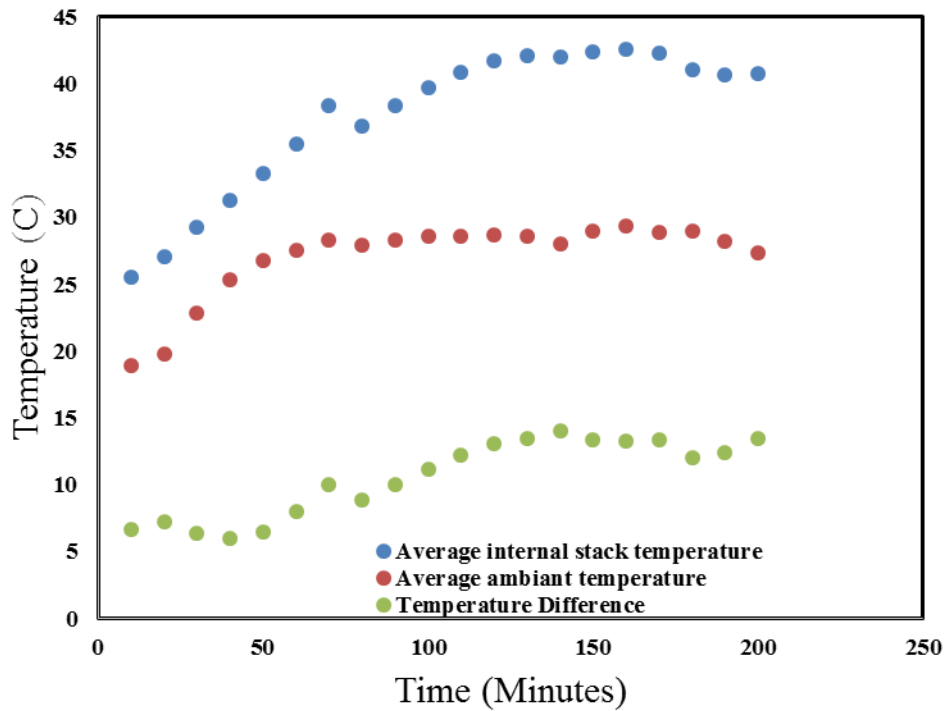


Figure 4.15: Recorded cell and ambient temperature data from the standalone solar powered methanol electrolysis system.

4.2.3 System Voltage and Current Density

While the system was designed with potentiometers to alter the current and voltage, they were not functioning properly when these tests occurred. Because of this, the system was set at constant values for the current and voltage. Because of clouds, and the changing angle of the sun, the amount of light that the solar panel received varied throughout the day. While it was expected to cause a large change in the power provided to the cell, it did not vary as greatly as might have been expected. This can be seen in Figure 4.16. Throughout the course of the experiment, the average voltage changed 0.03V and the average current density changed 0.115 A/cm².

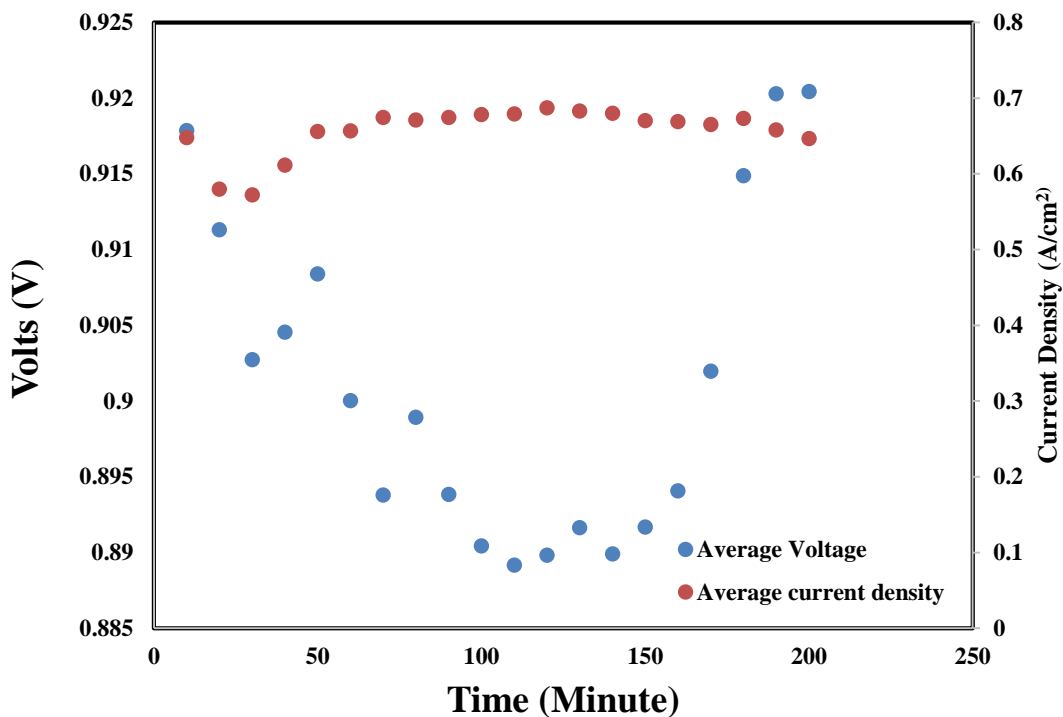


Figure 4.16: Average voltage and current density of the solar powered system between 25 °C and 40 °C

4.3 Concluding Remarks

Overall, it may be said that even though the original set of goals were perhaps overly ambitious and could not all be attained, the project was fundamentally successful in its main goals of both investigating the performance of the single cell methanol electrolyzer under a variety of operating conditions, and also in designing, constructing, and testing evidently the first solar powered methanol electrolyzer reported.

Chapter 5. Conclusions and Recommendations for Future Work

5.1 Single Cell Methanol Electrolyzer Performance

After analysis of the experimental data with the single cell, conclusions can be drawn regarding how altering operating conditions affect the methanol electrolyzer performance. It was found that increasing temperature and concentration changed the way the cell performs. Thus, while at room temperature, increasing concentration monotonically increases the performance of the cell. This trend, however, does not continue at elevated temperatures. As temperature increased, 5 M feed became higher performing than the 10 M feed, and after 40 °C, 3 M feed also became more efficient than the 10 M methanol feed. The best overall performance was found using a 3 M solution at 70 °C, while it is believed that the most optimal condition is 3 M at 60 °C. This is because of the lower cost of heating the solution to 60 than 70 °C, and the expected increased longevity of the membrane due to the milder operating temperature coupled with lower methanol concentrations. Higher methanol concentrations and higher operating temperatures can degrade the membrane more quickly.

Additionally, it can be concluded that for a given concentration, increasing the temperature increased the performance monotonically. The increase in performance was not equal however, with 3M and 5M displaying higher performance increases than 1M and 10M. The increase in performance at each temperature change was not equal as well. For 1M, 3M, and 10M, the greatest increase was in the upper temperature range, with 1M and 3M showing the best increase by changing from 50 °C to 60 °C, and 10M showing the best performance increase by changing from 60 °C to 70 °C. The 5M feed had the greatest change in performance when increasing the temperature from 20 °C to 30 °C.

It can also be concluded that there is a limit to the amount of current that can be added to the cell at certain temperatures and concentrations. For example in the 1M experiments, all of the tests were stopped between 0.8V and 0.9V, instead of going to higher voltages, as in other tests. This is because at lower concentrations all the methanol is depleted quicker than at higher concentrations. Mass transfer limitations also occurred at higher concentrations and lower temperatures. This is because the temperature did not allow electrolysis to occur as fast as the methanol was being brought into the system.

5.2 Standalone Solar Powered Methanol Electrolyzer System

While solar powered methanol electrolysis has been theorized in academic literature, it has apparently not been experimentally implemented prior to this project. Although polarization plots could not be generated from the data acquisition system that was used in the setup, valuable information was still gained, as well as proving the concept that hydrogen can be readily generated directly via solar power. Thus, a considerable buildup of pressure was accomplished in the hydrogen column as well as across the MEA. This shows that the hydrogen that is produced can be pressurized for use without using externally powered compressors. It also shows that by pressurizing the membrane, crossover is limited, increasing the performance and efficiency of the cell. This passive system also demonstrated that the solution can be fed into the cell via gravity, eliminating the need for a pump, thus simplifying the system and making it more efficient. The standalone system that was constructed and tested shows promise that with improvements, solar powered methanol electrolysis is a viable method of hydrogen production.

5.3 Recommendations for Future Work

Because of limited time constraints, not all of the originally planned experiments could be performed. One recommendation that can be made is finishing the test stand for the four individual

cells. By having access to this system, many more experiments could be conducted at once, allowing for far more extensive testing of various MEAs, membranes, and catalysts simultaneously, both in terms of performance and durability, in order to determine the optimal design of the methanol electrolyzer. Planned experiments that did not occur included using Nafion[®] 212, 115, 117 and XL membranes, with experiments run at 25, 45, 55, 65, and 75 °C as well as additional methanol concentrations to further optimize the operating conditions. With access to this system, future projects could be done on this system for many years to come.

If the four-cell test stand cannot be completed, then more operating conditions should be investigated by using the test set up in the FCC. For example, further tests at higher concentrations and higher temperatures can be done. Another recommendation for running tests in the FCC would be to obtain load box that allows an increase in the upper limit of the current that can be applied to the cell. Because of the limited current allowed, the upper limits of the 3M and 5M test could not be seen in the experiments reported here. Heating methods for the cell is another area where improvements could be made for controlling the cell temperature. While using the furnace worked for the tests that were done, it was a slightly difficult procedure that frequently caused the methanol temperature to go over the desired temperature.

Substantial future work could be carried out on with the solar powered electrolyzer system with improved design and components. By adding a mass flow meter to the system, data could be collected on how much hydrogen and carbon dioxide is being produced. With this data it could be determined whether the amount of hydrogen produced is more or less energy dense than the solar power that was put in to make it. Additionally, a solar heater would make the system more efficient. From there optimization of the system could occur in attempt to produce more hydrogen at similar operating conditions. Finally improved components could allow for polarization plots to be

generated for the solar methanol electrolyzer in order to more fully analyze and optimize the system's performance.

References

- Albo, J., Alvarez-Guerra, M., Castaño, P., & Irabien, A. (2015). Towards the electrochemical conversion of carbon dioxide into methanol. *Green Chemistry*, *17*(4), 2304-2324.
- Avasarala, B., & Haldar, P. (2009). Effect of surface roughness of composite bipolar plates on the contact resistance of a proton exchange membrane fuel cell. *Journal of Power Sources*, *188*(1), 225-229.
- Bi, W., & Fuller, T. F. (2008). Modeling of PEM fuel cell Pt/C catalyst degradation. *Journal of Power Sources*, *178*(1), 188-196. doi:10.1016/j.jpowsour.2007.12.007
- Bockris, J. O. (1975). *Energy: The Solar-Hydrogen Alternative*, Wiley, New York.
- California Hydrogen Business Council (2015), Power-to-Gas: The Case for Hydrogen White Paper, Los Angeles.
- Brown, L. F. (2001). A comparative study of fuels for on-board hydrogen production for fuel-cell-powered automobiles. *International Journal of Hydrogen Energy*, *26*(4), 381-397.
- Centi, G., & Perathoner, S. (2011). CO₂-based energy vectors for the storage of solar energy. *Greenhouse Gases: Science and Technology*, *1*(1), 21-35.
- Cloutier, C. R., & Wilkinson, D. P. (2010). Electrolytic production of hydrogen from aqueous acidic methanol solutions. *International Journal of Hydrogen Energy*, *35*(9), 3967-3984.
- Crabtree, G. W., Dresselhaus, M. S., & Buchanan, M. V. (2004). The hydrogen economy. *Physics Today*, *57*(12), 39-44.
- Datta, R., Martino, D. J., Dong, Y., & Choi, P. (2015). "Modeling of PEM Water Electrolyzer." In D. Bessarabov, H. Wang, H. Li, & N. Zhao (Eds.), *PEM Electrolysis for Hydrogen Production: Principles and Applications* (pp. 243-267). CRC Press.

- Dhar, B. M. (2013). How Do Solar Panels Work? by Live Science. Retrieved from <http://www.livescience.com/41995-how-do-solar-panels-work.html>
- Dunn, B., Kamath, H., & Tarascon, J. M. (2011). Electrical energy storage for the grid: a battery of choices. *Science*, 334(6058), 928-935.
- EIA (2011), <https://www.eia.gov/todayinenergy/detail.cfm?id=830>
- Elam, C. C., & Gregoire Padro, C. E. (2001). IEA agreement on the production and utilization of hydrogen: 2000 annual report.
- Florida Solar Energy Center. (n.d.). Hydrogen Basics - Production. Retrieved from <http://www.fsec.ucf.edu/en/consumer/hydrogen/basics/production.htm>
- Forbes *Why are solar panels so inefficient?* (2013, November 4)
- Fuel Cell Etc. (n.d.). Membrane. Retrieved from <http://fuelcellsetc.com/store/Nafion>
- Ganesh, I. (2014). Conversion of carbon dioxide into methanol—a potential liquid fuel: Fundamental challenges and opportunities (a review). *Renewable and Sustainable Energy Reviews*, 31, 221-257.
- Guenot, B., Cretin, M., & Lamy, C. (2015). Clean hydrogen generation from the electrocatalytic oxidation of methanol inside a proton exchange membrane electrolysis cell (PEMEC): effect of methanol concentration and working temperature. *Journal of Applied Electrochemistry*, 45(9), 973-981.
- Gumilar, A. (n.d.). Chemical Engineering Processing: Hydrogen Production By Steam Reforming. Retrieved from <http://chemeng-processing.blogspot.com/2010/05/hydrogen-production-by-steam-reforming.html>

- Halme, A., Selkäinen, J., Noponen, T., & Kohonen, A. (2016). An alternative concept for DMFC–Combined electrolyzer and H₂ PEMFC. *International Journal of Hydrogen Energy*.
- Hu, Z., Wu, M., Wei, Z., Song, S., and Shen, P. K., “Pt-WC/C as a Cathode Electrocatalyst for Hydrogen Production by Methanol Electrolysis,” *J. Power Sources*, **166**, 458-461 (2007).
- Hydrogenics. (2013). Electrolysis. Retrieved from <http://www.hydrogenics.com/technology-resources/hydrogen-technology/electrolysis>
- Jeffries-Nakamura, B., Narayanan, S. R., Valdez, T. I., and Chun, W., “Making Hydrogen by Electrolysis of Methanol,” NASA TECH BRIEF, **26**, No. 6 from JPL NEW TECHNOLOGY REPORT NPO-19948 (2002).
- Jentsch, M., Trost, T., & Sterner, M. (2014). Optimal use of power-to-gas energy storage systems in an 85% renewable energy scenario. *Energy Procedia*, *46*, 254-261.
- Jones, J. P., Prakash, G. K., & Olah, G. A. (2014). Electrochemical CO₂ reduction: recent advances and current trends. *Israel Journal of Chemistry*, *54*(10), 1451-1466.
- Jones, Geoffrey, and Loubna Bouamane. "Power from Sunshine': A Business History of Solar Energy." Harvard Business School Working Paper, No. 12–105, May 2012.
- Koraishy, B., Meyers, J. P., & Wood, K. L. (2009). *Manufacturing of membrane electrode assemblies for fuel cells* [Scholarly project]. In *Singapore University of Technology & Design*. Retrieved from http://www.sutd.edu.sg/cmsresource/idc/papers/2009-_Manufacturing_of_membrane_electrode_assemblies_for_fuel_cells.pdf
- Larminie, J., & Dicks, A. (2003). *Fuel cell systems explained*. West Sussex, England: John Wiley & Sons Ltd.

- Lamy, C., Guenot, B., Cretin, M., & Pourcelly, G. (2015a). Kinetics analysis of the electrocatalytic oxidation of methanol inside a DMFC working as a PEM electrolysis cell (PEMEC) to generate clean hydrogen. *Electrochimica Acta*, *177*, 352-358.
- Lamy, C., Guenot, B., Cretin, M., & Pourcelly, G. (2015b). (Invited) A Kinetics Analysis of Methanol Oxidation under Electrolysis/Fuel Cell Working Conditions. *ECS Transactions*, *66*(29), 1-12.
- Lamy, C., Jaubert, T., Baranton, S., & Coutanceau, C. (2014). Clean hydrogen generation through the electrocatalytic oxidation of ethanol in a Proton Exchange Membrane Electrolysis Cell (PEMEC): Effect of the nature and structure of the catalytic anode. *Journal of Power Sources*, *245*, 927-936.
- Lee, J. (2015, June 12). Is Solar Energy Sustainable? 4 Problems to Solve Before the Solar Revolution. Retrieved from <http://www.makeuseof.com/tag/solar-energy-sustainable-4-problems-stop-solar-revolution-tracks/>
- Lucas-Consuegra, A. D., Calcerrada, A., Osa, A. D., & Valverde, J. (2014). Electrochemical reforming of ethylene glycol. Influence of the operation parameters, simulation and its optimization. *Fuel Processing Technology*, *127*, 13-19.
- Mazloomi, K., Sulaiman, N. B., & Moayedi, H. (2012). Electrical efficiency of electrical hydrogen production. *International Journal of Electrochemical Science*, *7*, 3314-3326.
- Mitlitsky, F., Myers, B., and Weisberg, A. H., "Regenerative Fuel Cell Systems," *Energy & Fuels*, **12**, 56 (1998).
- Marbán, G., & Valdés-Solís, T. (2007). Towards the hydrogen economy? *International Journal of Hydrogen Energy*, *32*(12), 1625-1637.

- Muthumeenal, A., Pethaiah, S. S., & Nagendran, A. (2016). Investigation of SPES as PEM for hydrogen production through electrochemical reforming of aqueous methanol. *Renewable Energy*, *91*, 75-82.
- Narayanan, S. R., Chun, W., Jeffries-Nakamura, B., and Valdez, T. I U.S. Patent 6299744 (2001).
- Narayanan, S. R., Chun, W., Jeffries-Nakamura, B., and Valdez, T. I., “Hydrogen Generation by Electrolysis of Aqueous Organic Solutions,” U.S. Patent No. 6,432,284 B1, Aug. 13 (2002).
- NYSERDA. (2005). *Hydrogen Production – Steam Methane Reforming (SMR)* [Pamphlet]. Albany, NY: New York State Energy Research and Development Authority.
- Office of Energy Efficiency & Renewable Energy. (2006, May). *Equipment design and cost estimation for small modular biomass systems, synthesis gas cleanup, and oxygen separation equipment*. San Francisco, CA: Nexant Inc.
- Olah, G. A. (2005). Beyond oil and gas: the methanol economy. *Angewandte Chemie International Edition*, *44*(18), 2636-2639.
- Olah, G. A., Goeppert, A., & Prakash, G. S. (2008). Chemical recycling of carbon dioxide to methanol and dimethyl ether: from greenhouse gas to renewable, environmentally carbon neutral fuels and synthetic hydrocarbons. *The Journal of organic chemistry*, *74*(2), 487-498.
- Olah, G. A., Goeppert, A., & Prakash, G. S. (2011). *Beyond oil and gas: the methanol economy*. John Wiley & Sons.
- Palo, D. R., Dagle, R. A., & Holladay, J. D. (2007). Methanol steam reforming for hydrogen production. *Chemical Reviews*, *107*(10), 3992-4021.

- Perma Pure. (n.d.). All About Nafion. Retrieved from <http://www.permapure.com/resources/all-about-nafion-and-faq/>
- Pham, A. T., Baba, T., & Shudo, T. (2013). Efficient hydrogen production from aqueous methanol in a PEM electrolyzer with porous metal flow field: Influence of charge in grain diameter and material of porous metal flow field. *International Journal of Hydrogen Energy*, (38), 9945-9953.
- Pure Energies. (n.d.). Solar Trackers: Are they worth it? Retrieved from <https://pureenergies.com/us/how-solar-works/solar-trackers/>
- Rosenthal, N. S., Vilekar, S. A., & Datta, R. (2012). A comprehensive yet comprehensible analytical model for the direct methanol fuel cell. *Journal of Power Sources*, 206, 129-143.
- Rostrup-Nielsen, J. R., & Rostrup-Nielsen, T. (2002). Large-scale hydrogen production. *Cattech*, 6(4), 150-159.
- Rostrup-Nielsen, T. (2005). Manufacture of hydrogen. *Catalysis Today*, 106(1-4), 293-296.
- S.A. Grigoriev, V.I. Poremsky, V.N. Fateev, *Int. J. Hydrogen Energy* 31(2006) 171.
- Sasikumar, G., Muthumeenal, A., Pethaiah, S., Nachiappan, N., and Balaji, R., "Aqueous Methanol Electrolysis Using Proton Conducting Membrane for Hydrogen Production," *Int. J. Hydrogen Energy*, **33**, 5905 – 5910 (2008).
- Schlapbach, L., & Züttel, A. (2001). Hydrogen-storage materials for mobile applications. *Nature*, 414(6861), 353-358.
- Sethu, S. P., Gangadharan, S., Chan, S. H., & Stimming, U. (2014). Development of a novel cost effective methanol electrolyzer stack with Pt-catalyzed membrane. *Journal of Power Sources*, 254, 161-167.

- Stephan, D. W. (2013). Catalysis: A step closer to a methanol economy. *Nature*, 495(7439), 54-55.
- Stoll, R. E., & von Linde, F. (2000). Hydrogen-what are the costs? *Hydrocarbon Processing*, 42-45.
- Take, T., Tsurutani, K., and Umeda, M., “Hydrogen Production by Methanol-Water Solution Electrolysis,” *J. Power Sources*, **164**, 9-16 (2007).
- Tang, H., Peikang, S., Jiang, S. P., Wang, F., & Pan, M. (2007). A degradation study of Nafion proton exchange membrane of PEM fuel cells. *Journal of Power Sources*, 170(1), 85-92. doi:10.1016/j.jpowsour.2007.03.061
- Tawfik, H., Hung, Y., & Mahajan, D. (2007). Metal bipolar plates for PEM fuel cell—A review. *Journal of Power Sources*, 163(2), 755-767.
- Thanasilp, S., & Hunsom, M. (2010). Effect of MEA fabrication techniques on the cell performance of Pt-PD/C electrocatalyst for oxygen reduction in PEM fuel cell. *Fuel*, 89(12), 3847-3852.
- Tuomi, S., Santasalo-Aarnio, A., Kanninen, P., & Kallio, T. (2013). Hydrogen production by methanol–water solution electrolysis with an alkaline membrane cell. *Journal of Power Sources*, 229, 32-35.
- Uhm, S., Jeon, H., Kim, T. J., & Lee, J. (2012). Clean hydrogen production from methanol-water solutions via power-saved electrolytic reforming process. *Journal of Power Sources*, (198), 218-222.
- US DOE, *Bottling Electricity: Storage as a Strategic Tool for Managing Variability and Capacity Concerns in the Modern Grid*, Report of Electricity Advisory Committee, (2008).

US Dept. of Energy. (n.d.). Hydrogen Production: Natural Gas Reforming. Retrieved from <http://energy.gov/eere/fuelcells/hydrogen-production-natural-gas-reforming>, (2004)

US Department of Energy, *Grid Energy Storage*, http://www.sandia.gov/ess/docs/other/Grid_Energy_Storage_Dec_2013.pdf

Vilekar, S. A., Fishtik, I., & Datta, R. (2007). Topological analysis of catalytic reaction networks: Methanol decomposition on Pt (111). *Journal of Catalysis*, 252(2), 258-270.

Wikipedia (2016), *Energy Density*.

Yu, S., Li, X., Li, J., Liu, S., Lu, W., Shao, Z., & Yi, B. (2013). Study on hydrophobicity degradation of gas diffusion layer in proton exchange membrane fuel cells. *Energy Conversion and Management*, 76, 301-306.

Zhang, J., Thampan, T., & Datta, R. (2002). Influence of anode flow rate and cathode oxygen pressure on CO poisoning of proton exchange membrane fuel cells. *Journal of The Electrochemical Society*, 149(6), A765-A772.

Appendices

Standalone System Working Arduino Code:

```
// Arduino Data Acquisition Code by OPL II

// setup

void setup() {

  // initialize serial communication at 9600 bits per second:
  Serial.begin(9600);
}

// Data acquisition loop

void loop() {

  // read the input on analog pin 1:
  int CellVolt = analogRead(A1);
  float Voltage = CellVolt * (5.0 / 1023.0); //Hopefully we dont go over voltage
  int Current1 = analogRead(A0);
  float Current11 = Current1 * (5.0 / 1023.0); //DC DC converter voltage read
  float CurrentA = ((Current11-1.256)/(0.024167));
  int Current2 = analogRead(A2);
  float Current22 = Current2 * (5.0 / 1023.0); // post stack current measurement
  float CurrentB = (-1*((Current22/13.2)-37.8787)); //issue with sensor, removed

  int CellTemp = analogRead(A3); //Stack Temperature measurement
  float Vout = CellTemp * (5.0 / 1023.0);
  float R1 = (1000*((5/Vout)-1));
```

```

double LogR1 = log (R1);
double Log3 = pow (LogR1,3);
float StackTemperatureK = 1/(0.001032+(0.0002387 * LogR1)+(0.000000158* Log3));
float StackTemperatureC = (StackTemperatureK-273.15)-3.29; // corrected Thermistor reading

int H2Pres = analogRead(A4); // Column pressure measurement

float ColumnPress = H2Pres * (5.0 / 1023.0);

float Pressure = (ColumnPress*25) -(12.5);

int Ambienttemp= analogRead(A5);// thermistor located on breadboard

float AmbientTemperature= (Ambienttemp * (5.0 / 1023.0)-.5)*100;

Serial.print(Voltage);

Serial.print(",");

Serial.print(CurrentA);

Serial.print(",");

Serial.print(StackTemperatureC);

Serial.print(",");

Serial.print(Pressure);

Serial.print(",");

Serial.print(AmbientTemperature);

Serial.println(","); // print out the values we have

delay(1000); // One set of data per second

}

```

Step-by-Step Assembly of the Stack

1. The thickness of the entire stack was determined and four pieces of PFA Heat shrink were cut to just shorter than that length.
2. The insulating PFA heat shrink was then applied to four ¼” threaded clamping bolts.
3. Next a thick metal clamping washer followed by an insulating fiberglass washer were added to each bolt.
4. Each bolt was then pushed through one of four pre-drilled corner holes in the bottom titanium clamping plate.
5. The hydrogen side (cathode) bipolar flow plate was then added on top of the titanium clamping plate.
6. Pre-cut 15/1000” thick PTFE gasket, for the GDL Support Seal, is then slid onto the clamping bolts.
7. Pre-Cut gold plated mesh, for GDL support, is then placed in the open area provided in the GDL Support Seal.
8. Add pre-measured thinner PTFE gasket to determine specific GDL compression.
9. Align MEA with precut silicone gaskets on both sides, and carefully place it in the gap that is provided by the thinner compression gaskets.
10. From here steps 3-8 are repeated in reverse, making sure to properly align the carbon bipolar plate so that hydrogen will come out its own tube.
11. Each clamping bolt is then tightened down to hand tight in a diagonal pattern.
12. From there the predetermined inch pounds to compress the stack, usually 100 inch pounds, is applied to the stack in increments of 25 inch pounds, also in a diagonal pattern.

13. If installing a new MEA a manufacturer recommended break in period is suggested for optimal performance.